Alaska Department of Transportation & Public Facilities

Alaska University Transportation Center

Evaluation of MEMS-based In-place Inclinometers in Cold Regions

Margaret M. Darrow, Ph.D.
David. D. Jensen, E.I.T.

December 2012

Prepared By:

Alaska University Transportation Center
Duckering Building Room 245
P.O. Box 755900
Fairbanks, AK 99775-5900

Alaska Department of Transportation
Research, Development, and Technology Transfer
2301 Peger Road
Fairbanks, AK 99709-5399

INE/AUTC 12.38

FHWA-RD-AK-12-28

REPORT DOCUMENTATION PAGE

Form approved OMB No.

1. AGENCY USE ONLY (LEAVE BLANK)	2. REPORT DATE	3. REPORT TYPE AND DATES COVERED
FHWA-AK-RD-12-28	March 2013	Final Report (07/01/2009-12/31/2013)

4. TITLE AND SUBTITLE

Evaluation of MEMS-based In-Place Inclinometers in Cold Regions

5. FUNDING NUMBERS

AUTC #309022
DTRT06-G-0011
T2-09-06

6. AUTHOR(S)

Margaret M. Darrow, Ph. D., David D. Jensen, E.I.T.

7. PERFORMING ORGANIZATION NAME(S) AND ADDRESS(ES)
Alaska University Transportation Center
University of Alaska. Fairbanks
PO Box 755900
Fairbanks, AK 99775-5900

8. PERFORMING ORGANIZATION REPORT NUMBER

INE/AUTC 12.38

9. SPONSORING/MONITORING AGENCY NAME(S) AND ADDRESS(ES)

State of Alaska, Alaska Dept. of Transportation and Public Facilities
Research and Technology Transfer
2301 Peger Rd
Fairbanks, AK 99709-5399

10. SPONSORING/MONITORING AGENCY REPORT NUMBER

FHWA-AK-RD-12-28

11. SUPPLEMENTARY NOTES

12a. DISTRIBUTION / AVAILABILITY STATEMENT

No restrictions

12b. DISTRIBUTION CODE

13. ABSTRACT (Maximum 200 words)

Inclinometer probes are used to measure ground movement. While an industry standard, this technology has drawbacks, including costly trips for manual measurements, operator error, and limited measurements due to casing deformation. Relatively new MEMS-based in-place inclinometers (M-IPIs) consist of MEMS accelerometer segments separated variously by flexible joints or field-connection systems, and encased in watertight housing. M-IPIs provide nearly continuous ground movement measurements, accommodate greater ground movement due to their flexibility, and may contain temperature sensors. Two M-IPIs from different manufacturers were evaluated for three different vertical and horizontal applications in Interior Alaska. Each M-IPI was evaluated for ease of installation and subsequent retrieval, durability, and functionality in frozen ground. Measurements from both devices compared well to those from the inclinometer probe, indicating that these devices are suitable for use in cold regions. Field experience indicates that the installation procedure for each instrument is better undertaken at above freezing temperatures, due to required manual dexterity and the temperature requirements of casing adhesive. If used to measure both ground movement and temperature in frozen ground, the M-IPI temperature sensors should be calibrated. We recommend replacing cold-affected plastic components between installations to avoid unwanted breakage during re-installation.

14- KEYWORDS:

Inclinometer, MEMS, slope stability, Alaska, permafrost

15. NUMBER OF PAGES

122

16. PRICE CODE

N/A

17. SECURITY CLASSIFICATION OF REPORT	18. SECURITY CLASSIFICATION OF THIS PAGE	19. SECURITY CLASSIFICATION OF ABSTRACT	20. LIMITATION OF ABSTRACT
Unclassified	Unclassified	Unclassified	N/A

SI* (MODERN METRIC) CONVERSION FACTORS

APPROXIMATE CONVERSIONS TO SI UNITS

Symbol	When You Know	Multiply By	To Find	Symbol
		LENGTH		
in	inches	25.4	millimeters	mm
ft	feet	0.305	meters	m
yd	yards	0.914	meters	m
mi	miles	1.61	kilometers	km
		AREA		
in^2	square inches	645.2	square millimeters	mm^2
ft^2	square feet	0.093	square meters	m^2
yd^2	square yard	0.836	square meters	m^2
ac	acres	0.405	hectares	ha
mi^2	square miles	2.59	square kilometers	km^2
		VOLUME		
fl oz	fluid ounces	29.57	milliliters	mL
gal	gallons	3.785	liters	L
ft^3	cubic feet	0.028	cubic meters	m^3
yd^3	cubic yards	0.765	cubic meters	m^3
	NOTE: volumes greater than 1000 L shall be shown in m^3			
		MASS		
oz	ounces	28.35	grams	g
lb	pounds	0.454	kilograms	kg
T	short tons (2000 lb)	0.907	megagrams (or "metric ton")	Mg (or "t")
		TEMPERATURE (exact degrees)		
^oF	Fahrenheit	5 (F-32)/9 or (F-32)/1.8	Celsius	^oC
		ILLUMINATION		
fc	foot-candles	10.76	lux	lx
fl	foot-Lamberts	3.426	$candela/m^2$	cd/m^2
		FORCE and PRESSURE or STRESS		
lbf	poundforce	4.45	newtons	N
lbf/in^2	poundforce per square inch	6.89	kilopascals	kPa

APPROXIMATE CONVERSIONS FROM SI UNITS

Symbol	When You Know	Multiply By	To Find	Symbol
		LENGTH		
mm	millimeters	0.039	inches	in
m	meters	3.28	feet	ft
m	meters	1.09	yards	yd
km	kilometers	0.621	miles	mi
		AREA		
mm^2	square millimeters	0.0016	square inches	in^2
m^2	square meters	10.764	square feet	ft^2
m^2	square meters	1.195	square yards	yd^2
ha	hectares	2.47	acres	ac
km^2	square kilometers	0.386	square miles	mi^2
		VOLUME		
mL	milliliters	0.034	fluid ounces	fl oz
L	liters	0.264	gallons	gal
m^3	cubic meters	35.314	cubic feet	ft^3
m^3	cubic meters	1.307	cubic yards	yd^3
		MASS		
g	grams	0.035	ounces	oz
kg	kilograms	2.202	pounds	lb
Mg (or "t")	megagrams (or "metric ton")	1.103	short tons (2000 lb)	T
		TEMPERATURE (exact degrees)		
^oC	Celsius	1.8C+32	Fahrenheit	^oF
		ILLUMINATION		
lx	lux	0.0929	foot-candles	fc
cd/m^2	$candela/m^2$	0.2919	foot-Lamberts	fl
		FORCE and PRESSURE or STRESS		
N	newtons	0.225	poundforce	lbf
kPa	kilopascals	0.145	poundforce per square inch	lbf/in^2

*SI is the symbol for the International System of Units. Appropriate rounding should be made to comply with Section 4 of ASTM E380.
(Revised March 2003)

EXECUTIVE SUMMARY

Inclinometer probes are used to measure ground movement. While an industry standard, this technology has drawbacks, including costly trips for manual measurements, operator error, and limited measurements due to casing deformation. Relatively new to the industry, MEMS-based in-place inclinometers (M-IPIs) are composed of a series of MEMS accelerometer segments separated variously by flexible joints or field-connection systems, and encased in a watertight housing. M-IPIs provide nearly continuous ground movement measurements without frequent field trips, accommodate greater ground movement due to their flexibility, and may contain temperature sensors, useful for frozen ground applications. Since M-IPIs have not been evaluated fully for use in cold regions, two M-IPIs from different manufacturers were evaluated for three different applications in Interior Alaska: 1) to monitor creep in frozen ground (vertical installation); 2) to identify and monitor slide shear zones (vertical installation); and 3) to monitor thaw settlement under a newly-constructed embankment (horizontal installation). Each M-IPI was evaluated for ease of installation and subsequent retrieval, durability, and functionality in frozen ground.

Measurements from both devices compared well to those from the inclinometer probe, with small differences in measurements attributed to differences in the devices' geometry and flexibility. Temperature data analysis indicates that the M-IPI devices measured temperatures within ~0.4°F of those recorded by a thermistor string. In two separate installations, temperature readings from the M-IPI device served as a check on potentially faulty readings from another sensor, which was an unexpected benefit. In addition to the proposed test sites, one of the M-IPI devices was installed where a large amount of movement was anticipated. The device continued to read during shearing and provided meaningful measurements after shearing. The presence of the M-IPI in the quickly moving landslide provided much more data than we otherwise would have collected due to the remoteness of the installation.

Based on this analysis, these devices are suitable for use in cold regions. Field experience indicates that the installation procedure for each instrument is better undertaken at above freezing temperatures, however, due to required manual dexterity and the temperature requirements of casing adhesive that is typically available. We recommend that, if the needs of the project require the M-IPI device to produce measurements of both ground movement and temperature, the M-IPI temperature sensors are calibrated by the manufacturer before use. Additionally, we recommend replacing any needed cold-affected plastic components between installations to avoid unwanted breakage during re-installation.

TABLE OF CONTENTS

EXECUTIVE SUMMARY ..... **i**
TABLE OF CONTENTS ..... **ii**
LIST OF FIGURES ..... **iv**
LIST OF TABLES ..... **viii**
LIST OF APPENDICES ..... **viii**
ACKNOWLEDGEMENTS ..... **ix**
CHAPTER 1 BACKGROUND **1**
RESEARCH OBJECTIVES 2
M-IPI SUMMARY 2
CHAPTER 2 RESEARCH APPROACH **7**
SITE 1: RICH113 7
Geology and Background 7
Instrument Installation and Retrieval 7
SITE 2: CHITINA DUMP SLIDE 10
Geology and Background 10
Instrument Installation and Retrieval 11
SITE 3: LOST CHICKEN 12
Geology and Background 12
Instrument Installation 12
SITE 4: FROZEN DEBRIS LOBE-A (FDL-A) 13
Geology and Background 13
Instrument Installation 13
CHAPTER 3 FINDINGS **15**
RICH 113 15
M-IPI Analysis 15
Temperature Analysis 18
TDR Analysis 18
CHITINA DUMP SLIDE 21
M-IPI Analysis 21
TDR Analysis 25
Water Pressure and Temperature Analysis 25

LOST CHICKEN SITE 25
M-IPI Analysis 25
Temperature Analysis 33
FDL-A RESULTS 43
M-IPI Analysis 43
Temperature Analysis 43
DISCUSSION OF M-IPI SOFTWARE USE 47
CHAPTER 4 CONCLUSIONS, RECOMMENDATIONS, AND SUGGESTED RESEARCH 49
CHAPTER 5 REFERENCES 52

LIST OF FIGURES

Figure 1 Components of the Geodaq INC500 device 3

Figure 2 Overview of the Measurand SAA device 5

Figure 3 Location of the four research sites relative to Fairbanks and Anchorage 8

Figure 4 Relative locations of the measured casings at Rich113 16

Figure 5 Selected measurements and analysis from the Rich113 site 17

Figure 6 Comparison of measured temperatures 19

Figure 7 Measurements from the TDR cable 20

Figure 8 Relative locations of the measured casings and piezometer installation at the Chitina Dump Slide 22

Figure 9 Cumulative displacement measurements from the inclinometer probe for TH10-1551 23

Figure 10 Selected measurements and analysis from the Chitina Dump Slide site 24

Figure 11 Measurements from the TDR cable 26

Figure 12 Data from the vibrating wire piezometer. 27

Figure 13 Temperature readings from the INC500 device installed within TH10-1552 27

Figure 14 Uncorrected cumulative displacement measurements with time 29

Figure 15 Corrected SAA and inclinometer probe performance using the uncorrected data referenced to the near casing end 31

Figure 16 Comparison of SAA and inclinometer probe performance using corrected data (referencing the near end) 28

Figure 17 Corrected SAA data 32

Figure 18 Estimated embankment settlement based on (a) corrected inclinometer probe and (b) SAA data, and survey data from August 20 and October 6. 34

Figure 19 Comparison of casing orientation as measured by the inclinometer probe and based on survey data 35

Figure 20 Comparison of temperature measurements beneath the Lost Chicken embankment 36

Figure 21 2-Dimensional plot of temperatures versus time measured by the thermistor string 37

Figure 22 2-Dimensional plot of temperatures versus time measured by the SAA device 39

Figure 23 2-Dimensional plot of temperature versus time measured by the TAC device 40

Figure 24 Comparison of measured average daily air temperature and historical average daily air temperature obtained from NCDC 41

Figure 25 Measured daily average air and ground surface temperatures 42

Figure 26 Cumulative displacement measurements for TH12-9004 until the INC500 began to demonstrate signs of failure. 44

Figure 27 Evidence of failure of the INC500 at FDL-A 45

Figure 28 Temperature readings from TH12-9004 46
Figure A-1 Location of the drill rig for TH09-1510 54
Figure A-2 Configuration of coaxial (TDR) cable at the bottom of the guide casing prior to installation 54
Figure A-3 Conducting a “hallway” test with the INC500 and SAA devices wired into the ADAS enclosure 55
Figure A-4 Staging the INC500 device on sawhorses in March 2010 55
Figure A-5 Marking the INC500 for placement of centralizers 56
Figure A-6 Order of INC500 module serial numbers before installation 56
Figure A-7 Damage to centralizers due to improper alignment during the March 2010 installation 57
Figure A-8 Attaching the safety line to the lowest module 57
Figure A-9 Lowering the first INC500 module down the guide casing 58
Figure A-10 First INC500 module resting on fork 58
Figure A-11 Steps in the assembly of the INC500 modules 59
Figure A-12 Connecting the coupler assembly with machine screws 60
Figure A-13 Installing inner 1.05-in. PVC into guide casing for SAA device 60
Figure A-14 Preparing inner 1.05-in. PVC casing for SAA installation 61
Figure A-15 Installing the SAA device 61
Figure A-16 Completed Rich113 installation in March 2010 62
Figure A-17 Inside of ADAS enclosure 62
Figure A-18 Guide casing to flexible conduit adapter in place on TH09-1511 casing 63
Figure A-19 Final configuration of the Rich113 site 63
Figure A-20 Configuration of Rich113 ADAS 64
Figure A-21 Retrieving the INC500 in September 2010 to adjust the positioning of the centralizers 64
Figure A-22 Retrieving the SAA in August 2011, and replacing the device on the shipping reel 65
Figure A-23 Final configuration of the Rich113 site in August 2011 65
Figure A-24 “Hallway” test of the SAA device after retrieval from the Rich113 site 66
Figure A-25 “Hallway” test of the INC500 device after retrieval from the Rich113 site 66
Figure B-1 Tamping dry sand backfill around the guide casing 75
Figure B-2 Configuration of the coaxial (TDR) cable on the outside of the guide casing 75
Figure B-3 Attaching the coaxial (TDR) cable with hose clamps at 10-ft intervals 76
Figure B-4 Installing the INC500 within the guide casing 76

Figure B-5 Placement of vibrating wire piezometer on PVC casing for installation into TH10-1553 77
Figure B-6 Preparing the cement-bentonite grout for backfill into TH10-1553 77
Figure B-7 Overview of the Chitina installation 78
Figure C-1 Looking southeast towards the instrumented cross section 85
Figure C-2 Casings prior to backfill at the instrumented cross section 85
Figure C-3 Covering the casings with sand bedding 86
Figure C-4 Downhill toe of embankment with thermal berm and exposed casing ends 86
Figure C-5 Wrapping BeadedStream temperature acquisition cable (TAC) to thermistor cable for installation 87
Figure C-6 Alignment of TAC and thermistor cable 87
Figure C-7 Attaching the pull rope to the end of the TAC device 88
Figure C-8 Uphill termination of the casing containing the TAC and thermistor string 88
Figure C-9 PVC casing to flexible conduit adapter for the temperature measurement cables 89
Figure C-10 Installing the SAA device from the downslope end, pulling from the upslope end 89
Figure C-11 Installation of SAA device, showing shipping reel position relative to embankment and ADAS 90
Figure C-12 PVC casing to flexible conduit adapter for SAA installation 90
Figure C-13 Installing the dead-end pulley on the horizontal guide casing 91
Figure C-14 Routing pull rope for SAA through ABS end cap adapter 92
Figure C-15 Tapping ABS end cap adapter into the sand bedding to be flush with inner casing 92
Figure C-16 Filling annulus space with expanding foam to seal outer ABS end cap adapter in place 93
Figure C-17 Upslope casing ends secured 93
Figure C-18 Trimming the downslope guide casing for ABS end cap adapter 94
Figure C-19 Tapping ABS end cap adapter into the sand bedding for downslope guide casing 94
Figure C-20 Attaching 2 ¼-in. locking link to wire rope within guide casing 95
Figure C-21 Winding up excess wire rope from within casing assembly 95
Figure C-22 Taking manual inclinometer probe measurements 96
Figure C-23 Downslope guide casing termination 96
Figure C-24 Downslope casing ends secured 97
Figure C-25 Battery box and enclosure for ADAS 97
Figure C-26 Final ADAS configuration located near the downslope toe of the embankment 98
Figure C-27 Cracks in the thermal berm on September 14, 2012 98

Figure C-28 Changes at the ADAS during the fall of 2012 99
Figure D-1 Drilling TH12-9004 with tricone and casing 100
Figure D-2 Cement-bentonite grout during the back-filling process 100
Figure D-3 INC500 modules, staged and ready for installation 101
Figure D-4 Installing the INC500 within the guide casing in TH12-9004 101
Figure D-5 Examples of coupler damage 102
Figure D-6 Completed casing and instrument installation in TH12-9004 102
Figure D-7 Completed ADAS location and casing installation of TH12-9004 103

LIST OF TABLES

Table 1 Specifications for the three instruments compared 6
Table 2 Summary of results from various M-IPI installations 50
Table 3 Summary of pros and cons of each M-IPI device 51
Table F-1 “Parts list” for Geodaq M-IPI device 108
Table F-2 “Parts list” for Measurand M-IPI device 108
Table F-3 “Parts list” for typical ADAS installation 109

LIST OF APPENDICES

APPENDIX A: RICH113 INSTALLATION PHOTOGRAPHS AND BORING LOGS 54
APPENDIX B: CHITINA INSTALLATION PHOTOGRAPHS AND BORING LOGS 75
APPENDIX C: LOST CHICKEN INSTALLATION PHOTOGRAPHS 85
APPENDIX D: FDL-A INSTALLATION PHOTOGRAPHS AND BORING LOG 100
APPENDIX E: MANUFACTURER’S WEBSITES 107
APPENDIX F: “PARTS LISTS” FOR M-IPI DEVICES AND ADAS INSTALLATIONS 108

ACKNOWLEDGMENTS

This project was jointly funded by the Alaska Department of Transportation and Public Facilities (ADOT&PF) and the Alaska University Transportation Center (AUTC). We thank the members of the research committee overseeing this project for their valuable input and support throughout its duration. So many people with ADOT&PF made this project a success. We thank: J. Hoffman and T. Ansell for their support and on-site help with remote connections at Tazlina, M. Helkenn for preparation of the Chitina site for drilling, T. Straub for his help coordinating field work at Lost Chicken, and L. Woster, J. Currey, and S. Masterman for all of their support throughout this project. We also thank A. Parsons, S. Parker, P. Lanigan, J. Cline, C. Roach, R. Wagster, and K. Maxwell (ADOT&PF), and T. Haller, K. Obermiller, S. Huang, J. Yao, R. Daanen, and J. Simpson (UAF) for their hard work in the field; L. Danisch and J. Lemke for their willingness to address concerns and their patience with consistent questions; and M. Lilly and A. McHugh for their help in setting up smoothly functioning ADAS.

CHAPTER 1

BACKGROUND

Inclinometers are used widely in geotechnical engineering to measure ground movement for a variety of applications including slopes, embankments, bridges, and retaining wall structures. The traditional technology for vertical inclinometers relies on installing a grooved (or guide) casing into a drilled boring. An inclinometer probe fitted with wheels is manually lowered down the near-vertical casing. This type of instrument contains two force-balanced servo-accelerometers that measure its inclination (Durham Geo-Enterprises, Inc., 2011). Measurements, which consist of the orientation from true vertical of the inclinometer, are recorded at specified depth intervals. A series of such measurements are compared to each other and to the initial set of readings. In this manner, the profile of the casing is established at the time of each measurement. Plotting subsequent profiles allows changes in the casing to become apparent. Analysis of a series of such readings facilitates the identification of a zone or zones of movement, and the rate of movement in these zones. Measurements of horizontal casings for monitoring settlement are made in a similar fashion. Machan and Bennett (2008) provide a comprehensive overview of inclinometer types, their usage, and data analysis techniques.

Despite its place as an industry standard for the last 40 years, this technology has some drawbacks and shortcomings. Since the data is acquired manually, each dataset represents a trip to the field site. Depending on the remoteness of the project location, these trips (and thus, data acquisition) become an expensive part of the overall monitoring program. The measurement frequency may be reduced due to budget considerations, making interpolation of the recorded data necessary. The accuracy of the data collected using the inclinometer probe depends on the care of the individual taking the measurements, since the inclinometer must be consistently placed at the specified intervals. Differences in the skill levels and techniques of the various individuals collecting the data are integrated into each dataset, thereby introducing human error. Additional error may result from reading perturbations caused by dirt or debris becoming lodged in the casing grooves with time. The manual inclinometer instrument is a 2-ft long rigid device; its configuration limits the amount of deformation a casing can experience before readings are no longer possible. For landslides, the casing may deform at an upper elevation, preventing the passage of the inclinometer and thus leaving a lower shear zone undetected. Finally, the inclinometer casing itself has limited flexibility and will shear off when excessive ground movement occurs, ending the monitoring.

A relatively new type of geotechnical instrumentation incorporates Micro-Electro-Mechanical Systems (MEMS) accelerometers, which were first used for automotive airbags. MEMS-based in-place inclinometers (M-IPIs) are composed of a series of accelerometers that are connected with flexible joints and encased in watertight housing, making these devices suitable for direct burial in the ground. The M-IPI devices are reported to have high accuracy with results that correlate well with inclinometer probes (Barendse, 2008; Lemke, 2006). The shorter length and smaller diameter of M-IPI segments theoretically allow these instruments to record larger deformations and yet still be retrievable (Barendse and Machan, 2008). When the installation is accompanied by a remote power supply and a telemetry link, an M-IPI can provide nearly continuous observation of ground movement without multiple trips to the field. M-IPI manufacturers state that these devices are reusable, as they can be removed from one installation

and placed into another, resulting in further cost savings. Some M-IPIs also have integrated temperature sensors, which facilitate simultaneous ground movement and temperature readings.

It also should be noted that there are other configurations of in-place inclinometers, where individual sensors are positioned within a casing to capture expected movement. The sensors are mechanically connected to each other via cables or rods, and by signal cables with watertight connectors. Many of these in-place inclinometers now use MEMS tilt sensors. This group of instruments (as well as MEMS inclinometer probes) will not be discussed further here as they were not tested during this research project.

RESEARCH OBJECTIVES

Since this technology is relatively new, the use of M-IPIs has not been fully evaluated, especially in cold regions. M-IPIs potentially can be reused; however, new extraction techniques for use in frozen ground may need to be developed. As with any equipment used in cold regions, the durability of M-IPI at sub-freezing temperatures must be evaluated as well.

The overall goals of this research project were to evaluate the use of M-IPI for their versatility and accuracy in cold regions, for their ease of use and recoverability, and to compare their use against the existing manual methodology. To achieve these goals, we developed the following objectives:

1) To evaluate M-IPI devices for three different applications in Interior Alaska:
    - To monitor creep in frozen ground (vertical installation)
    - To identify and monitor a slide shear zone (vertical installation)
    - To monitor thaw settlement under a newly-constructed embankment (horizontal installation)
2) To compare two different M-IPI products to each other and to the existing manual method, identifying any benefits of one product over another;
3) To evaluate the extraction of M-IPI devices in order to evaluate their re-usability.

This report summarizes the vertical (and horizontal for one device) installations of two different M-IPI products: an INC500 Series In-Place Inclinometer (INC500) from GEODAQ; and the ShapeAccelArray (SAA) from Measurand. This report is not an endorsement of either product, but rather an independent evaluation of their use in cold regions. As this project represents the first time the Principal Investigator (PI) installed either of the M-IPI devices, this report also includes anecdotes from field work, and photographic summaries of each M-IPI installation in Appendices A through D. Manufacturer's websites and "parts lists" are provided in Appendices E and F, respectively.

M-IPI SUMMARY

The INC500 device consists of 8-ft long flexible modules that contain a series of MEMS-based accelerometer sensors, which measure tilt (see Figure 1). In a standard module, these biaxial sensors are located every 12 in., along with a temperature sensor that has a reported accuracy of ±3°F (GEODAQ, 2010) and is not calibrated unless specified by the customer. The modules are

Figure 1. Components of the Geodaq INC500 device. (a) Modules prepared for installation; the yellow arrow indicates a safety line attached to the lowest module. The other components necessary to complete an installation are (b) coupler assemblies, centralizers, a slotted fork to hold the INC500 within the casing, and (c) the GCM controller module. (Photographs by M. Darrow)

joined by underwater electrical connectors, and the connections are stiffened by a coupler assembly, in order to give the entire instrument length a uniform rigidity. Additionally, three to four centralizers are mounted along the length of each module. Each centralizer contains four stainless steel wheels that are designed to guide and orient the device within a guide casing. Because of its modularity, an INC500 device can be lengthen or shortened to accommodate the geometry of a given installation. The order of the modules as installed within the casing must be recorded, as this order is an input parameter into a setup file for the software program to calculate displacement (see Figure A-6). The INC500 must be installed so as to rest on the bottom of the casing. Because of the potential difference in length between the joined modules and the total casing depth, the INC500 may rest slightly lower or higher than the ground surface within the casing (J. Lemke, pers. comm., March 2010). The INC500 instrument acquired for this research contained bi-axial sensors oriented only for a vertical installation. The manufacturer can make a model for both vertical and horizontal applications, which requires additional sensors (J. Lemke, pers. comm., March 2011).

An SAA consists of rigid segments connected by special joints. Each segment contains MEMS gravity sensors that measure tilt (Measurand, 2010). The segments are grouped into octets, with a temperature sensor located about the midpoint of each octet. The temperature sensor has a reported accuracy of ±2.2°F, and is not calibrated unless specified by the customer. For a given installation, an SAA of a desired length is ordered from the manufacturer. The SAA is shipped on a reel from which it is directly installed in the field (see Figure 2). Table 1 is a summary of the specifications for both of these devices, as well as those of a Digitilt Inclinometer Probe, which served as the standard against which comparisons were made for this project. These specifications are a simplified representation of the complete discussion on the instruments' performance; for more detail, the reader is directed to the manufacturer's datasheets.

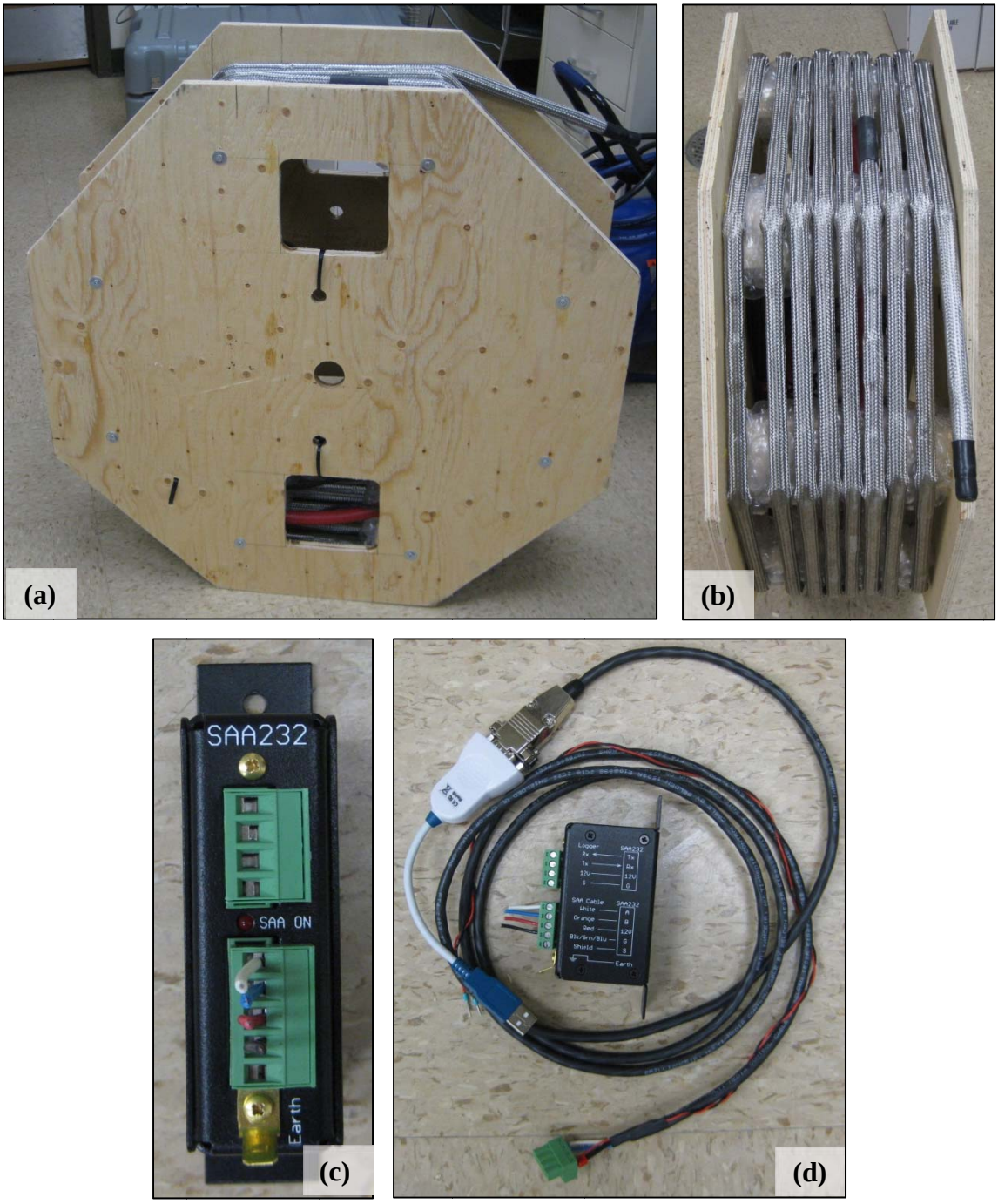

Figure 2. Overview of the Measurand SAA device. (a) The SAA on the shipment reel as viewed from the side and (b) on end. The SAA232 converter for use with a CR1000 data logger, (c) as viewed from the end and (d) on its side, with SAA232 to USB direct connection cable for pre-installation diagnostics. (Photographs by M. Darrow)

Table 1: Specifications for the three instruments compared. Values provided were taken (and in some cases, converted) from [1]Durham Geo-Enterprises (2011), [2]GEODAQ (2010), and [3]Measurand (2010). The symbol '*' represents data not available on the datasheet. ([†] The relationship between length and precision is not linear, as this information would suggest; we refer the reader to Measurand's datasheet for a more thorough discussion.)

Instrument	Digitilt Inclinometer Probe[1]	GEODAQ INC500[2]	Measurand SAA[3]
Range (typical, tilt)	±35° from vertical	±15° from vertical (for typical use)	±60° from vertical (range of software)
Resolution	0.0012 in. per 24 in.	0.01 in. per 96 in. (0.005 in. per 12 in.)	2 arc-seconds
Accuracy	*	0.04 in. per 96 in. (0.014 per 12 in.)	*
Precision	±0.05 in. per 50 readings (±0.01%FS)	*	± 0.06 in. / 100 ft[†]
Temperature Operating Range	-4 to +122°F	0 to 150°F	-4 to +158degF
Accuracy of uncalibrated temperature sensors	(not included)	±3°F	±2.2°F

CHAPTER 2

RESEARCH APPROACH

To achieve the overall research goals of evaluating MEMS-based in-place inclinometers (M-IPI) for use in cold regions and against the existing manual methodology, we installed the two M-IPI devices in vertical or horizontal configurations at four different research sites (see Figure 3). This chapter contains an overview of each site, consisting of some site history and geology, and a summary of the field work associated with the M-IPI installation and, for Sites 1 and 2, retrieval.

SITE 1: RICH113

Geology and Background

We evaluated both M-IPI devices in vertical installations at a site in south-central Alaska along the Richardson Highway at Milepost 113 (Rich113). At this location, the highway travels along an east-facing bluff overlooking the Copper River. The area has experienced movement for decades, requiring realignment of the highway away from the bluff edge in 1965.

Permafrost in this area is warm, with an average annual temperature of 31°F, and the subsurface consists of a 5-ft thick surficial silt layer, underlain by ice-rich, clayey soils. At approximately 52 ft below the ground surface (bgs), the soils become more ice-poor and coarser grained. It is at this soil transition that movement is occurring. Analysis of *in situ* measurements and soil creep tests indicates that the ice-rich clayey soils are experiencing creep, with velocities of up to 1 in. per year (Darrow et al., 2012).

Instrument Installation and Retrieval

Alaska Department of Transportation and Public Facilities (ADOT&PF) personnel conducted drilling programs in the area in 2003 and 2007, installing several guide casings. The existing installations and several years of recorded measurements made this site ideal for one of the M-IPI evaluation research locations. Together with ADOT&PF personnel, the PI installed additional guide casing during field work in November 2009. We drilled a total of three borings, one boring for the automated data acquisition system (ADAS) post, and two borings for the installation of grooved guide casing and 1-in. PVC for thermistor cable installation (see Appendix A for boring logs and photographs of the installation). We attached a coaxial cable, serving as a time-domain reflectometry (TDR) device, to the outside of the guide casing in TH09-1511 (see Figure A-2). The bottom end of the TDR cable was sealed with an end cap in the laboratory prior to the field work (see inset in Figure A-2). Following a method presented by Cortez et al. (2009), we affixed the coaxial cable with hose clamps at 10-ft depth intervals. Because of the warm permafrost in the area, the 2.75-in. guide casings were not grouted in place. Instead, dry sand was poured and tamped into the annulus space, typically in 1 to 3 in. lifts (see Figure B-1 for an example of this process for a different research site). All casings were measured using the traditional inclinometer probe in November 2009 to establish baseline readings.

The M-IPI instruments were ordered from the manufacturers after the drilling program was complete, since the exact length needed was known once back from the field. Upon receipt of the devices, a “hallway” test of both instruments was conducted to ensure that they were

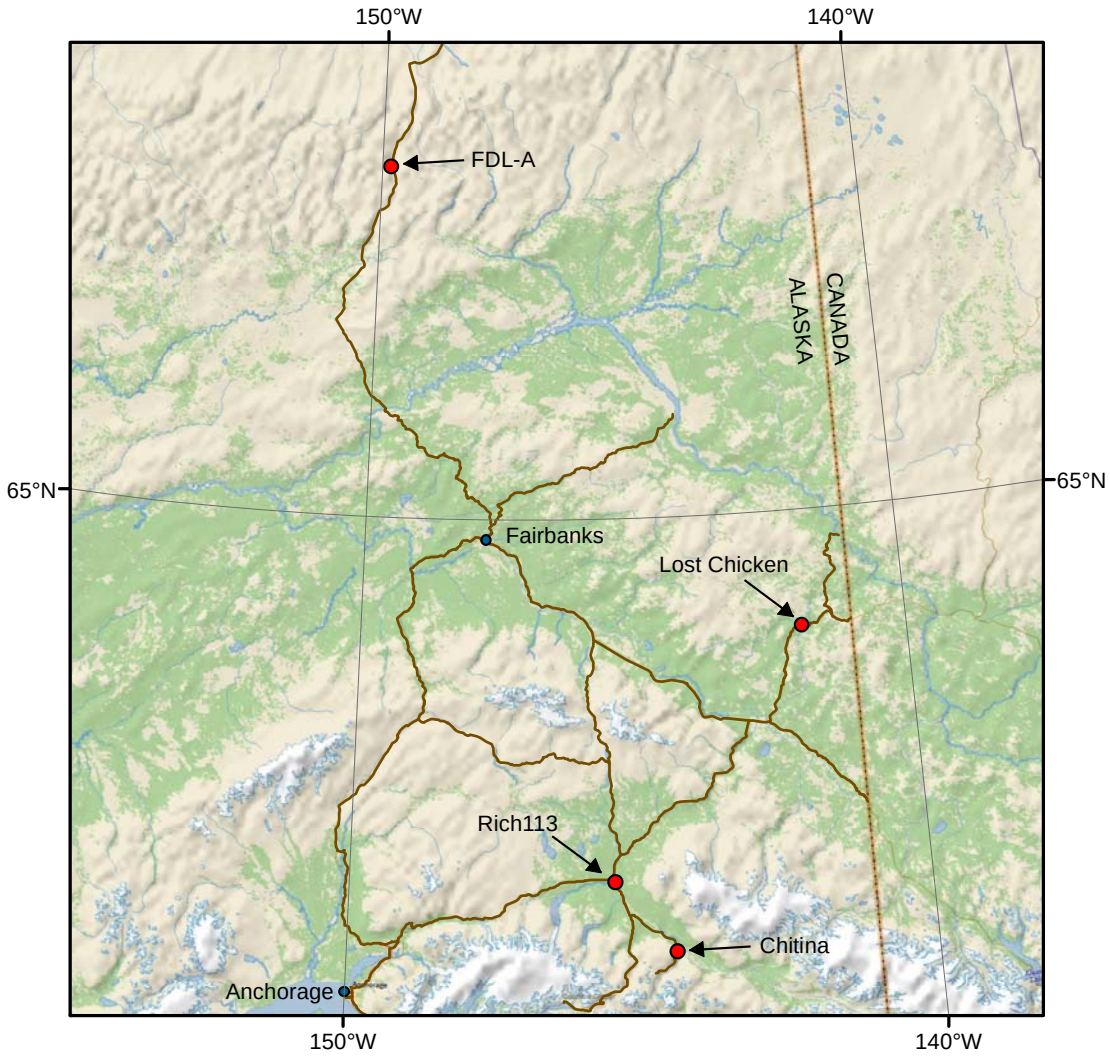

Figure 3. Location of the four research sites relative to Fairbanks and Anchorage. Each research site is indicated by a red circle, and major highways/roads are indicated by the brown lines. Base map courtesy of DeLorme and ESRI.

recording data and communicating well with the ADAS that would be used in the field (see Figure A-3). The INC500 device consisted of eight 8-ft-long modules; including the length of the cable/coupling at each connection, the total length of the INC500 was 67.5 ft. The SAA device consisted of eight standard octets, with an additional partial octet to achieve the desired length. As measured during the hallway test, the SAA was 68.7-ft long. Neither of these lengths included the connection cables.

The M-IPI instruments were installed by two people during a subsequent trip to the field in March 2010, during which temperatures ranged from 0°F in the morning to 30°F mid-day in the sun. The INC500 coupler assemblies required ten machine screws and each centralizer required two machine screws to secure firmly around the module (see Figure 1b and Figures A-4 through A-12 for installation steps of the INC500). In the field, we used both a screwdriver and a cordless drill to secure these screws. Installing the screws presented a challenge at sub-freezing temperatures because of lost dexterity due to gloves and searching for screws dropped into the snow. The PI unknowingly oriented the centralizers 90° off from their correct orientation (when correctly oriented, the centralizers fit into a longitudinal notch along the module). This resulted in some strain in the plastic and a few broken centralizers (see Figure A-7). Because of the incorrect orientation, the modules did not easily slide into the guide casing; rather, effort was required to push the INC500 to its appropriate depth. The guide casing then was filled with propylene glycol to prevent the freezing of any water that might accumulate inside the casing due to condensation and/or leaks. The entire process took two people about four hours to complete.

The manufacturer of the SAA recommends that this device be installed within a 1.05-in. dia. electrical PVC casing (see Figures A-13 through A-15 for installation steps of the SAA). The SAA fits snuggly into this smaller diameter casing, which is more flexible than the larger 2.75 in. guide casing. Since the focus of the M-IPI evaluation project was to compare the instrument responses only, using two different casing sizes would have introduced another variable to evaluate. As a compromise, we installed the 1.05-in. dia. electrical PVC casing within the 2.75 in. guide casing, with the annulus backfilled with tamped dry sand. For a snug fit inside the 1.05-in. dia. casing, the SAA joints should be in compression (Measurand, 2008). At the time of this installation, the manufacturer recommended cutting notches into the top of the 1.05-in. casing; once the SAA was installed within the casing, a hose clamp locked the SAA into position (see Figure A-14). As we wanted to secure the top of the guide casings, it was necessary to cut a slot into the guide casing to access the hose clamp with a screwdriver (see Figures A-13 through A-15). Instructions for the PVC glue indicated that it must be used at temperatures above 50°F, and that the glued connections must sit for one hour before adherence is complete. Since the actual temperatures during installation in March were much lower than those suggested and the necessary time was not available, we modified the recommended procedure. To keep it warm, the PVC glue was kept inside the PI's jacket until needed. Then, to speed up the assembly process, we glued two 10-ft long sections together. We then attached them to the 1 in. casing already inserted into the outer casing. In hindsight, this was a poor choice, as the 20 ft of PVC casing swaying in the air was difficult to hold steady while being affixed to the casing down the borehole. The installation of the SAA within the inner PVC casing proceeded without difficulty. This entire installation including the inner PVC casing took about two hours.

Both of the instruments were wired into an ADAS, which was powered from a battery bank recharged by a solar panel (see Figures A-16 and A-17). A data logger recorded measurements

every six hours, and data was transmitted from the site via a radio telemetry link. We returned to the site in May 2010 to add adapters to better transition between the guide casing and the flexible conduit (see Figure A-18). Figures A-19 and A-20 are photographs of the site, showing the three different casings that were measured and the ADAS. Installing all of the instrumentation at this site took about 1 ½ days to complete.

It was not until the summer of 2010, and during the installation of a second INC500 at another location, that the PI recognized the incorrect positioning of the centralizers at Rich113. In September 2010, we returned to the Rich113 site to correct this error. The INC500 was extracted from the casing, the centralizers were rotated, and then the device was reinstalled (see Figure A-21). Once removed from the casing the device was inspected for damage. Some of the connectors demonstrated twisting of the pins; however, this produced no detrimental effect on the device, which was reinstalled into the casing. During this second installation, the INC500 device traveled smoothly along the guide casing to its appropriate depth. Based on the second installation, September 3, 2010 was designated as the baseline reading for the INC500, SAA, and inclinometer probe devices. The analysis of results presented in Chapter 3 uses the data from September 3, 2010 until August 16, 2011.

We extracted both devices at the Rich113 site on August 16, 2011, and dismantled the ADAS, leaving only the existing casings in place (see Figures A-22 and A-23). Extracting the SAA took about thirty minutes with two people, with most of that time spent adjusting the device on the shipment reel. Three people were involved with the extraction of the INC500, which took about forty minutes. During retrieval, we examined each instrument for signs of wear. Overall retrieval went very well, and the entire dismantling of the site, including extraction of the thermistor string and removal of the ADAS, took about five hours.

In January 2012, we conducted another set of "hallway" tests upon returning from the field to ensure the proper operation of each device (see Figures A-24 and A-25). To test the SAA, we laid it on the floor and connected it directly to a lap top computer to view real-time data. We walked the length of the device, gently raising a portion of it as we walked alongside it. The inset in Figure A-24 is an illustration of watching this "bump" move down the length of the device, indicating good working condition. For the INC500, we connected two to three modules together and to the data logger, and then held them tightly and as still as possible in a stairwell, logging for about fifteen minutes. We then reviewed the data, which indicated that each set of modules functioned correctly.

SITE 2: CHITINA DUMP SLIDE

Geology and Background

Less than a mile beyond Chitina, Alaska, a slow-moving slide intersects the McCarthy Road. As the area was previously used as the town dump, this site of slope instability has received the infamous title of the "Chitina Dump Slide" (CDS). In and near the slide area, the soils consist of surficial organic silt overlying silty clay with sand and gravel, overlying bedrock at depth. Located in discontinuous permafrost, a recent study suggests that thermal effects of the dump may have contributed to movement of the slide (Obermiller et al., in press).

Instrument Installation and Retrieval

As this site was known to demonstrate movement in a well-defined shear zone, we installed the INC500 in a vertical orientation for evaluation. Working with an ADOT&PF drill crew, we drilled four borings within the active slide area during June 2010: one for the ADAS post, two for installation of guide casing, and one for installation of a vibrating wire (VW) piezometer (see Appendix B for installation photographs and boring logs). Drilling indicated that the shear zone was between 15 and 20 ft bgs. As with the Rich113 site, the annular space around the guide casing was backfilled with tamped dry sand (see Figure B-1). A coaxial (TDR) cable was attached to the outside of the casing installed in TH10-1552, attached with hose clamps at 10-ft intervals (see Figures B-2 and B-3).

We installed a second, previously-unused set of INC500 modules to a depth of 50.5 ft bgs in TH10-1552. It was during this installation, which took two people about two hours to complete, when the PI understood that the centralizers on the INC500 at Rich113 were installed incorrectly. We did not see evidence of strain in the centralizers at CDS, although some of the threaded inserts popped out of the plastic coupler assemblies (see Figure B-4b). This was corrected by continuing to tighten each screw, which pulled the insert back into the plastic.

To evaluate the effect of water pressure on slope movement, we installed a VW piezometer in TH10-1553 at a depth of 15.8 ft bgs. In all of the borings, the soils transitioned from moist to wet organic silt to clay between 15 and 16 ft bgs. We also encountered buried trash at and slightly below these depths, indicating movement of the organic silt. We attached the VW piezometer to the outside of 1-in. diameter PVC casing, which was used to place the instrument at the correct depth (see Figure B-5). Following a method presented by McKenna (1995), Mikkelsen (2002), Mikkelsen and Green (2003), and Contreras et al. (2008), we used a cement-bentonite grout as backfill around the VW piezometer (see Figure B-6), which worked effectively.

The INC500 and VW piezometer were wired into an ADAS, which was powered from a battery bank recharged by a solar panel (see Figure B-7a). The power/data cable that shipped with the INC500 modules was not long enough for this installation; however, we simply spliced the cable with additional four-conductor 18 gage cable purchased locally. A data logger recorded measurements every 6 hours, and data was transmitted via a satellite telemetry link. Overall, the drilling and installation of all instrumentation at this site took three days to complete.

A week later, the PI returned to CDS to collect manual measurements of the guide casing. The measurements indicated that the slide had moved during that time, and new cracks on the embankment were apparent. The movement of CDS demonstrated its potential as a discontinuous permafrost location for evaluation of an M-IPI device, but it also raised concerns about being able to retrieve the device. We tested this by lifting the INC500 about 6 in. up on July 30, 2010. The instrument moved smoothly within the casing without any signs of binding. Satisfied with these results, we replaced the device in the casing, leaving it until the final retrieval on September 4, 2010. After extracting the INC500, we took readings of both slotted casings with the manual inclinometer probe. We also dismantled the ADAS, leaving only the existing casing in place (see Figure B-7b). The cables for the TDR and VW piezometer were coiled into a canvas bag attached to the casing for TH10-1552, in case future readings were needed. In May 2011, the PI made another trip to the site. Manual readings of the casings were no longer possible, as both casings had sheared over the winter.

SITE 3: LOST CHICKEN

Geology and Background

East of Chicken, the Taylor Highway crosses Lost Chicken Creek. The area is underlain by ice-rich silt and massive ice to the underlying bedrock surface about 50 ft bgs. Replacement of a culvert in 2004 resulted in thawing of the foundation soils below a portion of the highway (Darrow, 2008). This stretch of the highway was realigned in 2012, located closer to the bedrock outcropping along the valley walls. The realigned embankment consisted of portions of air-convected embankment (ACE) with a thermal berm on the downslope side. As part of the construction project, the contractor installed casing within the embankment for the horizontal M-IPI and temperature sensor installation.

Instrument Installation

In June 2012, we traveled to the Lost Chicken location to observe the installation of the casing for the horizontal inclinometer probe, SAA, and temperature sensors (see Figures C-1 through C-3, and Appendix C for additional installation photographs). Due to the construction schedule, we were unable to install the M-IPI devices during this trip. Prior to returning to the site, we calibrated the thermistor string that was retrieved from the Rich113 research site. The calibration indicated that, with the exception of two thermistor beads that failed during its initial use, the thermistor string was functioning correctly.

In mid-July 2012, we returned to the Lost Chicken location to install temperature sensors (see Figures C-5 through C-9), the SAA device (see Figures C-10 through C-12), and the ADAS. This field work included installing a dead-end pulley for the inclinometer probe measurements (see Figure C-13). This device allows one person to make measurements with the probe from one end of the embankment, rather than requiring two people (i.e., a person on either side of the embankment) and radio communication for synchronized actions to procure measurements. We also installed a digital temperature acquisition cable (TAC) from BeadedStream alongside the thermistor string (see Figures C-5 through C-9), in order to test the accuracy and reliability of this fairly new temperature measurement sensor. Both the SAA and the thermistor string were originally installed at the Rich113 location. As they were made for that location, they were of insufficient length to stretch under the entire embankment at Lost Chicken. We chose to locate them on the downslope side of the embankment so as to focus on measurements of the temperatures and movement below the thermal berm and the thermal berm-ACE interface. These devices were installed into casing rather than placed into trenches for a direct burial primarily due to the construction scheduling, and to allow for future extraction and reuse on a different project.

The SAA and temperature sensors were wired into an ADAS, which was powered from a battery bank and recharged by a solar panel (see Figures C-25 and C-26). The TAC was attached to its own data logger that was stored in an ABS casing extension at the toe of the embankment (see Figure C-9). The installation of all of the instrumentation, which went smoothly, took two full days to complete. During the initial installation, we took the initial sets of readings with the manual inclinometer probe (see Figures C-21 through C-23).

We returned to the site on July 23, August 6 and 20, September 1 and 14, and October 6, 2012 (approximately when the highway closed for the winter) to make manual measurements with the inclinometer probe. The frequency of trips allowed us to observe changes in the embankment

and the ADAS post-construction. In mid-September, we noted cracks on the side slope of the thermal berm (see Figure C-27). The ADAS site also experienced some changes during the fall. In July, the contractor installed the wooden post using a weed burner to thaw the ice-rich soils at the ADAS location. When we arrived at the site, the vegetation was disturbed, and surface runoff was draining past the ADAS location. Figure C-28a shows the configuration of the ADAS upon completion of the installation in mid-July. By October 6, the surface had settled at least 6 in. due to thawing of the ice-rich soils (see Figure C-28b). We adjusted the battery box at that time to provide adequate slack on the wiring; however, this action will need to be performed repeatedly for the long-term maintenance of this ADAS.

SITE 4: FROZEN DEBRIS LOBE-A (FDL-A)

Geology and Background

In the summer of 2012 and upon recommendation of the research committee overseeing this project, we extended the research by further testing the INC500 device in another vertical installation. The research site was Frozen Debris Lobe-A (FDL-A) at MP219 on the Dalton Highway, a slow-moving landslide that is encroaching on the highway at this location. Although previously identified in the area, FDLs have never been studied in detail. Analysis of remotely sensed imagery indicated that FDL-A was moving at an average rate of 0.4 in. per day between 1955 and 2008, and reconnaissance visits to the site suggested a variety of movement mechanisms, such as permafrost creep, debris flows along the over-steepened toe, and basal sliding (Daanen et al., 2012). Prior to the 2012 drilling program, however, we did not know the internal structure of the lobe, nor did we have any *in situ* measurements of movement.

Instrument Installation

We installed the INC500 in September 2012 and as part of a project to investigate FDL-A (Darrow et al., in press). We suspected that FDL-A might move quickly enough so as to make retrieval of the M-IPI device impossible. Thus, the reasons for this installation were 1) to collect important data from FDL-A to determine its mode, location, and rate of movement, and 2) to determine how much movement the INC500 device could withstand before it no longer functioned. Dasenbrock (2010) presented such a study for the SAA device, but to the best of the PI's knowledge, a similar study had not been conducted for the INC500.

Where drilled, FDL-A was fairly homogeneous, mostly consisting of silty sand with gravel. The boring in which the INC500 was installed intercepted white mica schist bedrock at 86.5 ft bgs (see Appendix D for the boring log and installation photographs). To reach the total depth required, we combined modules used both at the Rich113 and CDS locations; thus this was the second installation for these modules. We installed the device to 100 ft bgs (see Figures D-3 and D-4). Because of the casing length and the overall length of the connected modules, approximately 1.5 ft of the uppermost INC500 module was above the ground surface within the casing. During the installation, some of the plastic couplers cracked, and a few threaded inserts popped out of the couplers and could not be pulled back by tightening the screw (see Figure D-5). All of these components were installed previously for up to 17 months in a cold propylene glycol-water mixture, which may have affected the plastic, causing it to become brittle. Otherwise, as this was the fourth time that the PI had installed this device (with an extra retrieval and installation at the Rich113 site), the installation proceeded relatively quickly, with two people completing the installation in about an hour. In addition to the M-IPI, we attached two

VW piezometers and a thermistor string to the outside of the casing in TH12-9004. We backfilled the casing using cement-bentonite grout (see Figure D-2). All of these instruments were wired into an ADAS, which was powered from a battery bank recharged by a solar panel (see Figures D-6 and D-7). A data logger recorded measurements every six hours. Details on the instrument's performance at the FDL-A site are provided in Chapter 3.

CHAPTER 3

FINDINGS

RICH 113

M-IPI Analysis

For spatial reference of the measured locations, Figure 4 is a photograph of the casing locations relative to each other and the bluff edge. Figure 5a and b are plots of cumulative displacement obtained from the three instruments. The readings collected with the traditional inclinometer probe (shown as green diamonds and labeled with the prefix "SI" in each figure) indicate movement occurring at approximately 55 ft bgs, with between 0.5 and 0.6 in. of cumulative displacement within the analyzed time frame. Although small, this movement is consistent in depth and character with that previously recorded for this site.

We installed the INC500 inside a guide casing within the boring TH09-1511 (see Figure 4). When we extracted the M-IPI device, we measured the casing with the inclinometer probe for comparison. Thus, the cumulative displacements from the INC500 and the inclinometer probe shown in Figure 5a are directly comparable. Visual analysis indicates that the two sets of readings are very similar, with a maximum difference in readings of 6.89×10^{-2} in. Readings from equivalent depths for these two instruments are plotted in Figure 5c. The solid red line at 45° indicates a 1:1 relationship. For each pair of readings, the precision (or repeatability) of the inclinometer probe and INC500 is shown as horizontal or vertical whiskers, respectively. Examination of the measurement pairs indicates that each point lies within the precision of the inclinometer probe device; thus, the readings cannot be differentiated from each other.

We installed the SAA within the two concentric casings in boring TH09-1512. Because of the inner 1.05-in. dia. PVC casing required for the SAA installation, we were unable to make direct comparisons with inclinometer probe readings from the same casing. Instead, Figure 5b contains inclinometer probe measurements of TH07-1711, another boring approximately 4 ft away (see Figure 4). Between 67 and 70 ft, the SAA readings indicate no cumulative displacement. Although 10-20 ft of installation within a stable stratum is recommended (Cornforth, 2005; Dunnicliff, 1993), these readings indicate that the bottom of the SAA was anchored into soil below the zone of movement. The inclinometer probe readings indicate no movement below 55 ft, whereas SAA readings demonstrate approximately 1.17×10^{-1} in. of cumulative displacement below this depth. Above this depth, visual analysis indicates similarity between the two sets of readings, with a maximum difference of 8.7×10^{-2} in. occurring at approximately 47 ft bgs. Readings from equivalent depths for the SAA and inclinometer probe are plotted in Figure 5d, also shown with a red line indicating a 1:1 relationship and pairs of whiskers representing the precision of each instrument. A cluster of points near the origin and another for the largest readings deviate from the 1:1 relationship by more than the precision of the inclinometer probe. Rather than assuming this deviation from the inclinometer readings is due to inaccuracy, other possibilities must be considered. The sets of readings are from two different casings. Although close to each other, it is possible that the soil is deforming slightly differently between these two locations. Additionally, the inner casing may have shifted within the sand backfill after installation, despite the careful tamping of the sand. Otherwise, there is close agreement

Figure 4. Relative locations of the measured casings at Rich113. Vertical arrows are labeled with the test hole identifiers. The edge of the bluff overlooking the Copper River is immediately beyond the spruce trees behind the installations, and the Richardson Highway is behind the photographer. (Photograph by M. Darrow)

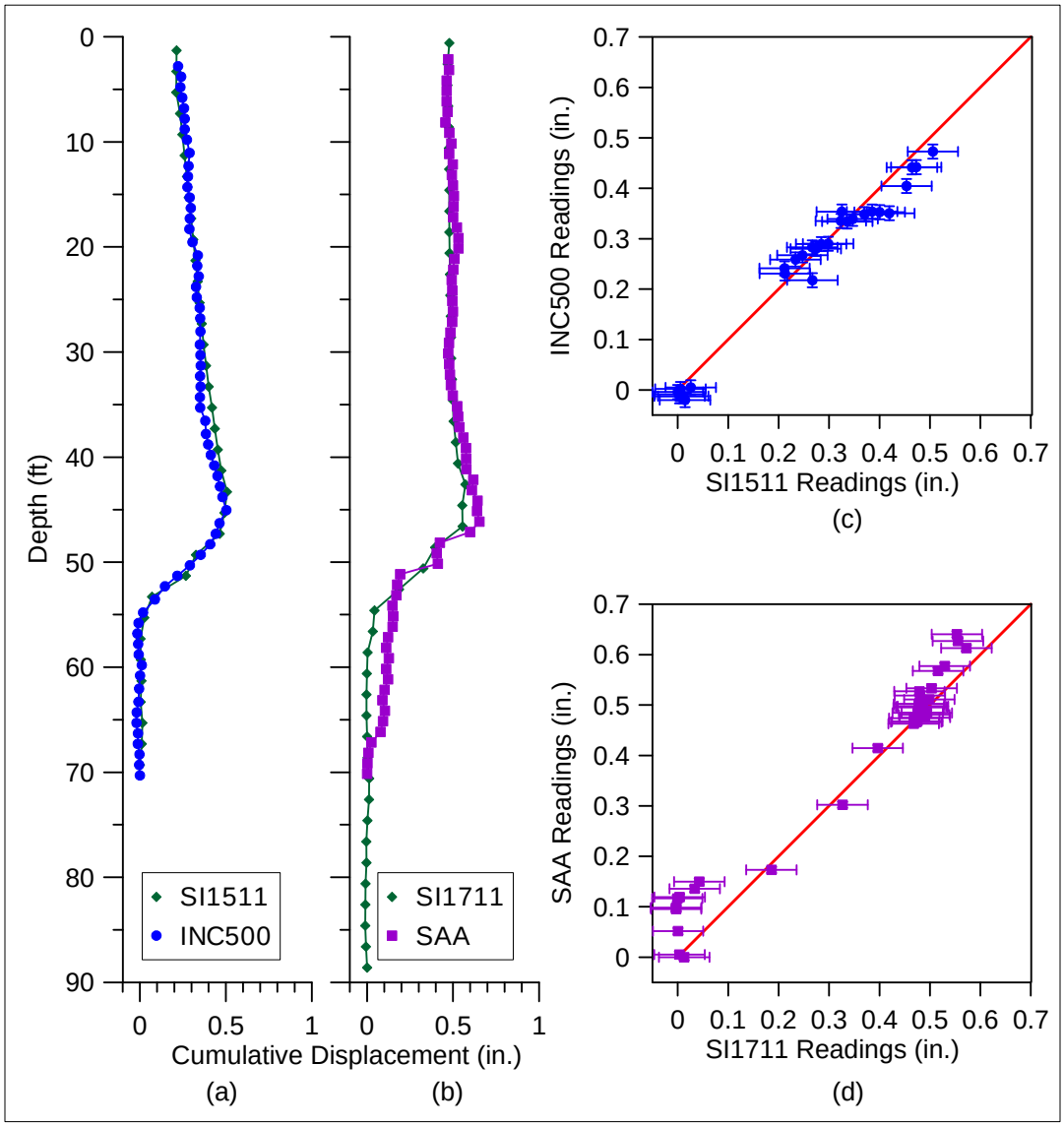

Figure 5. Selected measurements and analysis from the Rich113 site. (a) Readings from the INC500 and inclinometer probe for a single installation (TH09-1511); (b) Readings from the SAA and inclinometer probe for two adjacent installations (TH09-1512 and TH07-1711, respectively); (c) Comparison of INC500 and inclinometer probe measurements shown in (a); (d) Comparison of SAA and inclinometer probe measurements shown in (b).

between the readings of the two devices, and overall there is good agreement in the amount of total deformation recorded.

Temperature Analysis

The temperature measurements from the two M-IPI devices were compared against those collected from a thermistor string, which was installed in a second 1-in. dia. casing within TH09-1512. Each thermistor bead within the string has a reported accuracy of ±0.2ºF (Measurement Specialties, 2008), and the entire string was calibrated in an ice bath. Thermistor measurements were recorded at 8-ft intervals along the length of the string, with the exception of the thermistor at 41.1 ft bgs, which ceased to report data after the installation (see Figure 6a). Since the temperature sensors in the INC500 and SAA were not positioned at the exact same depths as the thermistor beads, readings from the two nearest sensors above and below each thermistor bead were interpolated for the required thermistor depth. These are the values that are shown in Figure 6b for the INC500 and Figure 6c for the SAA. Data from three different days in 2010 are shown for each of the devices (see Figure 6a-c); each device measured the same temperature ±0.02ºF for the lowest two depths, indicating a consistent temperature within the permafrost and stability of each measurement device throughout the six months presented.

Next, the INC500 and SAA data were compared to the thermistor string data. Figure 6d, Figure 6e, and Figure 6f are plots of all three devices for June 1, August 1, and December 1, 2010, respectively. Each data point is plotted with horizontal whiskers indicating the reported accuracy of the sensor. Each cluster of measured temperatures falls within the ranges of accuracy for both instruments. On average for these three days, the INC500 and SAA sensors were within 0.41ºF and 0.39ºF of the thermistor measurements, respectively. While temperatures plotted with these devices are able to demonstrate the general trend of temperature with depth, this ~0.4ºF offset would make analysis of activity in the active layer or identification of the permafrost table problematic. This issue may be addressed by using an M-IPI device with calibrated temperature sensors.

TDR Analysis

We first attempted to read the coaxial cable serving as the TDR device in March 2010 during the installation of the M-IPI devices. Unfortunately, we were unable to obtain data as the cable reader unit did not function. We suspected that this was due to the effect of cold weather on the batteries, as they did not hold a charge well. We were successful in obtaining readings in July and September, 2010.

Figure 7a contains the results of the TDR measurements taken in July and September. The September readings shown were adjusted to eliminate the overall variation of impedance between the two data sets. The “lows” in impedance indicated by arrows represent the locations of the hose clamps that crimped the cable at 10-ft intervals; the “low” near the 30-ft depth is not as apparent as the others. There are no obvious additional “lows” to represent shearing of the TDR cable. Figure 7b is a plot of the difference in impedance between the September and July readings. The variation between these sets of readings appears to be random, and does not indicate any additional crimping of the cable that would suggest a shear zone. One of the noted limitations of the TDR method is that it is much less sensitive to bending than to shearing (O’Connor and Dowding, 1999). This may explain the apparent lack of movement measured

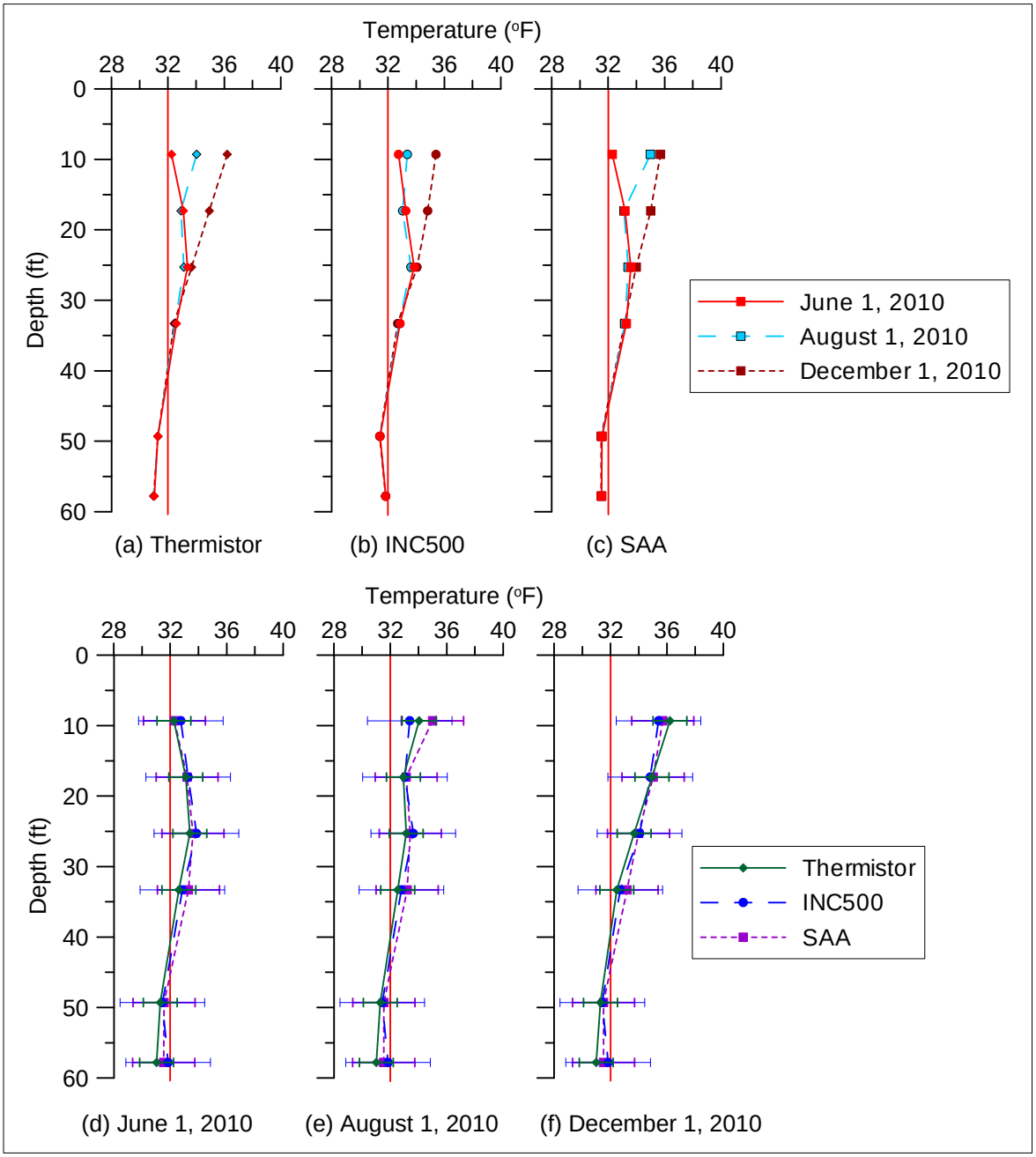

Figure 6. Comparison of measured temperatures. The graphs (a), (b), and (c) are measured temperatures from the thermistor string, INC500, and SAA devices, respectively. Data for three different days are shown for each device. The graphs in (d), (e), and (f) are comparisons of the measured data from all of the three instruments for June 1, 2010, August 1, 2010, and December 1, 2010, respectively.

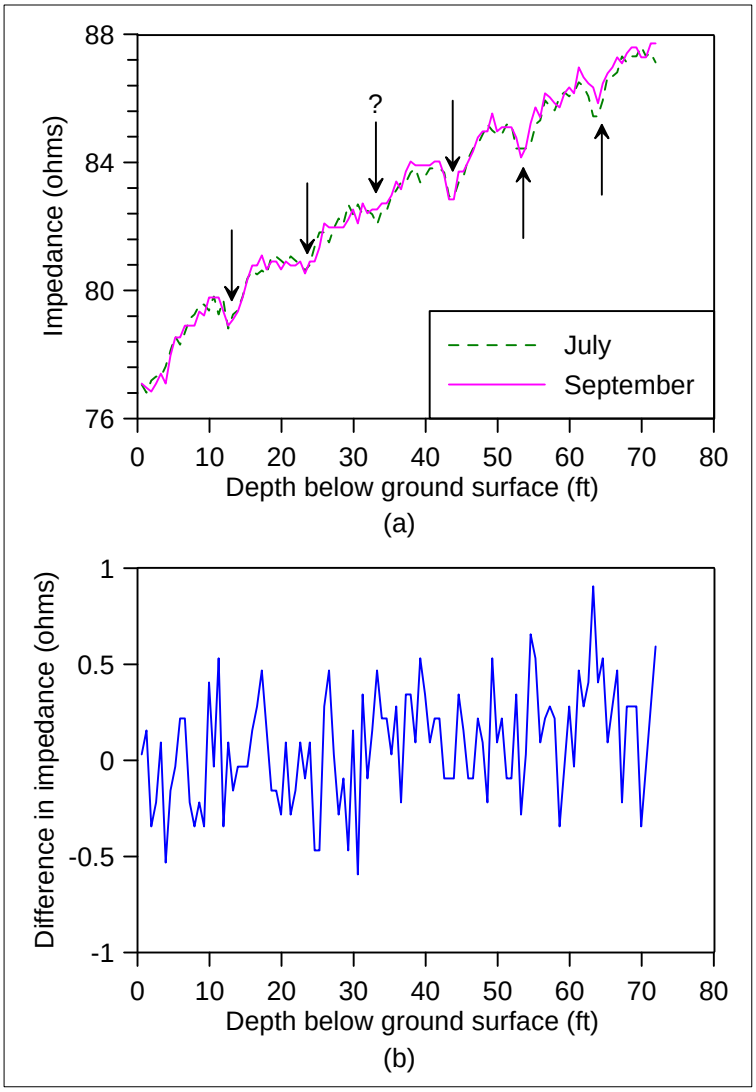

Figure 7. Measurements from the TDR cable. (a) Readings from July and September; the September readings were corrected to account for the overall difference in impedance from July. Impedance "lows" (indicated by arrows) indicate positions of the hose clamps (the "low" near 30 ft bgs is not as apparent). (b) Difference in impedance between the July and September readings.

using the TDR device at Rich113 since the creep movement is similar to bending. The TDR device also may not indicate the zone of movement at Rich113 due to the backfill method. Turner (2006) noted that a grout mix must be stiff enough to deform the coaxial cable when shearing. The dry sand backfill, although potentially frozen, may have been loose enough so as to provide space for the cable to move rather than crimping it.

CHITINA DUMP SLIDE

M-IPI Analysis

For spatial reference of the measured locations, Figure 8 is a photograph of the casing locations relative to each other. As a first step in analysis, inclinometer probe measurements were used to evaluate the effectiveness of tamping the sand backfill around the casing within the boring. Voids created by bridging within the loosely poured sand into the annular space in a boring often are evident in sagging of the casing within a few weeks after the initial installation. The data collected during the summer of 2010 was evaluated by assigning two different initial dates, June 17 (date of installation) and June 25 (one week later). Below the shear zone, these sets of readings differed by 0.03 in. at the most; thus, we considered any sagging of the casing as minor, and used June 17 as the initial reading for the rest of the analysis. Figure 9b contains all of the cumulative displacement measurements from 2010, which indicate a shear zone between 14.3 and 18.3 ft bgs and about 1.7 in. of movement over the three month measurement period.

Measurements obtained using the INC500 are presented in Figure 10. We "lifted" the device about 6 in. within the casing on July 30, 2010 to ensure that it was not binding in the casing. While this exercise indicated that retrieval of the device was still possible, it had an effect on the data, as the INC500 readings after the move were noticeably different (see Figure 10a). All subsequent data obtained from the INC500 was adjusted to account for the "lift". Figure 10b contains a comparison of the INC500 measurement of TH10-1552, the inclinometer probe measurement of TH10-1552 immediately after retrieval of the M-IPI device, and the inclinometer probe measurement of TH10-1551. All readings from the two casings compare well to each other, demonstrating about 1.7 in. of total movement. While the shear zone is well defined in Figure 10b, among the readings there is some variation on the exact depth of where it begins. For each set of readings, the bottom of the shear zone was identified; for the inclinometer probe readings of TH10-1551 and the INC500 readings of TH10-1552, the two closest depths bracketing the movement were averaged. The resulting depths are 17.3 ft bgs for TH10-1551 (inclinometer probe), and 17.5 ft bgs and 17.4 ft bgs for TH10-1552 (inclinometer probe and INC500, respectively). Overall there is a difference of 0.2 ft. As the casings were not surveyed and tied into a benchmark for absolute elevation, readings are relative to the ground surface. Thus, this difference in depth can be partially attributed to small changes in the ground surface elevation between the two casing locations. This, however, does not explain the difference between measurements from the same casing with different devices, as indicated by the comparison plot shown in Figure 10c. Instead, we must consider the geometry of the measurement device and the placement of the reading over the measurement interval. The inclinometer probe is 2-ft long and rigid. Additionally, the plotted depths were determined using the "auto-depth adjustment" setting within the software program. This means that the plotted point is placed at the depth of the upper set of wheels on the probe, rather than the depth

Figure 8. Relative locations of the measured casings and piezometer installation at the Chitina Dump Slide. Vertical arrows are labeled with the test hole identifiers; the installations were located on a drill bench downhill of the roadway embankment. This photograph was taken from the McCarthy Road embankment looking east towards the Copper River. (Photograph by M. Darrow)

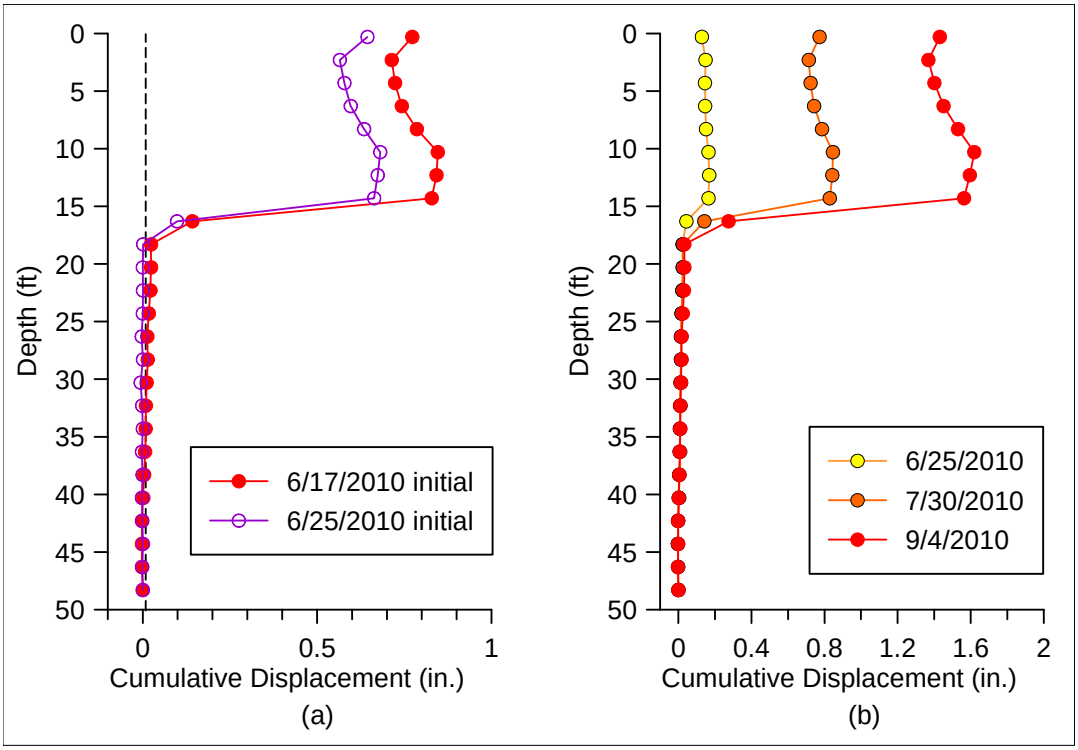

Figure 9. Cumulative displacement measurements from the inclinometer probe for TH10-1551. (a) Evaluation of slump of the casing within the tamped sand backfill using two different start dates (note the enlarged horizontal scale for better resolution); (b) all cumulative displacement measurements from 2010.

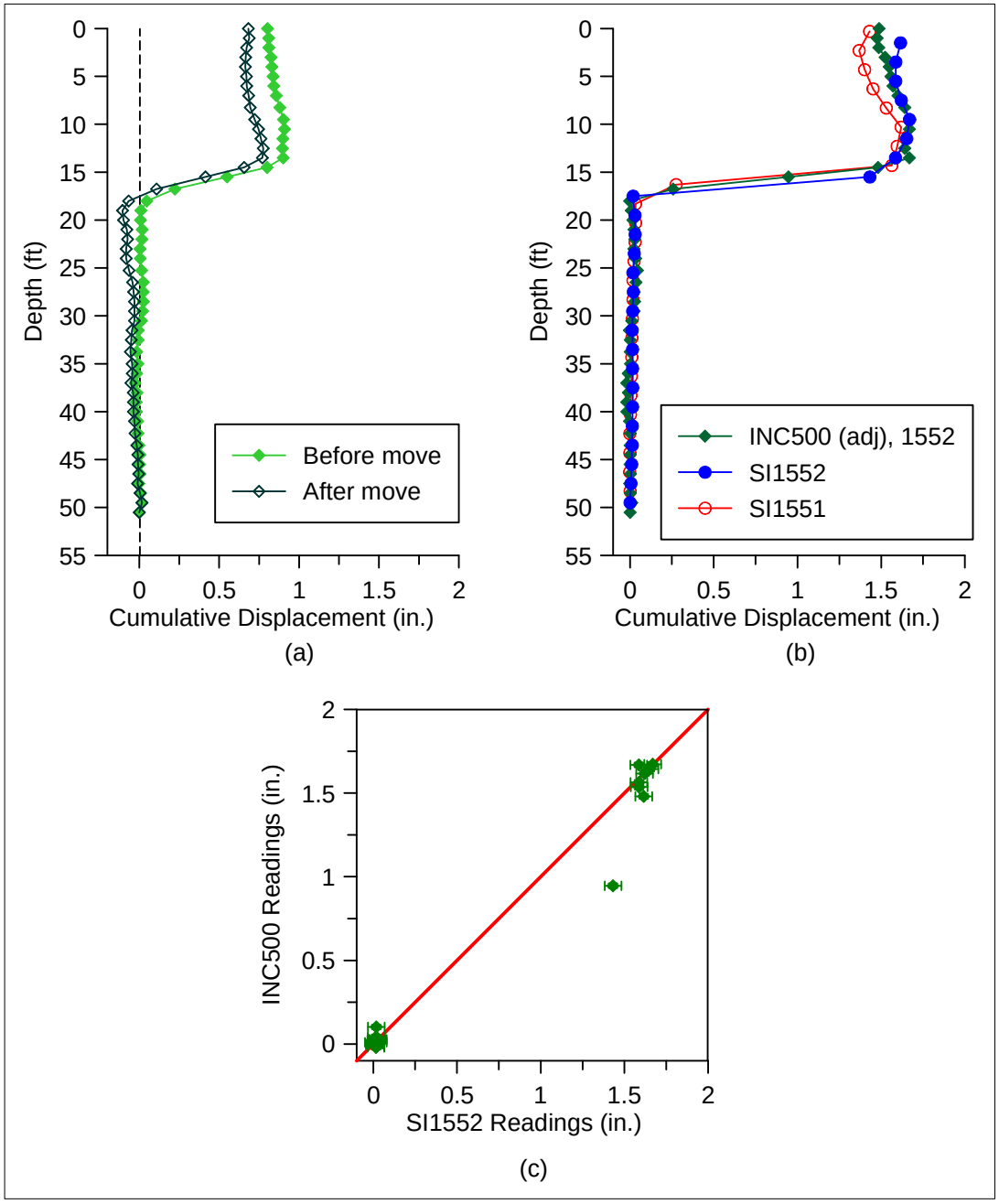

Figure 10. Selected measurements and analysis from the Chitina Dump Slide site. (a) Evaluation of the effects of "lifting" the INC500 device on July 30, 2010; (b) Readings from the inclinometer probe for two adjacent installations (TH10-1551 and TH10-1552) and adjusted readings from the INC500 for TH10-1552; (c) Comparison of INC500 and inclinometer probe measurements shown in (b).

indicated by the cable length. The INC500 is a more flexible device, with measurements taken at 1-ft to 1.25-ft intervals (depending on where modules are connected) along its length. This higher frequency of measurements may better constrain the sliding surface.

TDR Analysis

Figure 11a contains the results of the TDR measurements taken in June, July, and September 2010. The latter two sets of readings were adjusted to eliminate the overall variation of impedance. The "lows" in impedance indicated by arrows represent the locations of the hose clamps that crimped the cable at 10-ft intervals. As with the TDR at the Rich113 location, there are no obvious additional "lows" to represent shearing of the TDR cable. Figure 11b is a plot of the difference in impedance between the June and July, and June and September sets of readings. The variation between these sets of readings appears to be random, and thus does not indicate any additional crimping of the cable that would suggest a shear zone. Although there was more movement during the measurement period at CDS than at Rich113, the backfill method was the same. The dry sand backfill, although potentially frozen, may be loose enough so as to provide space for the cable to move rather than crimping it.

Water Pressure and Temperature Analysis

The data collected from the VW piezometer at 15.8 ft bgs in TH10-1553 is presented in Figure 12. In addition to water pressure, the device recorded temperature via a thermistor that had an accuracy of ±0.9ºF. The VW piezometer indicated a steady decrease in water pressure over the measurement period. This trend may reflect the loss of water from the cement-bentonite grout. The measured temperatures demonstrated an unusual trend, with an initial decrease in temperature followed by a steady rise. Additionally, all of the reported temperatures were below freezing, which is not supported by the observations made during drilling. The reasons for this trend are not known at this time. A longer data set, which may have helped to explain the observations, was not possible given the removal of the ADAS in September 2010.

Figure 13 contains plots of temperatures from the INC500 for four days during the measurement period. The first data set from June 18 demonstrates the heat effects from drilling, which quickly dissipated. Temperatures below 22 ft reached a pseudo-equilibrium by July 1 and changed very little during the remaining measurement period, with an average temperature of 35.8ºF. This average temperature corresponds well to those measured during drilling. Although the sensors were not calibrated, the INC500 temperature measurements supported the field observations and alerted us to the unusual behavior of the temperature sensor in the VW piezometer.

LOST CHICKEN SITE

M-IPI Analysis

Figure 15 contains plots of the cumulative displacement for the inclinometer probe and SAA device for all of the six days of manual measurements (i.e., 7/23, 8/6, 8/20, 9/1, 9/14, and 10/6) following the initial installation, and Figure 15 contains plots comparing readings from these two instruments for each of the six manual measurement days. The software for each of these devices calculates vertical displacement relative to one fixed end that is assumed not to move; for Figure 15, this is the near end. The data were exported from the software for each instrument and plotted together using Origin Pro spreadsheet software. Since the SAA did not extend across

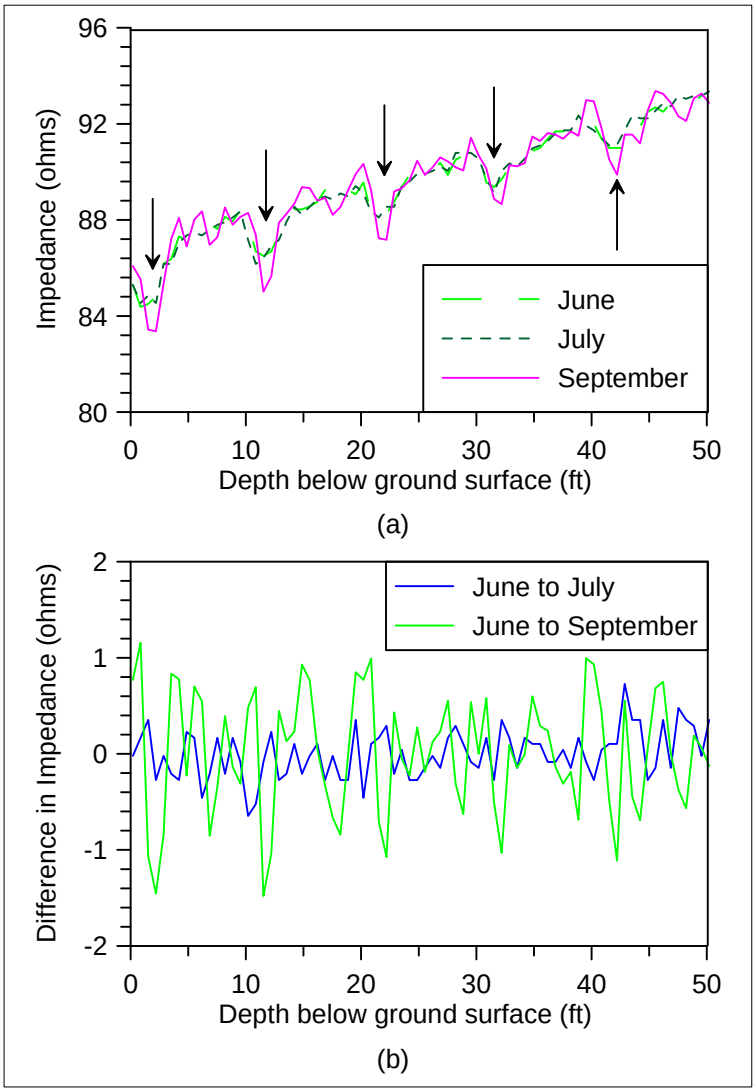

Figure 11. Measurements from the TDR cable. (a) Readings from June, July, and September 2010; the July and September readings were corrected to account for the overall difference in impedance from June. Impedance "lows" (indicated by arrows) indicate positions of the hose clamps. (b) Difference in impedance between June and July and June and September readings.

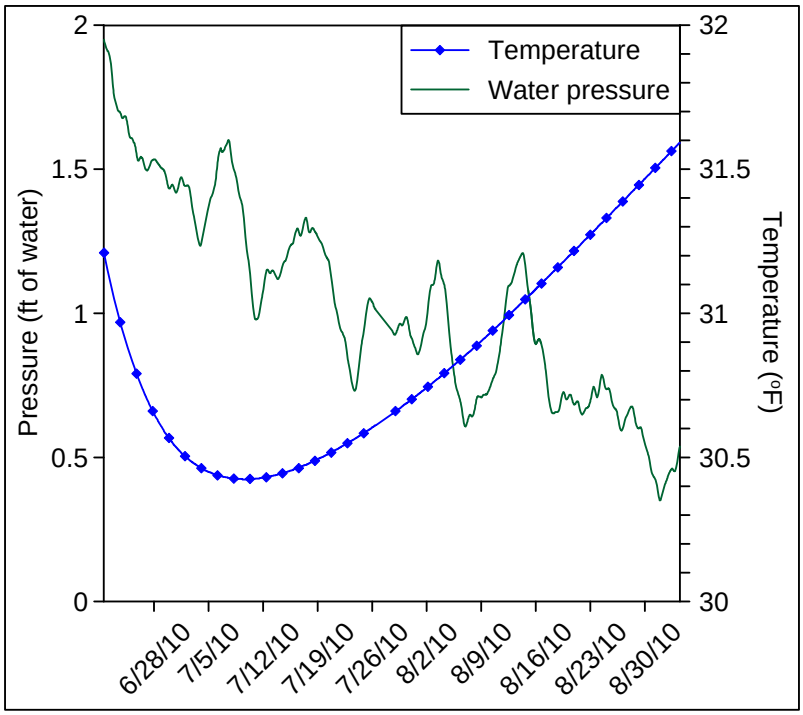

Figure 12. Data from the vibrating wire piezometer. In addition to water pressure, the device reports temperature with a thermistor that has ±0.9°F accuracy.

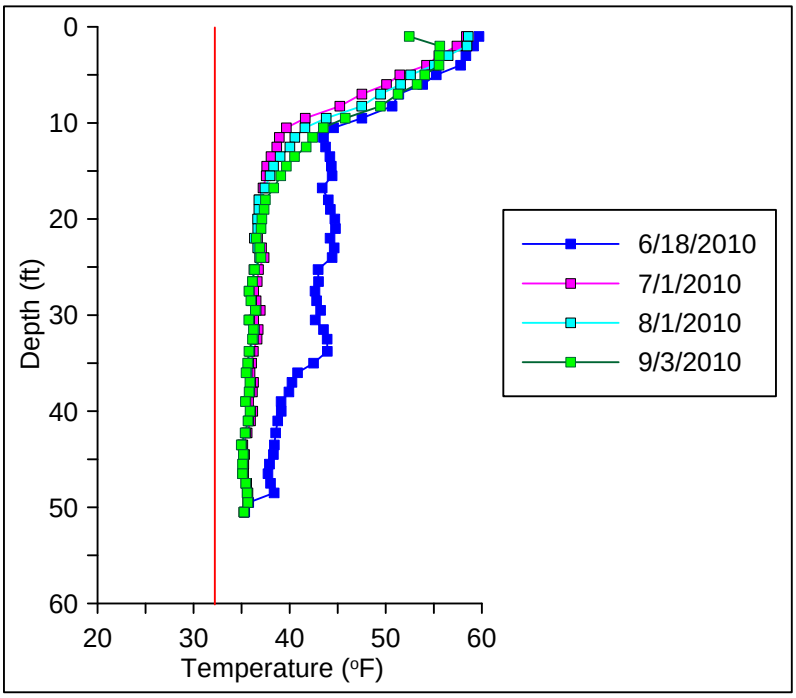

Figure 13. Temperature readings from the INC500 device installed within TH10-1552. The phase-change temperature is indicated by the vertical red line.

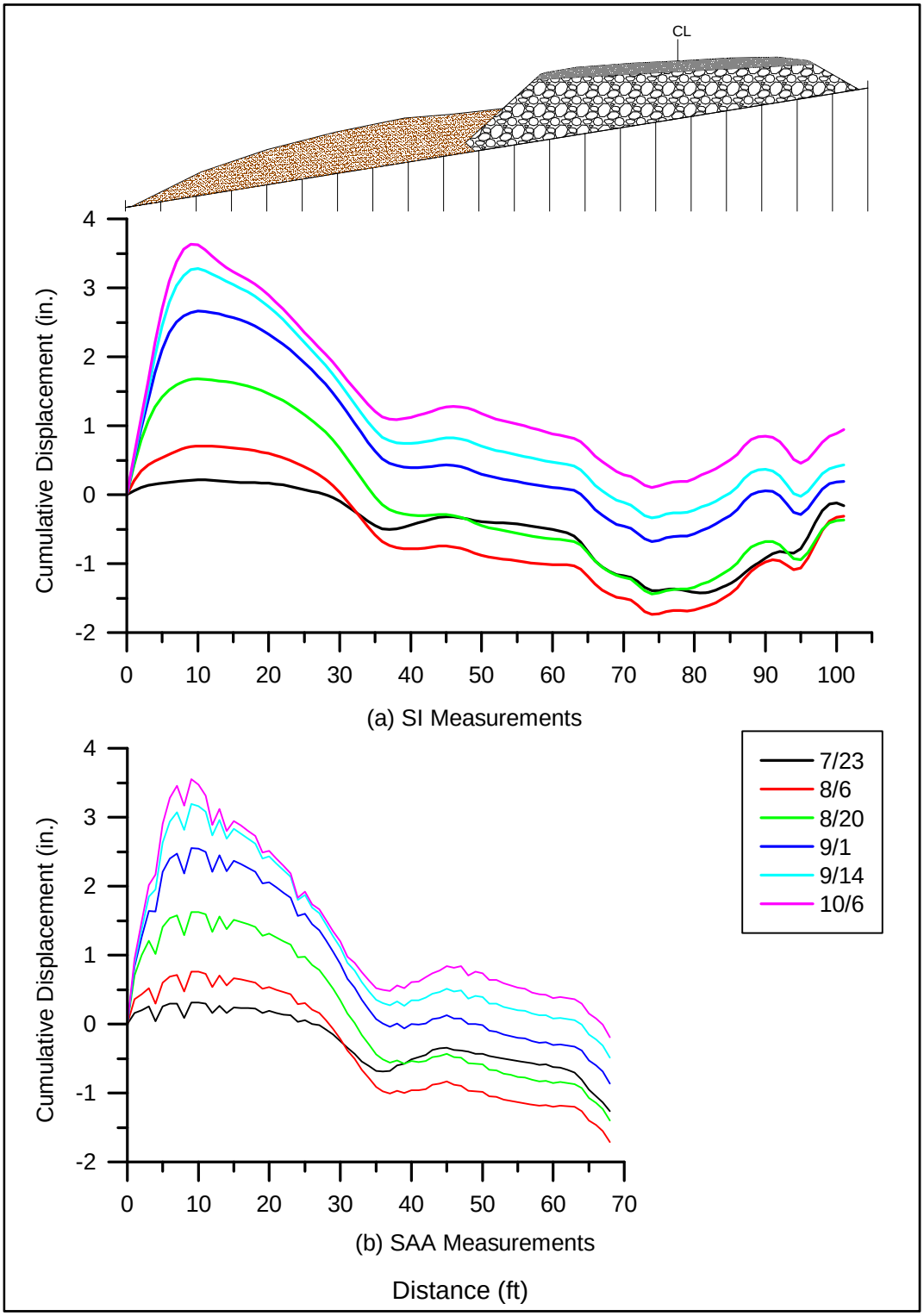

Figure 14. Uncorrected cumulative displacement measurements with time. (a) Inclinometer probe measurements, and (b) SAA measurements. Both reference the near end.

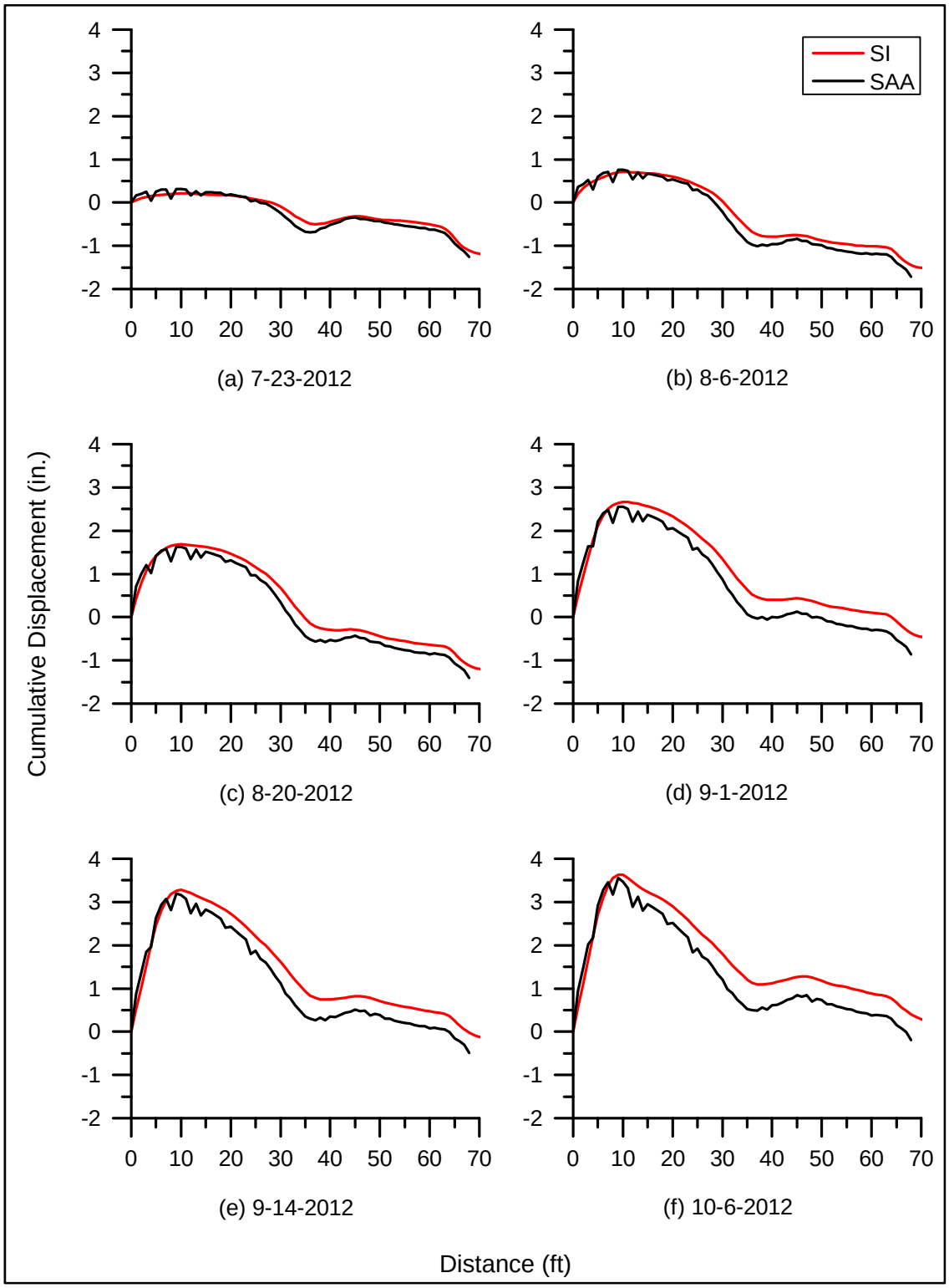

Figure 15. Comparison of SAA and inclinometer probe performance using the uncorrected data referenced to the near casing end.

the entire embankment width, readings from this device were limited to the interval from 0 to 68 ft. Measurements from both instruments suggest that the bottom of the embankment is rising over time. This is erroneous as the embankment should move only downwards due to post-construction settlement during the summer months (some upward movement could occur as a result of frost heaving during sub-freezing temperatures). As displayed in Figure 15, both instruments demonstrate the same trend in displacement; however, the difference in cumulative displacement recorded by each instrument increases slightly over time with a maximum difference of 0.69 in. This difference may be due to differential settlement of the near end of each casing.

As neither software program corrected for the downward movement of the fixed casing end at the time the SAA was purchased for this project (newer versions of the software account for change in elevation), the exported data was adjusted manually in a spreadsheet in order to determine the actual settlement. We made some assumptions before performing these calculations: 1) All movement of the embankment occurred vertically and only downward due to soil consolidation and thaw settlement during the measurement period. 2) As no point along the casing was moving upwards, then any upward displacement recorded by the instruments was due solely to the downward movement of the casing end. The only way any point along the casing length could move upwards is if the casing end was moving downwards at a faster rate. 3) Therefore, if any point along the casing was not moving or at least moving downward at a slower rate than the casing end, then the downward movement of the casing from one reading to the next was referenced to that particular point. There are errors inherent in these assumptions. For example, error may occur if the points that appeared to be moving up were actually moving down; however, the amount of error is dependent on the rate at which the point was moving relative to the casing end. Using these assumptions, the greatest error would occur when the rate of downward movement at points along the casing approached the same rate of downward movement as the casing end.

We applied these assumptions to correct the measured cumulative displacement. In a spreadsheet, the difference in cumulative displacement was taken for each pair of consecutive readings for each point along the casing, and the maximum positive difference was identified. If there was no positive value, we assumed that the casing end did not move and that all points were moving down relative to the casing end; however, this did not occur for this measurement period. Once the maximum positive difference was identified, the incremental displacement was added to the readings from the first day, and the maximum positive displacement was subtracted. This is summarized by Equation 1:

$$CD_{final} = CD_{T_1} + \left(CD_{T_2} - CD_{T_1}\right) - MAX\left(CD_{T_2} - CD_{T_1}\right) \quad \text{Eqn. 1}$$

where *CD* indicates cumulative displacement, and the subscripts *final*, T_1, and T_2 represent the corrected value, time of first reading, and time of second reading, respectively. Figure 16 is a comparison of the corrected data, which illustrates slightly better agreement between sets of readings from the two devices, with 0.61 in. as the greatest difference between pairs of readings. Regardless, it is evident that both instruments reveal nearly identical changes in deformation over time. Figure 17 contains two plots of corrected SAA data, using both a biweekly and daily time difference between pairs of readings. Calculating differences in cumulative displacement between daily readings results in greater overall settlement.

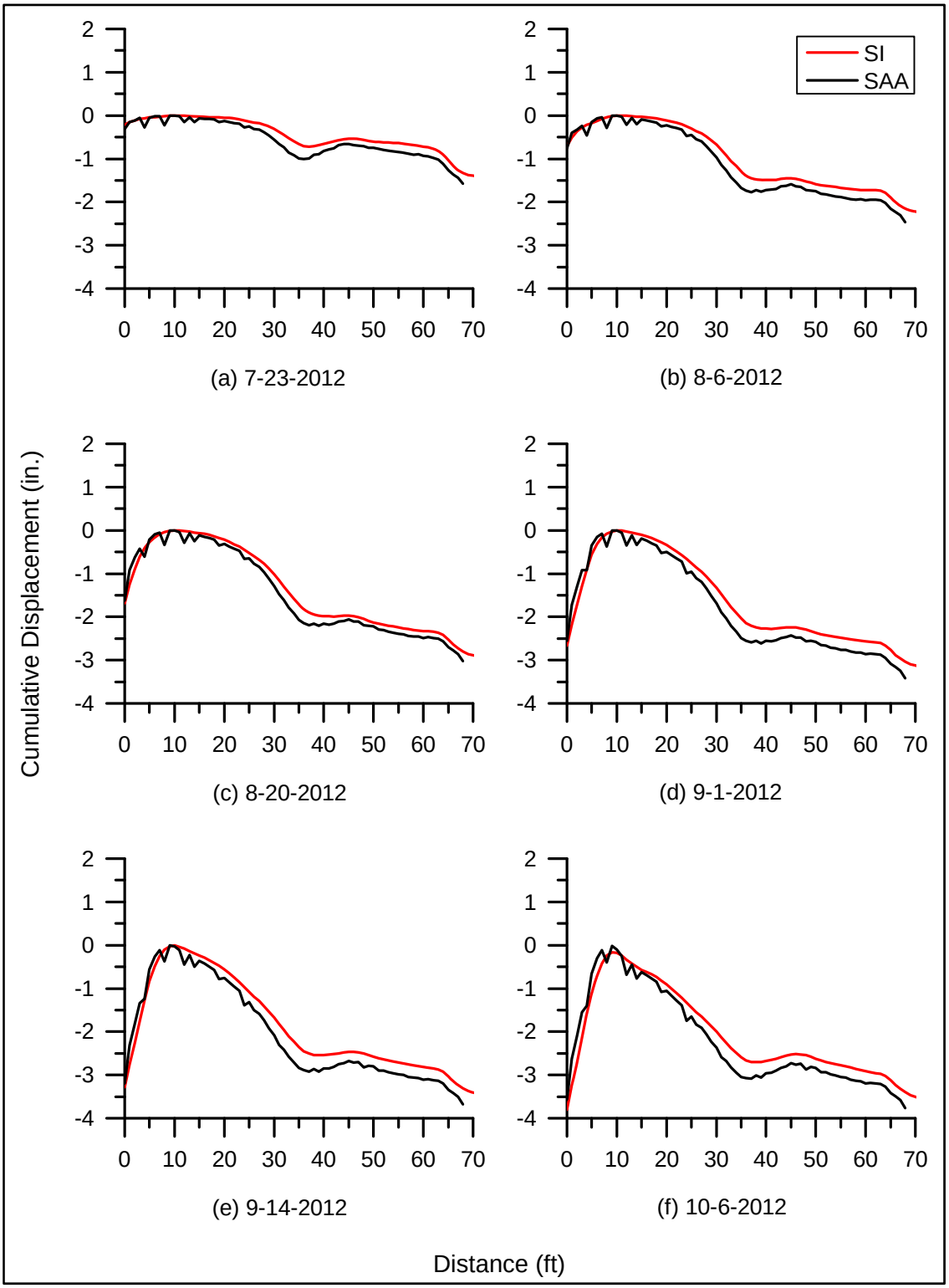

Figure 16. Comparison of SAA and inclinometer probe performance using corrected data (referencing the near end). The SAA data in (d), (e), and (f) have been adjusted to account for differential settlement of the near end of the casing.

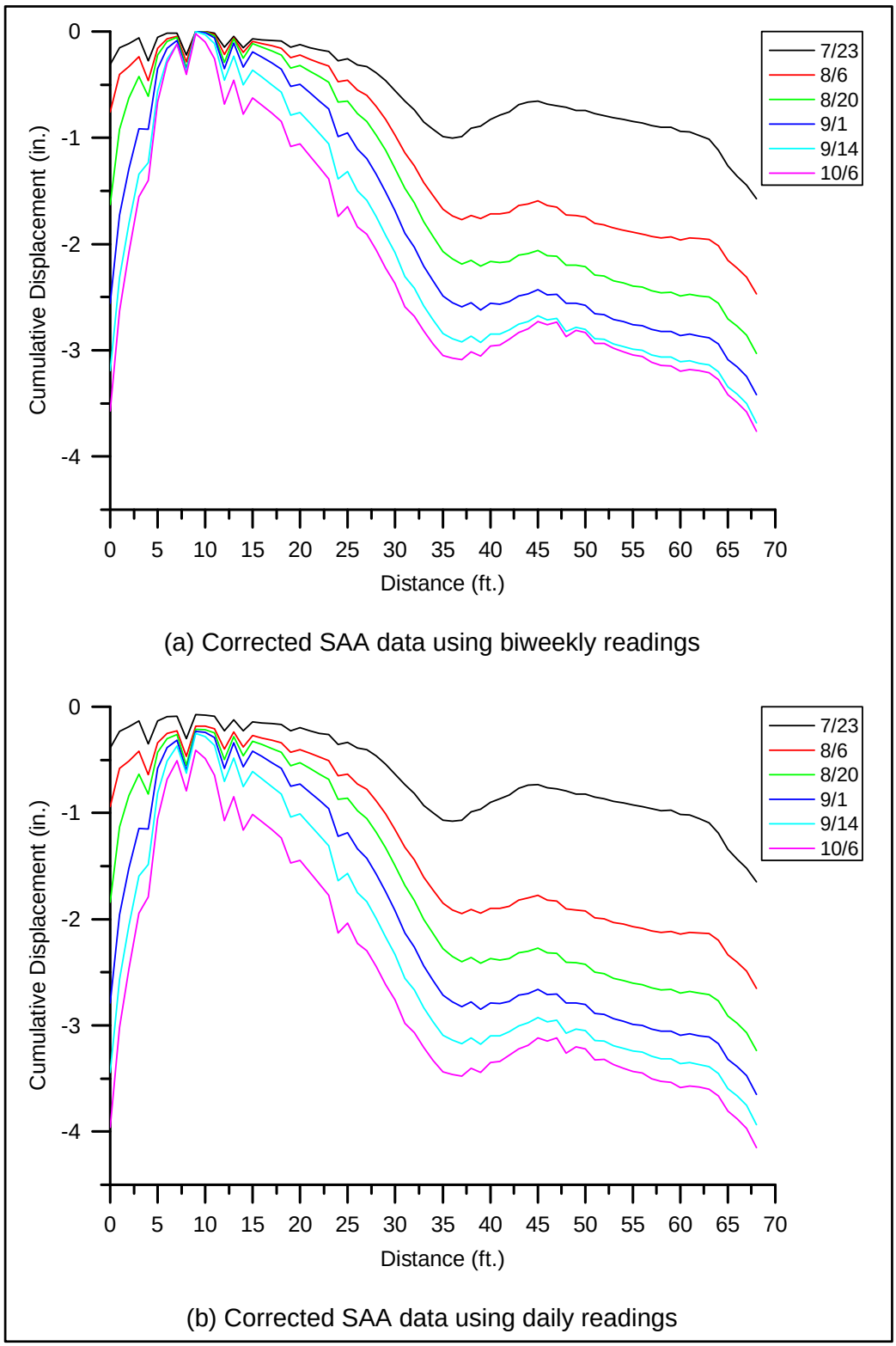

Figure 17. Corrected SAA data. These data were adjusted by (a) comparing biweekly measurements and (b) daily measurements. Data are shown for dates corresponding to manual inclinometer probe measurements.

The most effective and precise way to determine overall settlement is to survey the casing ends immediately after installation and during each measurement with the inclinometer probe. Due to equipment and scheduling issues, we were only able to obtain reliable survey data for August 20 and October 6. Between these two dates, the survey data indicated that the near end of the casing settled 3.85 in., and the far end settled 3.31 in. We adjusted the inclinometer probe and SAA data starting on August 20 to account for the surveyed settlement; these final data are shown in Figure 18. Correcting the data using this combination of methods yields an overall settlement of approximately 5.5 in. over the measurement period, with the greatest settlement at the toe of the thermal berm and under the ACE near the embankment centerline. It must be stressed, however, that this value is an underestimate of the total settlement, as it does not include settlement that occurred prior to August 20.

Finally, as with the vertical inclinometer probe, the horizontal inclinometer probe must be checked for "drift" or systematic errors. We attempted to check for drift by comparing survey data of the casing ends to measurements obtained using the inclinometer probe for a given set of readings. Figure 19 illustrates the results of this comparison for the initial reading of the casing in the field on July 11. While we could not use the July 11 survey data for the overall settlement analysis (as we were missing essential data for absolute elevation calculations), we were able to use the data for the analysis of relative elevation. The total inclinometer probe casing length was 105.16 ft from end to end. For each set of measurements, we took inclinometer readings from 1.5 ft to 102.5 ft (as measured from the near end of the casing). These start/stop points were selected due to the length of the probe and cable limitations associated with the dead end pulley. The ends of the casing were surveyed, creating gaps (1.5 ft at the near end and 2.66 ft at the far end) between the inclinometer probe measurements and the surveyed ends, as illustrated in Figure 19. We extrapolated the inclinometer probe readings to the casing ends. Comparison of the extrapolated cumulative deviation data to the survey data indicates a maximum difference of 0.14 in. between these two measurement methods. After this initial measurement, enough settlement of the casing ends occurred that made checking instrument drift impossible using this method. Despite these limitations, the similarity of the data trends shown in Figure 16 suggests stable readings. Future sets of readings should be examined for increasing separation between data sets from different instruments, which could suggest instrument drift.

Temperature Analysis

Figure 20 is a comparison of the temperature measurements from the thermistor string, SAA device, and TAC device for August 1, September 1, and October 1, 2012. The thermistor and SAA data points include "whisker plots" indicating the range of accuracy, which is $\pm 0.2^{o}$F and $\pm 2.2^{o}$F, respectively. Not shown with whiskers, the accuracy of the TAC sensors is ±0.18ºF. Prior to this installation, we recalibrated the thermistor cable in an ice bath, which indicated that some of the thermistors had failed. These sensors are not shown in Figure 20. On average, temperatures measured by the thermistor string and the TAC differ by ±0.3ºF, and the temperatures measured by the thermistor string and the SAA differ by ±0.4ºF. Considering the accuracy for all of the devices, these temperature measurements are comparable.

Figure 21 is a 2-dimensional contour plot of temperature versus time as measured by the thermistor string. The sensors are located beneath the embankment at 22, 30, 38, 46, 54, 70, and 79 ft from the downslope toe. Measurements were recorded hourly and averaged daily.

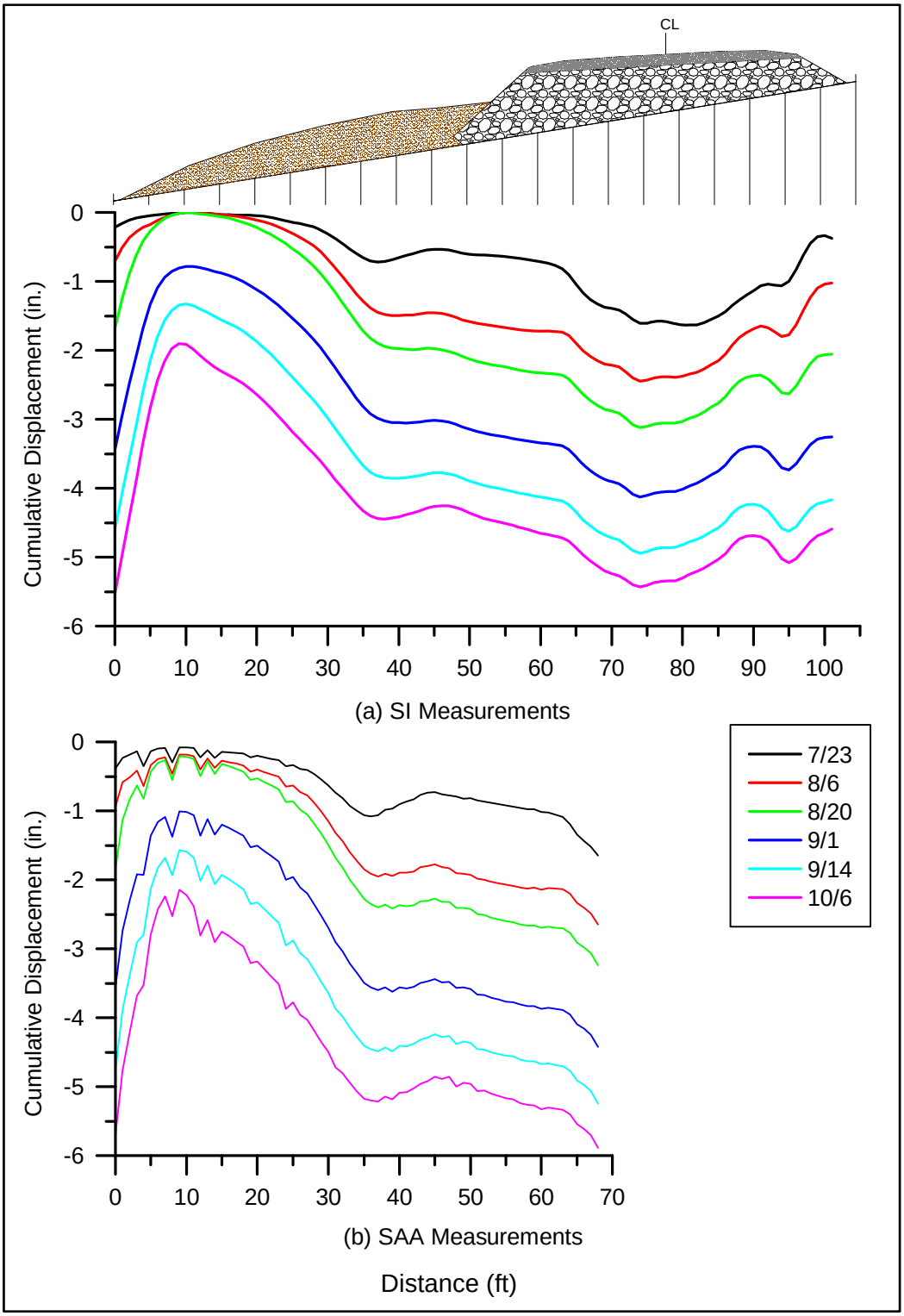

Figure 18. Estimated embankment settlement based on (a) corrected inclinometer probe and (b) SAA data, and survey data from August 20 and October 6.

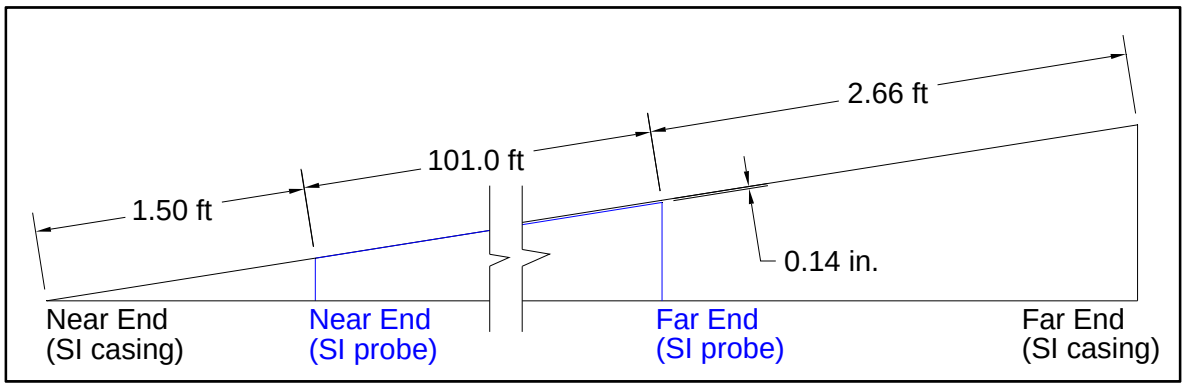

Figure 19. Comparison of casing orientation as measured by the inclinometer probe and based on survey data. Measurements were collected on July 11, 2012.

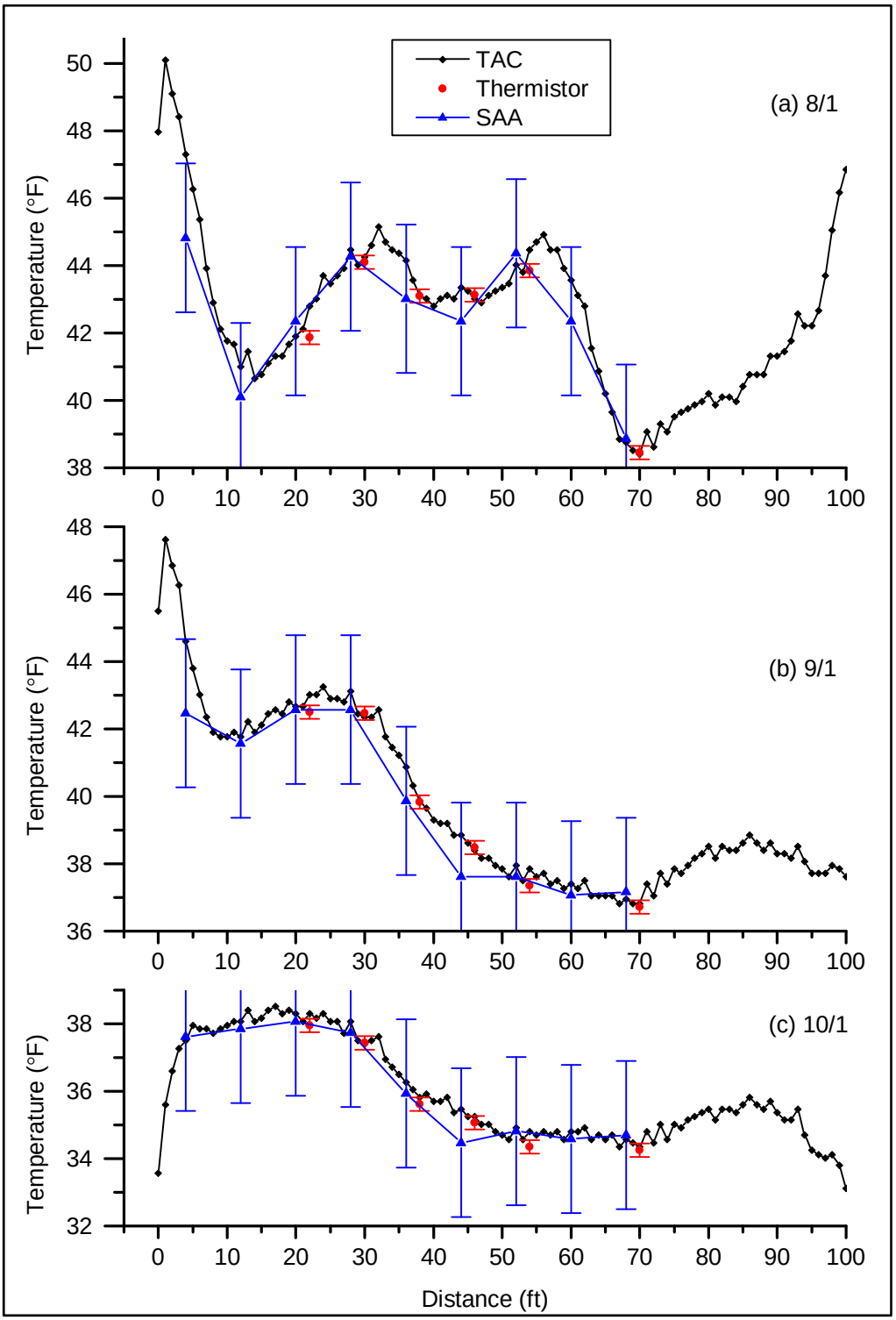

Figure 20. Comparison of temperature measurements beneath the Lost Chicken embankment. (a) Readings from August 1; (b) Readings from September 1; and (c) Readings from October 1. "Whiskers" illustrate the accuracy of the thermistors (±0.2ºF) and the SAA temperature sensors (±2.2ºF); the accuracy of the TAC sensors is ±0.18ºF, although no whiskers are shown.

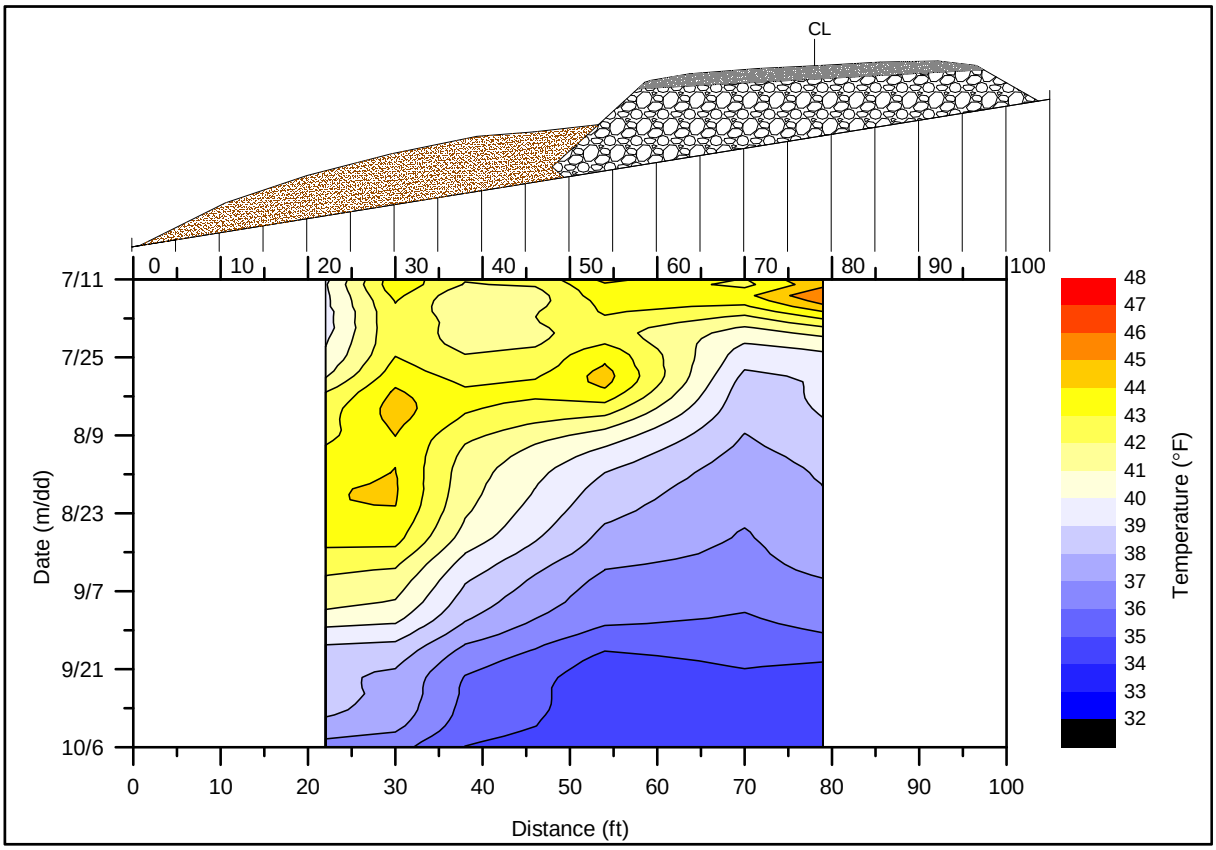

Figure 21. 2-Dimensional plot of temperature versus time measured by the thermistor string. Data presented is from July 11 to October 6, and a schematic of the final placement of thermal berm (left) and ACE (right) is provide for reference.

Figure 22, another 2-dimensional plot, represents the temperatures versus time measured by the SAA device. For the SAA, temperature sensors are located every 8 ft between 4 and 68 ft from the downslope toe, a spacing which provides greater resolution of temperature measurements. Temperatures were recorded once every 24 hours with this device. Finally, Figure 23 is a 2-dimensional plot of temperature versus time as measured by the TAC device. This device has a temperature sensor located every foot from 0 to 100 ft, which provides exceptional resolution of temperature measurements. Temperatures were recorded every 12 hours with the TAC device. As a function of the instrument spacing and overall length, the TAC device produced the highest resolution temperature plot and the most spatial coverage; however, where these different strings of sensors overlap, all three data sets demonstrate similar trends. There was a distinct difference in the rate of cooling between the thermal berm and the ACE during the measurement period. On October 6, the temperature beneath the thermal berm was approximately 37-38ºF, whereas the temperature beneath the ACE was approximately 34-35 ºF. Very apparent in Figure 23, and to a lesser extent in Figure 22, is the noticeable temperature fluctuation present near the embankment toes. These sensors are experiencing a greater impact from short term variations in air temperature due to less material covering the casings.

Figure 24 is a comparison of the measured average daily air temperature at the Lost Chicken location and the historical average daily air temperature from the National Climatic Data Center (NCDC). The historical climate data measured at nearby Chicken were obtained online from Golden Gate Weather Services (http://ggweather.com/normals/daily_AK.html). The dataset covers the period from 1981 to 2010. The measured temperatures at the site follow the same trend as the historical temperatures. In addition to air temperature sensors, we placed several CS109 temperature sensors on different surfaces to measure surface temperatures throughout the year. One sensor was placed just at the surface of the moss in an undisturbed area. Another sensor was placed at the toe of the thermal berm and left exposed at the surface, and the final sensor was installed level with the ground surface on the top of the thermal berm near the toe of the ACE. Figure 25 contains plots from each of these sensors, indicating that the measured surface temperatures and air temperatures are similar throughout the summer. The plots begin to differ after the first snowfall around September 30, when the ground surface temperatures remain fairly constant at 31.9ºF, while the air temperature continues to fluctuate. These data will be used in future thermal modeling of the Lost Chicken embankment.

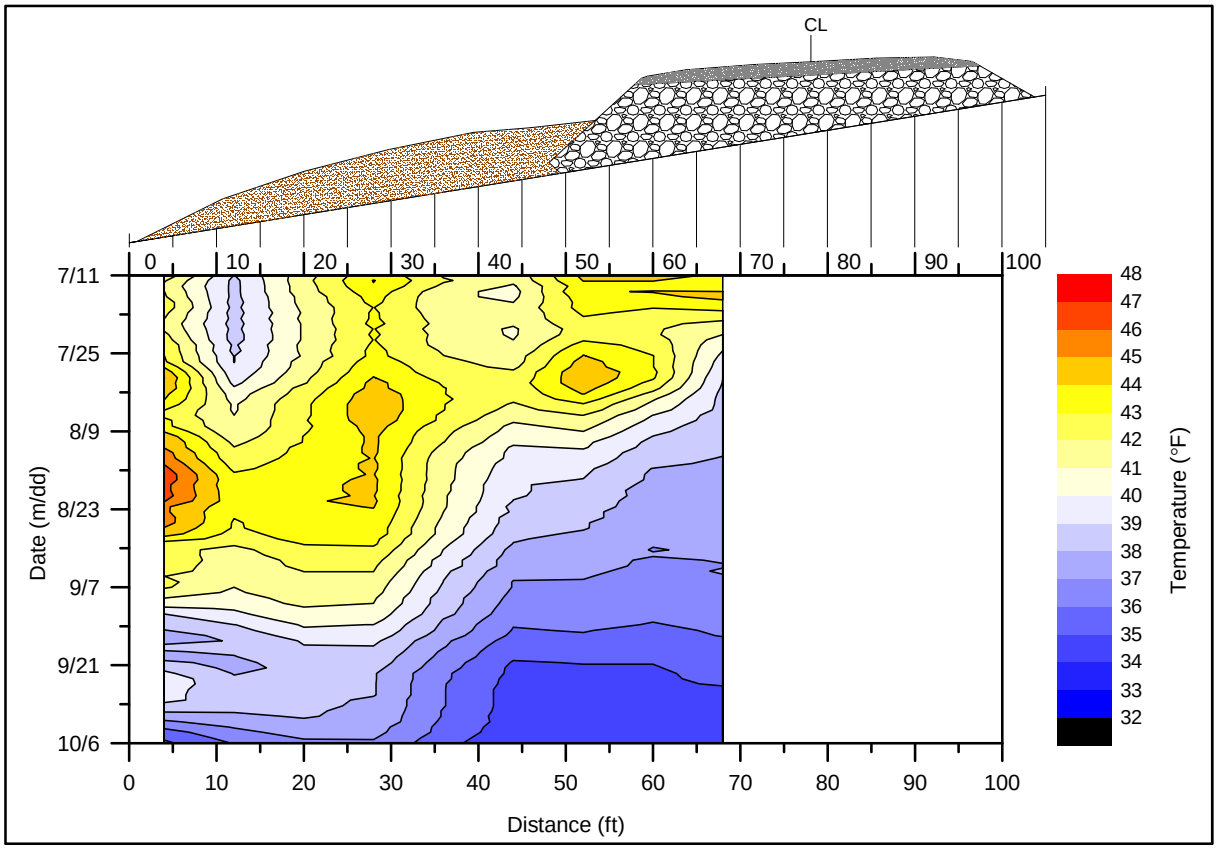

Figure 22. 2-Dimensional plot of temperatures versus time measured by the SAA device. Data presented is from July 11 to October 6, and a schematic of the final placement of thermal berm (left) and ACE (right) is provide for reference.

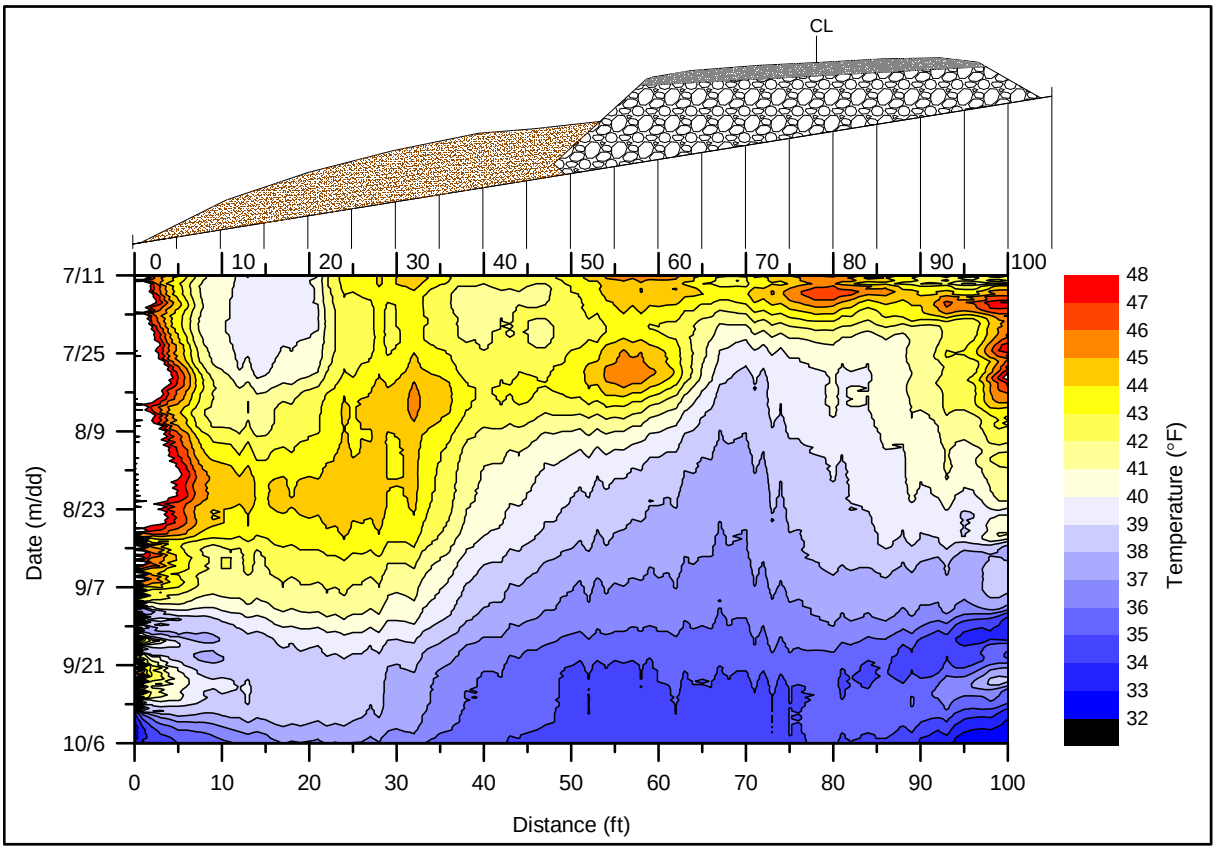

Figure 23. 2-Dimensional plot of temperature versus time measured by the TAC device. Data presented is from July 11 to October 6, and a schematic of the final placement of thermal berm (left) and ACE (right) is provide for reference.

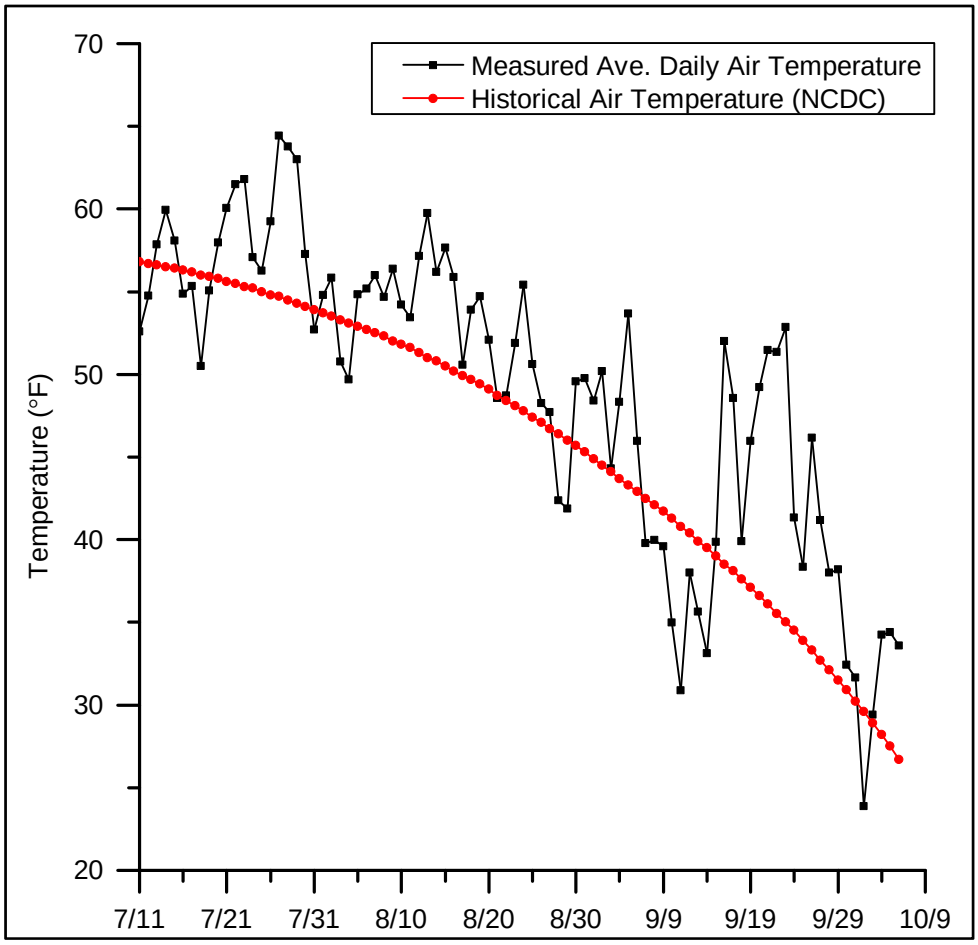

Figure 24. Comparison of measured average daily air temperature and historical average daily air temperature obtained from NCDC.

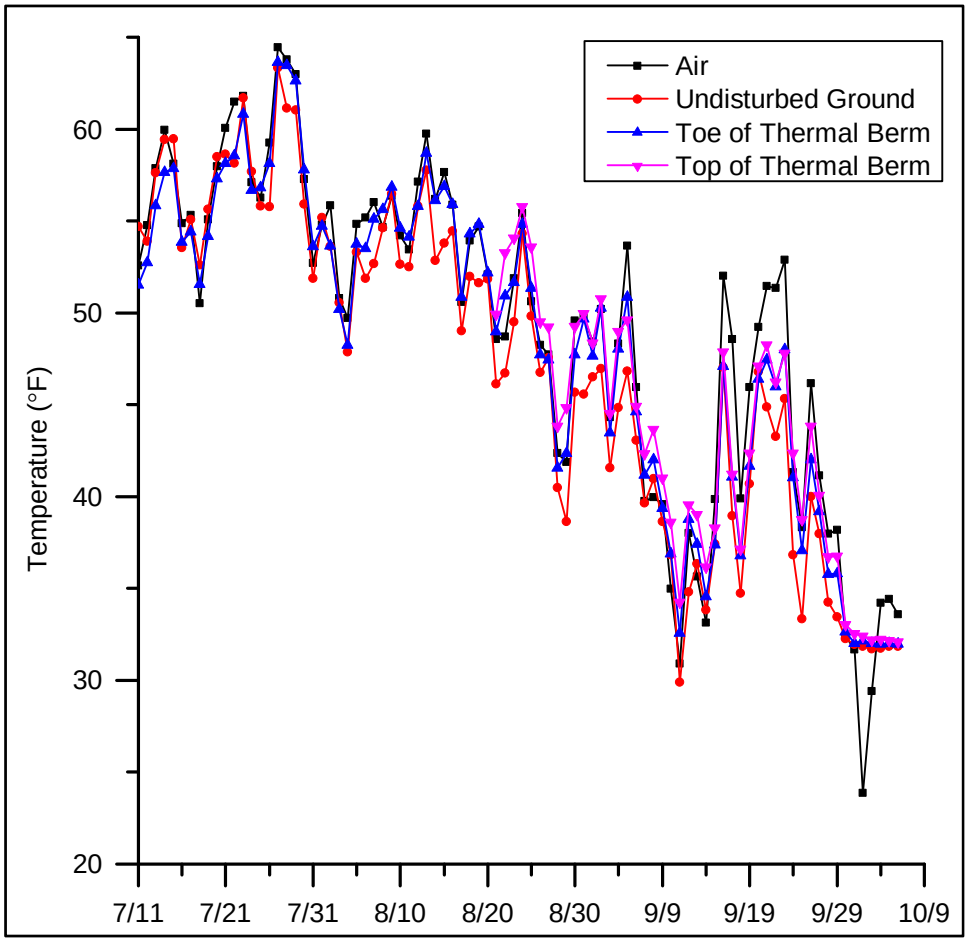

Figure 25. Measured daily average air and ground surface temperatures.

FDL-A RESULTS

M-IPI Analysis

Figure 26 contains plots of cumulative displacement from the INC500 device installed in TH12-9004. We corrected the data using vector summation (Cornforth, 2005) to determine the direction and magnitude of maximum movement. We also corrected for the cumulative change in depth of the sensors, as horizontal movement along the shear zone pulled the M-IPI device further down into the casing. Originally at 1.5 ft above the ground surface, horizontal movement within the shear zone pulled the INC500 down within the casing to 0.3 ft bgs, which correlated well with visual observations. These adjusted readings indicate movement within a well-developed shear zone between 66 ft and 74 ft bgs. Movement was fairly consistent over the measurement period, with a total of 31.2 in. of movement at the surface in about 31 days.

Early in the morning of October 24, the M-IPI began to record apparent "retrograde motion" upslope between 67 and 70 ft bgs (see Figure 27a). Considering an earlier failure of a thermistor string and the subsequent failure of a piezometer below this depth, we suspected that a few of the INC500 sensors were damaged in the shear zone. The manufacturer of the device agreed, indicating that the sensors "probably deformed or rotated within the housing" (J. Lemke, pers. comm., Nov. 2012). The INC500 continued to record downslope motion above the shear zone, with episodes of "retrograde motion" intermixed (see Figure 27b and Figure 27c). Despite the damaged sensors, the entire INC500 continued to record data, acquiring reasonable measurements of cumulative displacement below the depth of 70.5 ft. Then on October 31, the INC500 sensors below 66 ft bgs ceased reporting data (see Figure 27c). The manufacturer suggested that either the cable was physically pulled apart, or perhaps more likely, that one of the underwater connectors between modules pulled apart (J. Lemke, pers. comm., Dec. 2012). The sensors above the shear zone, however, continued to report movement and temperature data. In the summer of 2013, the PI intends to return to the FDL-A site and try to retrieve the upper modules from the casing, which may confirm how the modules became detached.

During the FDL-A research project, scheduling allowed the research team to return to the site every two to three weeks for manual measurements with the inclinometer probe. Considering the rate of movement, only one or two additional sets of readings could have been obtained before the inclinometer probe could no longer pass the shear zone and/or the casing sheared. Thus, the presence of the M-IPI device at this site delivered much more data than we otherwise would have collected.

Temperature Analysis

The M-IPI device provided additional data in another way. Figure 28a contains a temperature profile of TH12-9004, showing temperatures collected about a month apart from each other. The measurements collected on September 29 demonstrated elevated temperatures due to the drilling process (having not yet reached a pseudo-equilibrium). Most of these temperatures, however, fit the trend that developed with depth during the equilibrating process. One exception to this is the temperature measured at 85 ft bgs in TH12-9004. The temperature recorded by a VW piezometer at 85.5 ft bgs (i.e., "P2") also is plotted in Figure 28a. As the P2 temperature fits the expected trend, the likely explanation for the higher temperature is that it represents a malfunctioning thermistor. Unfortunately, all thermistors below 60 ft bgs failed on October 11, 2012. On October 26, the P2 unit also failed. Another exception to the stable temperature trend is illustrated with data collected on November 23 (see Figure 28a). Starting on November 9, the

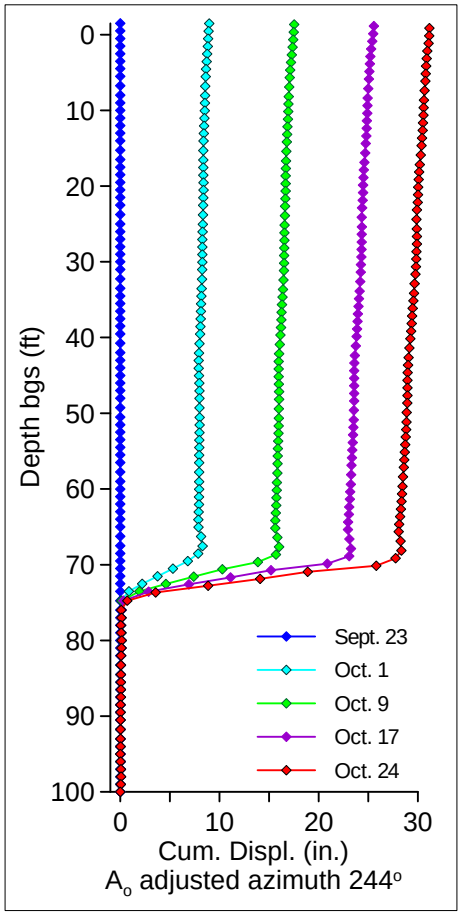

Figure 26. Cumulative displacement measurements for TH12-9004 until the INC500 began to demonstrate signs of failure.

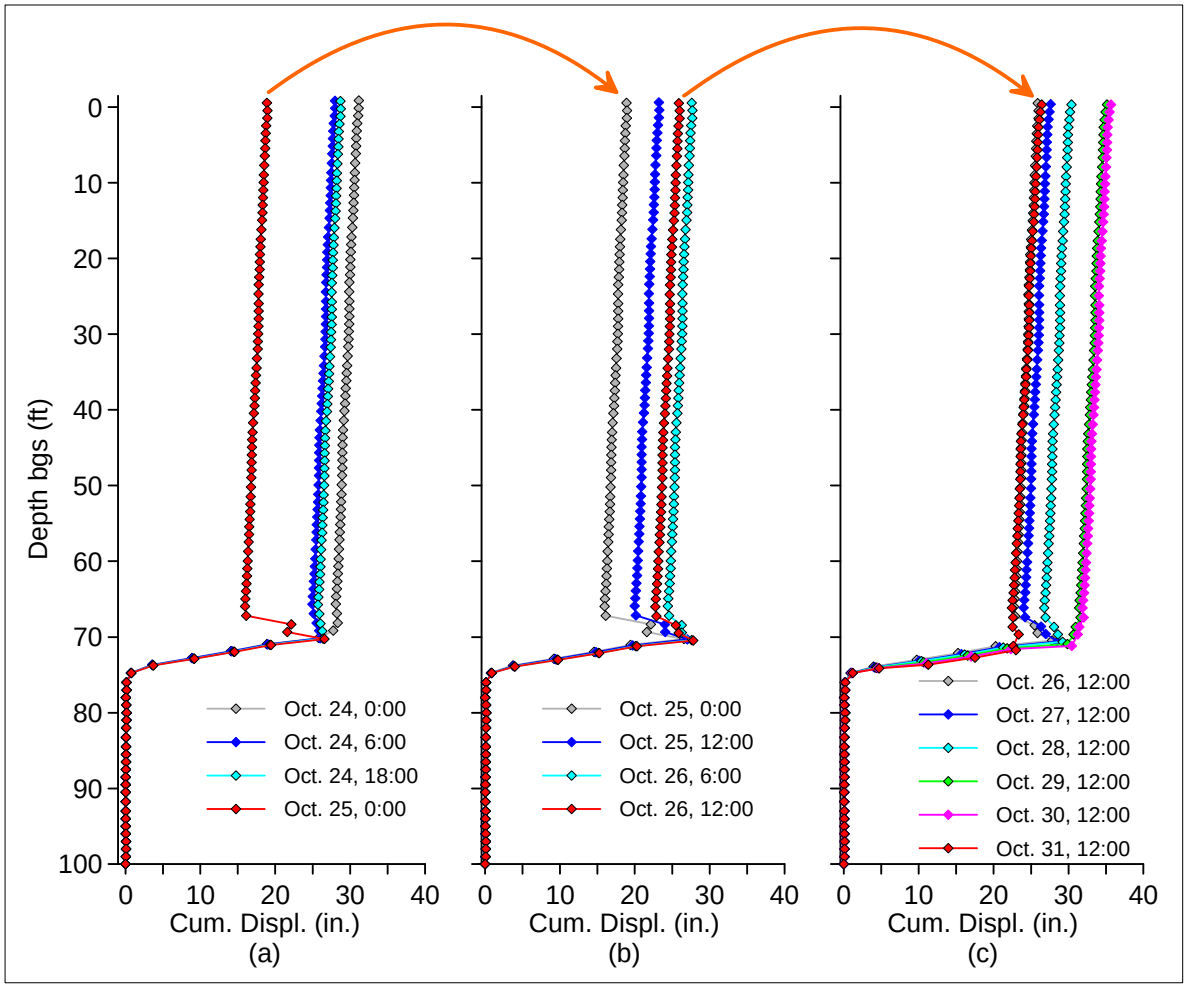

Figure 27. Evidence of failure of the INC500 at FDL-A. (a) Apparent "retrograde motion" began at 6:00 on October 24, with major "retrograde motion" at 0:00 on October 25. (b) The lobe above the shear zone continued to move downslope, with another episode of "retrograde motion" on October 26 at 12:00. (c) Final readings of the INC500 until failure of the lower modules after October 31 at 12:00. For each plot, the set of readings in gray represents the last reading from the previous plot (for (a), this is the last reading shown in Figure 26). The sequence of readings is given the same color scheme, with red indicating "retrograde motion".

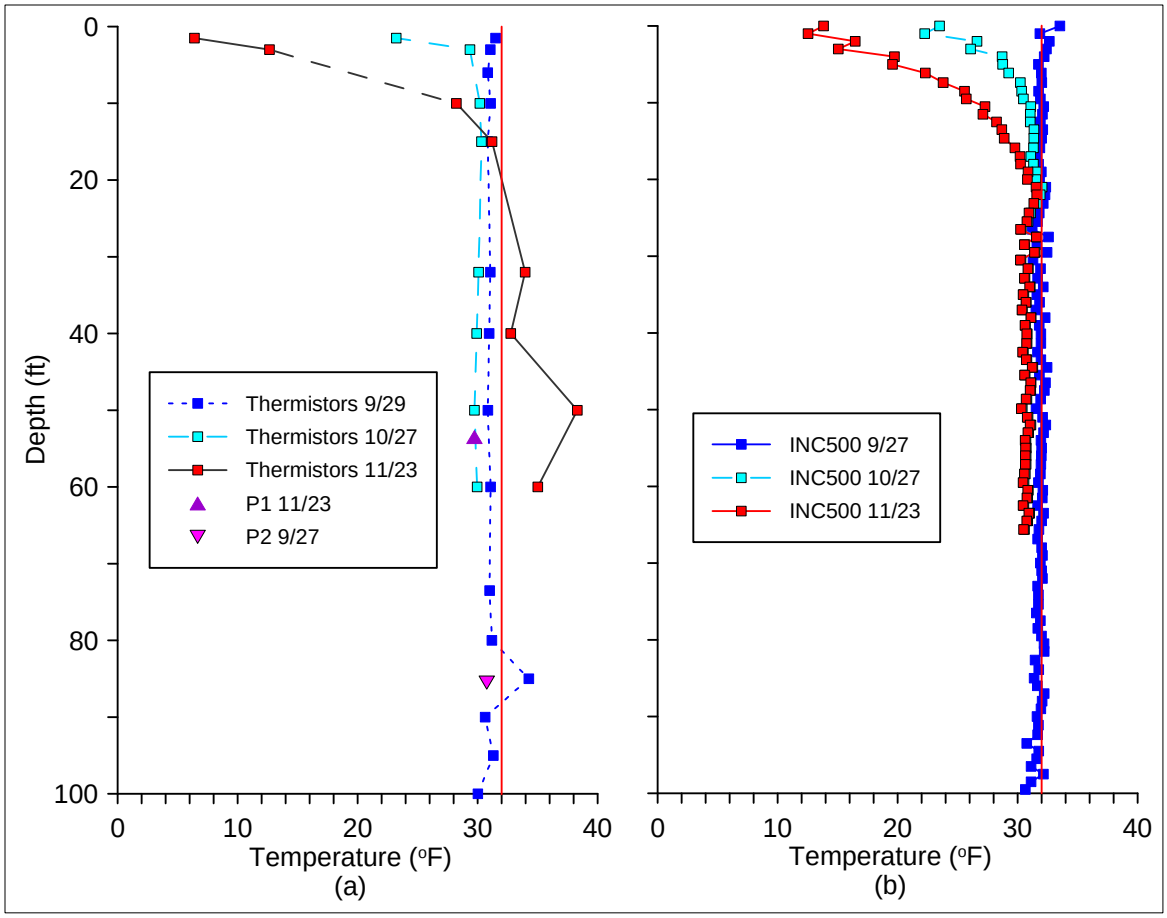

Figure 28. Temperature readings from TH12-9004. (a) Temperature readings from the thermistor string and two VW piezometers attached to the outside of the casing; "P1" and "P2" are readings from the vibrating wire piezometers installed at 53.5 and 85.5 ft bgs, respectively. (b) Temperature readings from the INC500. Nearest pairs of readings were averaged to reduce the scatter. For both plots, the phase-change temperature is indicated by the vertical red line.

remaining thermistors at depth began reporting a steady increase in temperature resulting in above-freezing values, as indicated by the erratic temperature profile from November 23; yet the VW piezometer located at 53.5 ft bgs (i.e., "P1") measured 29.7ºF, matching the previous temperature trend. Figure 28b is a plot of temperatures obtained using the INC500 device installed within TH12-9004. To reduce some of the temperature variability to illustrate data trends better, nearest pairs of readings were averaged together. The INC500 stopped reporting accurate temperatures below 65.5 ft bgs on October 24; however, the data above this depth are sufficient to indicate below freezing temperatures. Thus, the M-IPI data confirmed that the thermistors below 15 ft bgs began to malfunction on November 9, likely the result of glycol entering the cable and affecting the measured resistance.

DISCUSSION OF M-IPI SOFTWARE USE

In addition to the M-IPI installation, most of the research sites required the installation of other instrumentation. We chose to use CR1000 data loggers in each ADAS to accommodate multiple devices, which is not necessarily the routine configuration for M-IPI data collection and storage. The following discussion covers some data management issues that arose during this project, but it must be stressed that these issues may not be typical due to the nature of this research. Also, this discussion covers software that was first acquired in 2010, and in some cases, updated over the course of the research project. The reader is encouraged to investigate the most recent software versions from the companies' web sites (see Appendix E for websites as of December 2012). During this research project, instructions for the use of each program were readily available from each manufacturer, as well as supplemental clarifications as needed. Finally, just as the Digitilt Inclinometer Probe served as the standard against which comparisons were made for the M-IPI devices, software for each M-IPI device was compared against the use of the DigiPro for Windows software (ver. 1.34.1), which served as the data management software for the manual inclinometer probe.

The power budget was a concern for all of the sites. The CDS ADAS was located in rugged terrain along the Copper River with dense vegetation to the south, resulting in less than optimum solar exposure. The lack of daylight and snow cover on the solar panel at the Rich113 site taxed the power supply during the winter months. Thus, we needed to adjust initial programming of the CR1000 to manage the power budget for each site better. The program changes had an unforeseen effect on data management, as data acquired after the program change had to be "spliced" together with previously acquired data and the header information for the specific installation to develop a complete set. As this process was time consuming and introduced the possibility for human error, we recommend that thorough consideration be given to frequency of readings during the initial programming of the data logger.

The program INCVIEW V1.0a Beta was used for the INC500 data processing. This program currently is not provided by the manufacturer; instead web-based programs and apps are available for data retrieval and manipulation (J. Lemke, pers. comm., December 2012). The INCVIEW program required a set-up file developed in Excel that contained the order of modules as installed within the guide casing. Then the program called for the data file collected from the CR1000 data logger. The program allowed the user to view the data in a variety of ways, including cumulative and incremental displacement and displacement history with time. The data could not be corrected for a depth offset from the ground surface within the casing, nor was there an orientation correction for the potential misalignment of the casing grooves during the

initial installation. To perform these data corrections, the desired data sets were exported from the M-IPI program and imported into Excel. For this project, we contacted the manufacturer to parse out the temperature data set using a proprietary program. Once parsed out, the temperature data were easy to work with in a spreadsheet. At the time of this writing, the manufacturer indicated that web-based software could be modified easily to display temperature readings upon the request of a client (J. Lemke, pers. comm., December 2012).

During the research project, we had to acquire a new manual inclinometer probe. As a result of changing instruments, bias shift occurred in the readings, which was corrected with user-defined offsets within the DigiPro program. The M-IPI data sets were examined for bias shift as well, and we identified bias shift in the INC500 readings. The INCVIEW V1.0a Beta program allowed the user to correct for bias shift by selecting the zone over which this error occurred (i.e., the zone below the shear zone); the program then calculated and applied a displacement correction to the data profile.

SAA3D was the main program used for the SAA data processing. After appending the raw data to account for any CR1000 program changes, the data file and a project information file were placed into a unique file structure required by the SAA programs. Next, the program SAACR_raw2data ver. 1.24 was used to convert the CR1000 output into a form that the SAA3D program could read. The SAA3D program compiled the data, which then could be "rotated" within the display window to see changes in orientation with time. The program provided multiple ways to view the data with time and in space, including the traditional "SI plot."

The SAA3D did not correct for depth offset from the ground surface within the vertical casing, nor settlement of the fixed end of a horizontal casing installation. To perform this data correction, the desired data sets were exported from the M-IPI program and imported into Excel. The program also did not perform bias shift corrections. It did allow retrieval of temperatures measured by the SAA device. For this research project, the temperatures were exported and analyzed using Excel.

CHAPTER 4

CONCLUSIONS, RECOMMENDATIONS, AND SUGGESTED RESEARCH

We investigated the performance of two M-IPI devices in a variety of installations (see Table 2 for a summary of the types of installations). Both devices measured creep in frozen ground, the INC500 measured movement within shear zones at two different installations, and the SAA measured the settlement under a newly placed embankment over ice-rich permafrost. The results indicate that the two M-IPI devices tested provide data that correlate well to those obtained with the manual inclinometer probe. Deviations between readings from the M-IPI device and the inclinometer probe are attributed to differences in the devices' geometry and flexibility. Each device recorded temperatures within 0.4ºF of those reported by the thermistor string. In two separate installations, the INC500 temperature readings served as an additional set of measurements to check potentially faulty readings from another temperature sensor, which was an unexpected benefit of this device.

Each device was retrievable and operational after the initial field use, indicating that the devices can be reused. Each device also demonstrated versatility. The SAA was used successfully in both vertical and horizontal installations. Because of its modular nature, the INC500 was installed in three different locations that required different M-IPI lengths. In addition to the originally proposed test sites, we also installed the INC500 at a site where we anticipated large amounts of movement. This M-IPI device continued to read during shearing and provided meaningful temperature data after shearing. The presence of the M-IPI in the quickly moving landslide provided much more data than we otherwise would have collected due to the remoteness of the installation.

Based on this analysis, these devices are suitable for use in cold regions. Field experience indicates that the installation procedure for each instrument is better undertaken at above freezing temperatures, however, due to required manual dexterity and the temperature requirements of casing adhesive that is typically available. We recommend that, if the needs of the project require the M-IPI device to produce measurements of both ground movement and temperature, the M-IPI temperature sensors are calibrated by the manufacturer before use. Additionally, we recommend replacing the plastic components for the INC500 after an extended installation to avoid breakage during re-installation.

While this research indicates that either M-IPI device is suitable for use in cold regions, the selection of the device depends on the needs of the user. Table 3 is a summary of the various pros and cons of each device as experienced during this research project. Please note that the summary is not intended to endorse nor exclude either device. Also, both manufacturers were very amenable to providing solutions to problems encountered during this research. We suspect that many of the items that are listed in the "cons" column have not been requested in the past by users, and that the technology and services will continue to improve as these instruments become more widely used.

Table 2. Summary of results from various M-IPI installations. Comparison of M-IPI movement and temperature measurements to inclinometer probe and thermistor measurements, respectively. The corrected readings from the Lost Chicken installation follow the method discussed in Chapter 3.

M-IPI device	Type of installation and location	Maximum deviation from inclinometer probe readings	Average deviation from inclinometer probe readings	Same casing?	Deviation from thermistor readings
INC500	Vertical, Rich113	6.89×10^{-2} in.	$2.31 \times 10^{-2} \pm 1.63 \times 10^{-2}$ in.	Yes	±0.4ºF
SAA	Vertical, Rich113	1.17×10^{-1} in.	$3.96 \times 10^{-2} \pm 3.74 \times 10^{-2}$ in.	No	±0.4ºF
INC500	Vertical, CDS	4.86×10^{-1} in.	$5.99 \times 10^{-2} \pm 1.10 \times 10^{-1}$ in.	Yes	---
SAA	Horizontal, Lost Chicken	6.06×10^{-2} in. (corrected)	$2.78 \times 10^{-2} \pm 1.24 \times 10^{-1}$ in.	No	±0.4ºF
INC500	Vertical, FDL-A	N/A	N/A	N/A	N/A

Table 3. Summary of pros and cons of each M-IPI device. Please note that this summary is based on the results of this research and is not intended to endorse nor exclude either device.

Geodaq INC500	
PRO	CON
Modular; can be shortened or lengthened so as to fit multiple installations	Screws are required to join modules
Suitable for vertical installation	Use for both horizontal and vertical installations must be specified
Oriented and positioned within slotted guide casing by centralizers	Plastic coupler assemblies and centralizers may require replacement between installations
Sheared; still reported data during shearing and above shear zone	Separated to no longer provide data below shear zone
Records temperature	Temperature measurement devices not typically calibrated
Interfaces with CR1000 data logger	
Software provides views of cumulative and incremental displacement, XY displacement plots, and displacement vs. time plots	Temperature data must be parsed out of data set by manufacturer upon request
Software corrects for bias shift	Software does not correct for depth offset from ground surface within casing, nor orientation correction
Measurand SAA	
PRO	CON
Easy installation from shipment reel	Fixed length ordered from manufacturer
Suitable for both horizontal and vertical installations	
(From Dasenbrock, 2009) Sheared, continued to report data	
Records temperature	Temperature measurement devices not typically calibrated
Interfaces with CR1000 data logger	
Software provides different data views, including surface plots, absolute shape plots, Z slice (XY plots), displacement vs. time plots, SI plots, as well as rotation of the data in a 3-D setting; provides orientation correction	Software does not correct for bias shift nor depth offset from ground surface within casing
Software provides viewing of temperatures measured by SAA device	

CHAPTER 5

REFERENCES

Barendse, M. B. "Field evaluation of a MEMS-based, real-time deformation monitoring system." *Geotechnical Instrumentation News* (March 2008) pp. 41-44, http://www.bitech.ca/pdf/GeoTechNews/2008/GIN_March08.pdf

Barendse, M. B., and G. Machan. (2008). "In-place MEMS inclinometer strings – evaluation of an evolving technology." *TRB 88th Annual Meeting Compendium of Papers DVD*, 12 p.

Contreras, I. A., Grosser, A. T., Ver Strate, R. H. "The use of the fully-grouted methods for piezometer installation, part 1." *Geotechnical Instrumentation News* (June 2008) pp. 30-37, http://www.bitech.ca/pdf/GeoTechNews/2008/GIN_June08.pdf

Cornforth, D. H. *Landslides in Practice: Investigations, Analysis, and Remedial / Preventative Options in Soils*, John Wiley and Sons, Inc., Hoboken, NJ. (2005) 596 p.

Cortez, E. R., Hanek, G. L., Truebe, M. A., Kestler, M. A. *Simplified User's Guide to Time-Domain-Relfectometry of Monitoring of Slope Stability*: U.S. Dept. of Agriculture, Forest Service (September 2009) 25 p.

Daanen, R. P., Grosse, G., Darrow, M. M., Hamilton, T. D., Jones, B. M. "Rapid movement of frozen debris-lobes: implications for permafrost degradation and slope instability in the south-central Brooks Range, Alaska." *Natural Hazards and Earth System Science*: Vol. 12, No. 5 (May 2012), pp. 1-17, doi:10.5194/nhess-12-1-2012.

Darrow, M. M. *Taylor Highway MP 64 to Canadian Border Rehabilitation*, Federal Project No. STP-0785(11)/State Project No. 66446: Northern Region, Alaska Department of Transportation and Public Facilities (August 2008) 133 p.

Darrow, M. M., Bray, M. T., Huang, S. L. "Analysis of a Deep-Seated Landslide in Permafrost, Richardson Highway, South-Central Alaska." *Environmental and Engineering Geoscience*: Vol. 18, No. 3 (August 2012), pp. 261-280, doi:10.2113/gseegeosci.18.3.261

Darrow, M. M., Daanen, R. P., Simpson, J. M. *Monitoring and Analysis of Frozen Debris Lobes, Phase 1 – Final Report*: Alaska University Transportation Center and Alaska Department of Transportation and Public Facilities (in review), 63 p.

Dasenbrock, D. D. "Automated landslide instrumentation programs on US Route 2 in Crookston, MN." *Proceedings of the University of Minnesota 58th Annual Geotechnical Engineering Conference, St. Paul, MN* (February 2010) pp. 165-185.

Dunnicliff, J. *Geotechnical Instrumentation for Monitoring Field Performance*: John Wiley and Sons, Inc., Hoboken, NJ. (1993) 577 p.

Durham Geo-Enterprises, Inc., 2011. *Digitilt Inclinometer Probe datasheet*: Durham Geo-Enterprises, Inc., Mukilteo, WA.

GEODAQ, Inc., 2010. *INC500 Series In-Place Inclinometer datasheet*: GEODAQ, Inc., Sacramento, CA.

Lemke, J. (2006). "In-place inclinometers using a low-g accelerometer network." *ASCE Conf. Proc.* 187, 65-70.

Machan, G., and V. G. Bennett. "Use of inclinometers for geotechnical instrumentation on transportation projects." *Transportation Research E-Circular E-C129* (October 2008) 92 p.

McKenna, G. T. "Grouted-in installation of piezometers in boreholes." *Canadian Geotechnical Journal*: Vol. 32, No. 2 (April 1995) pp. 355-363, 10.1139/t95-035

Measurand, Inc. *Measurand ShapeAccelArray (SAA) Specifications*: Measurand, Inc., Fredericton, NB, Canada (2010).

Measurand, Inc. *ShapeAccelArray (SAA) Installation Guide*: Measurand, Inc., Fredericton, NB, Canada (2008).

Measurement Specialties, Inc. *44033RC Precision Epoxy NTC Thermistor*: Measurement Specialties, Inc., Shrewsbury, MA (2008).

Mikkelsen, P. E. "Cement-bentonite grout backfill for borehole instruments." *Geotechnical Instrumentation News* (December 2002) pp. 38-42, http://www.bitech.ca/pdf/GeoTechNews/2002/GIN_Dec2002mikkelsen.pdf

Mikkelsen, P. E., and G. E. Green. "Piezometers in fully grouted boreholes." *Symposium on Field Measurements in Geomechanics, FMGM 2003, Oslo, Norway* (September 2003) 10 p.

O'Connor, K. M. and C. H. Dowding. *GeoMeasurements by Pulsing TDR Cables and Probes*: CRC Press, New York, NY (1999) 402 p.

Obermiller, K. O., Darrow, M. M., Huang, S. L., Chen, G. "Site investigation and slope stability analysis of the Chitina Dump Slide (CDS), Alaska." *Environmental and Engineering Geoscience*: (in press).

Turner, J. P. *Time Domain Reflectometry for Monitoring Slope Movements*: Wyoming Department of Transportation, Cheyenne, WY, FHWA-WY-03/02F (June 2006) 58 p.

APPENDIX A: RICH 113 INSTALLATION PHOTOGRAPHS AND BORING LOGS

Figure A-1. Location of the drill rig for TH09-1510. Photograph taken in November 2009 from the Richardson Highway embankment. (Photograph by M. Darrow)

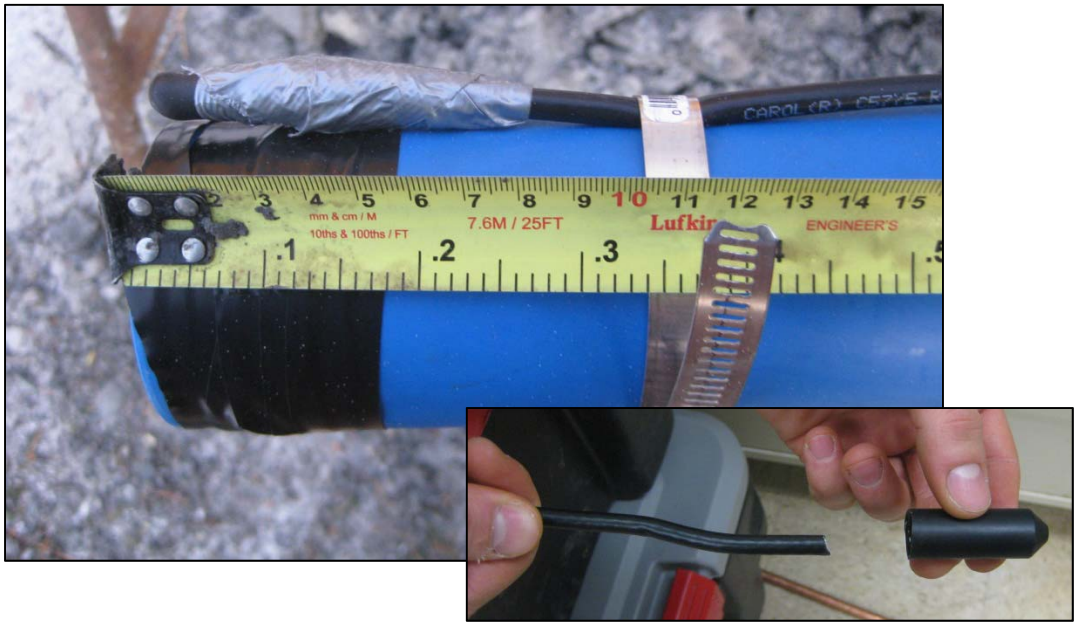

Figure A-2. Configuration of coaxial (TDR) cable at the bottom of the guide casing prior to installation. Inset illustrates sealing the cable end with an adhesive cap. (Photographs by M. Darrow, Nov. 2009)

Figure A-3. Conducting a “hallway” test with the INC500 and SAA devices wired into the ADAS enclosure. (Photograph by M. Darrow, March 2010)

Figure A-4. Staging the INC500 device on sawhorses in March 2010. (Photograph by M. Darrow)

Figure A-5. Marking the INC500 for placement of centralizers. (Photograph by M. Darrow, March 2010)

Figure A-6. Order of INC500 module serial numbers before installation. It is good practice to record this order both in a field book and through photographs. (Photograph by M. Darrow, March 2010)

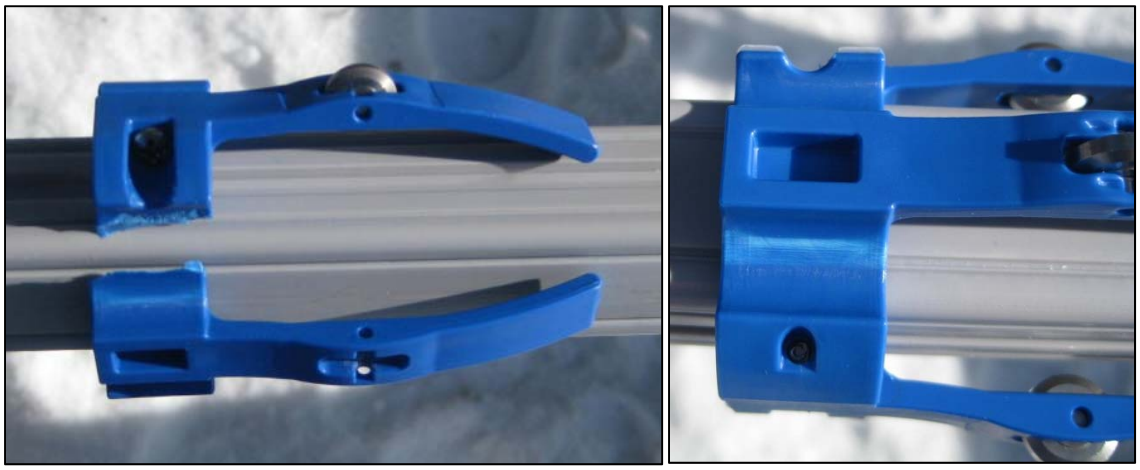

Figure A-7. Damage to centralizers due to improper alignment during the March 2010 installation. (Photographs by M. Darrow)

Figure A-8. Attaching the safety line to the lowest module. (Photograph by M. Darrow, March 2010)

Figure A-9. Lowering the first INC500 module down the guide casing. (Photograph courtesy of A. Parsons, March 2010)

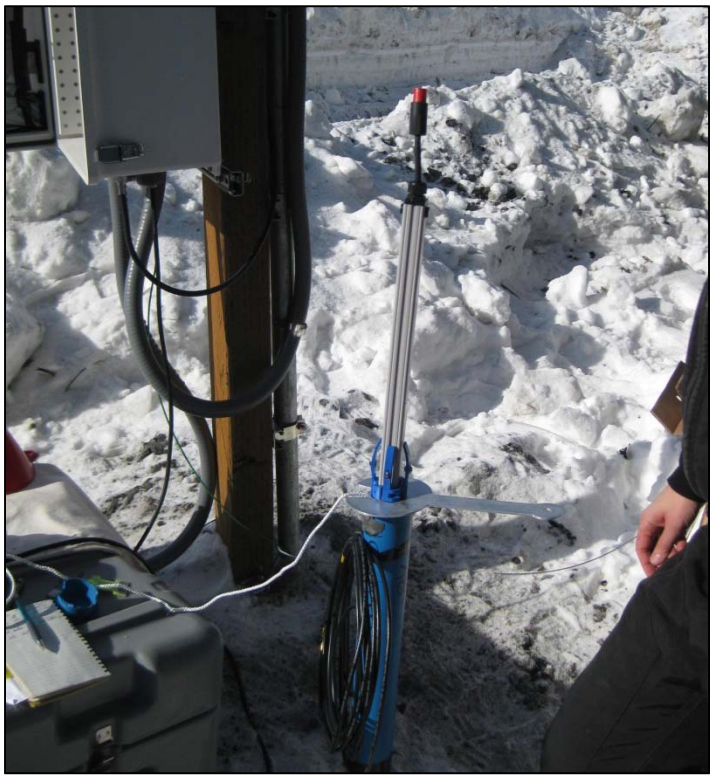

Figure A-10. First INC500 module resting on fork. (Photograph courtesy of A. Parsons, March 2010)

Figure A-11. Steps in the assembly of the INC500 modules. (a) Spraying the connections with silicon; (b) plugging the water-tight connectors together; (c) screwing the threaded connections together for the water-tight connection; (d) connected modules; e) attaching the coupler assembly. (Photographs courtesy of A. Parsons, March 2010)

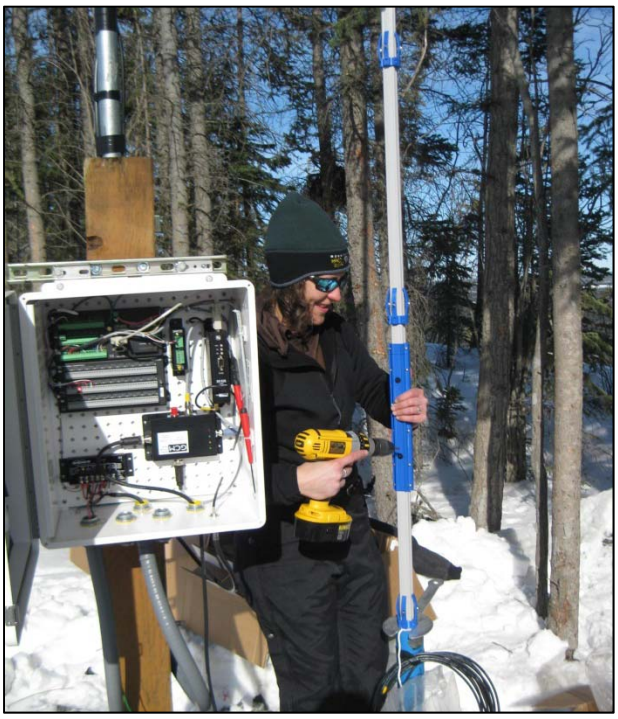

Figure A-12. Connecting the coupler assembly with machine screws. (Photograph courtesy of A. Parsons, March 2010)

Figure A-13. Installing inner 1.05-in. PVC into guide casing for SAA device. Slot cut into the guide casing was to allow tightening of the hose clamp at the top of the PVC casing (see Figure A-14). White 1-in. PVC to the left was for a thermistor string. (Photograph by M. Darrow, March 2010)

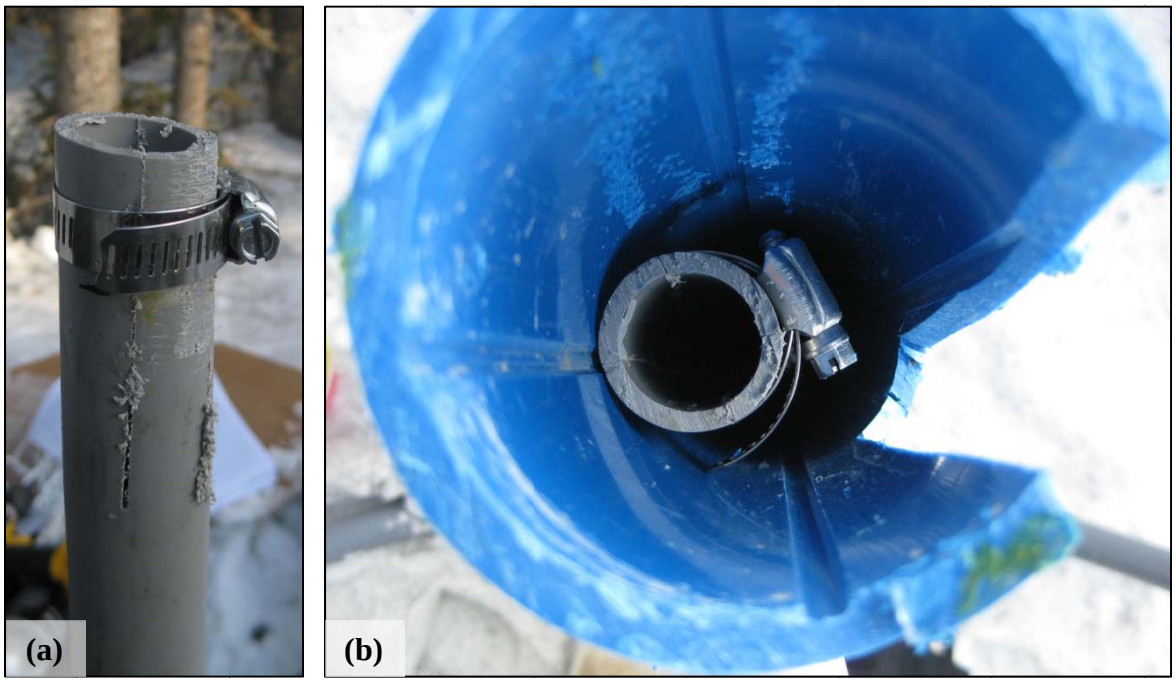

Figure A-14. Preparing inner 1.05-in. PVC casing for SAA installation. (a) Notches cut at the top of 1.05-in. PVC with hose clamp; (b) looking down the guide casing at the location of the inner 1.05-in. PVC casing. (Photographs by M. Darrow, March 2010)

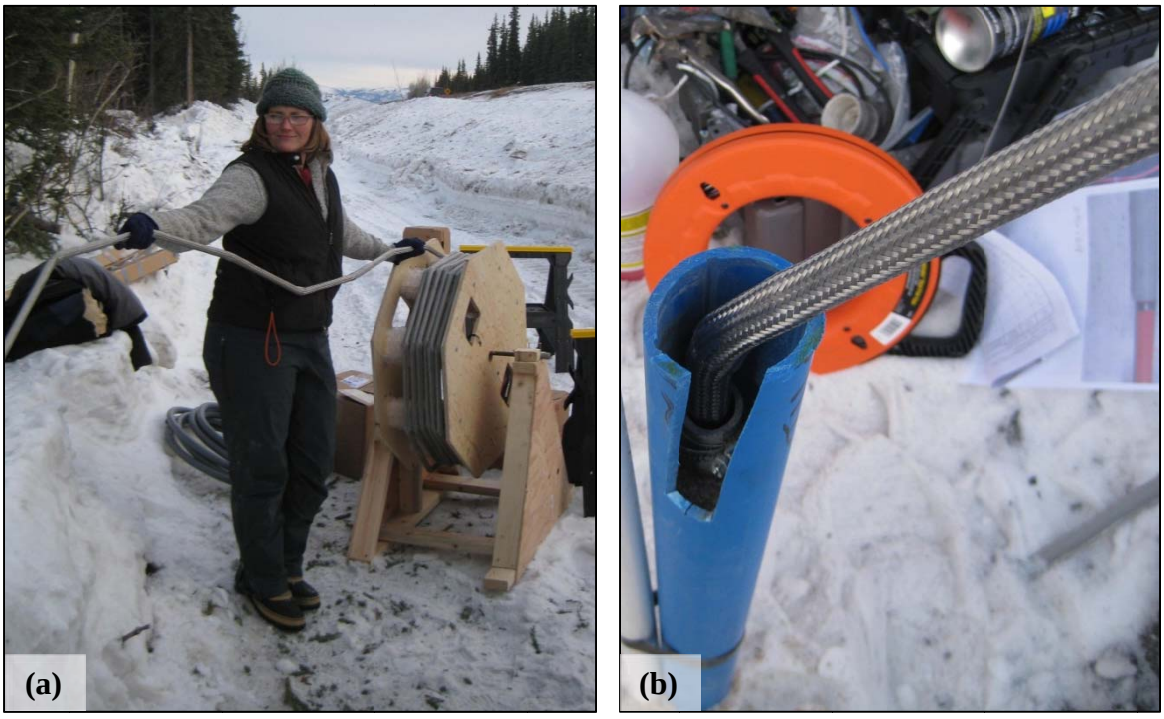

Figure A-15. Installing the SAA device. (a) Guiding the SAA off of the shipment reel, and (b) into the inner 1.05-in. PVC casing. (Photographs by M. Darrow, March 2010)

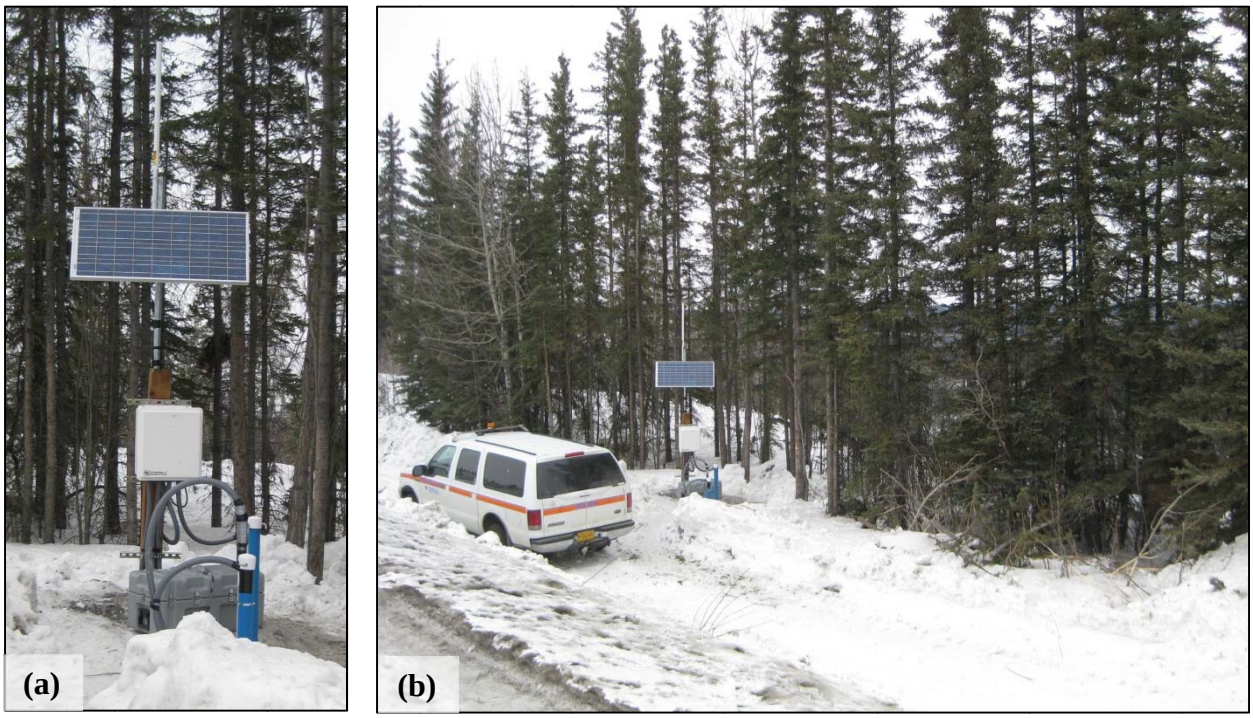

Figure A-16. Completed Rich113 installation in March 2010. (a) ADAS with battery box and casings. (b) Taken from the Richardson Highway, this photograph illustrates the installation site relative to the embankment and the edge of the bluff (just past the spruce trees). (Photographs by M. Darrow)

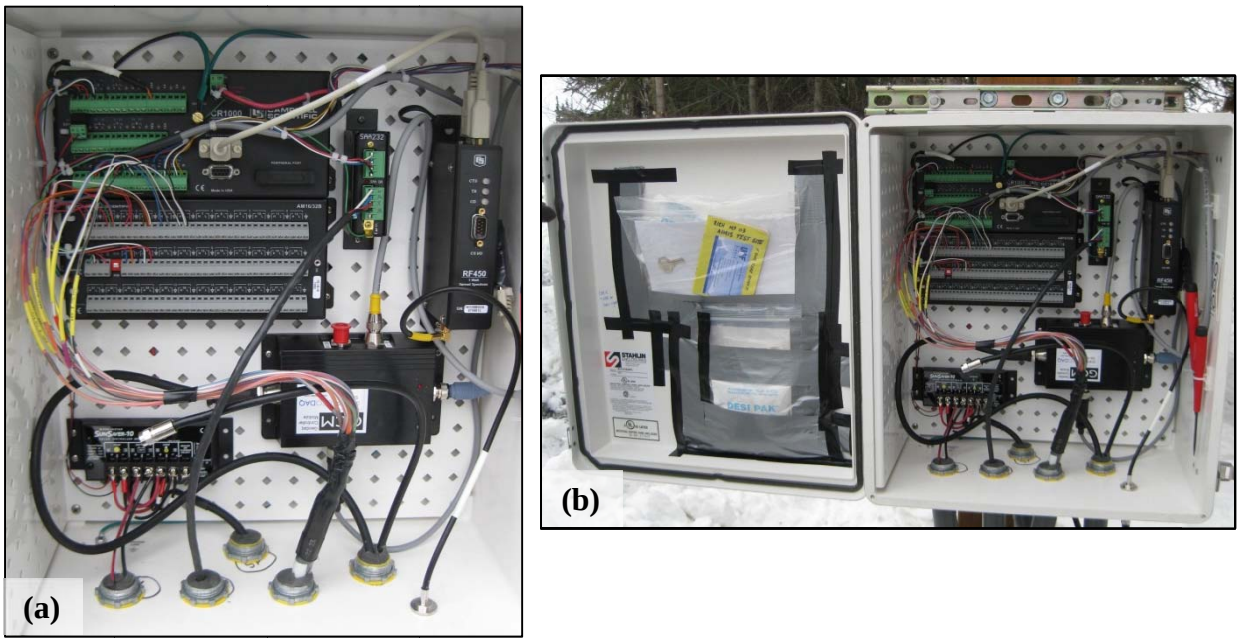

Figure A-17. Inside of ADAS enclosure. It is good practice to document the final wiring of the site through (a) close-up views and (b) general views of the enclosure. This facilitates later trouble-shooting. (Photographs by M. Darrow, March 2010)

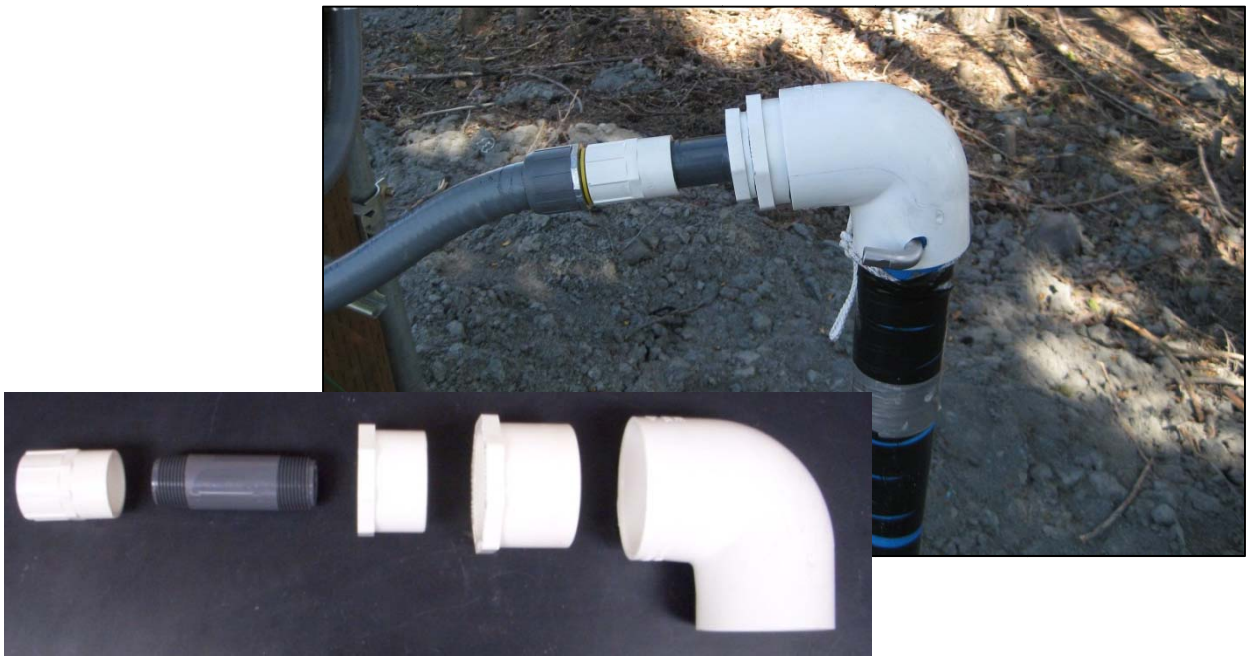

Figure A-18. Guide casing to flexible conduit adapter in place on TH09-1511 casing. Inset illustrates the various PVC fittings that comprise the adapter. (Photographs by M. Darrow, May 2010)

Figure A-19. Final configuration of the Rich113 site. (a) Complete ADAS overview; (b) TH07-1711 in foreground with battery box and ADAS; TH09-1511 is to the right. (Photographs by M. Darrow, Aug. 2011)

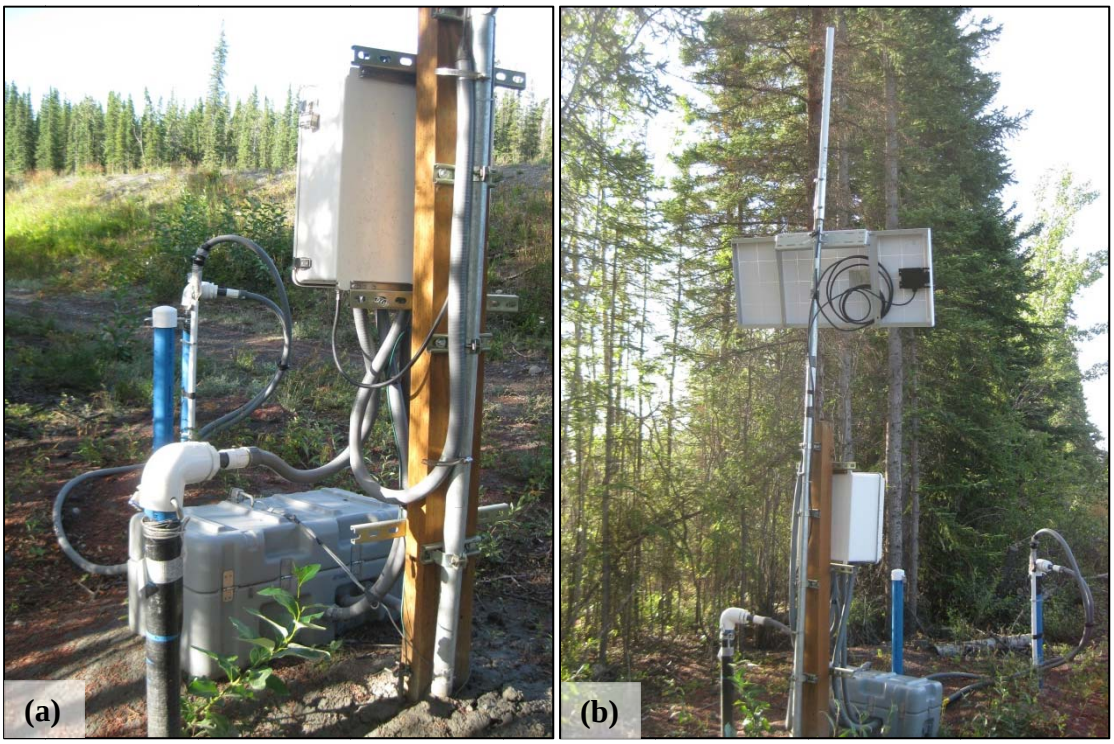

Figure A-20. Configuration of Rich113 ADAS. (a) View of the back side of the post with Richardson Highway in background; (b) rear of solar panel showing connectors. (Photographs by M. Darrow, Aug. 2011)

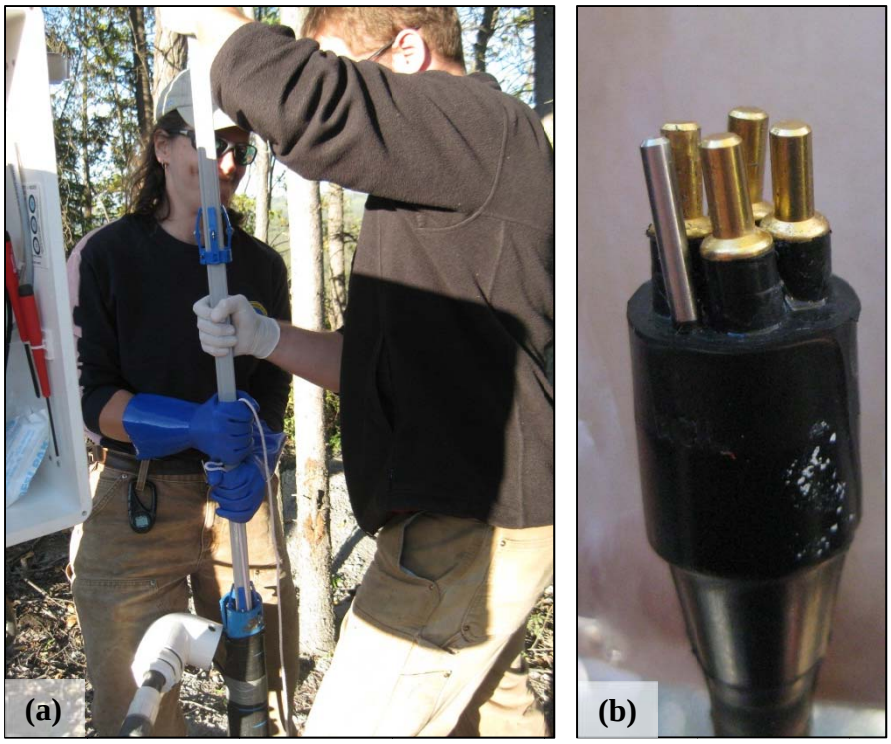

Figure A-21. Retrieving the INC500 in September 2010 to adjust the positioning of the centralizers. (a) Pulling the INC500 from the guide casing. (b) Some of the connectors demonstrated twisting. (Photographs courtesy of S. Huang)

Figure A-22. Retrieving the SAA in August 2011, and replacing the device on the shipping reel. (Photograph courtesy of J. Yao)

Figure A-23. Final configuration of the Rich113 site in August 2011. The post that supported the ADAS was cut off at the ground surface. Only the guide casings remain for manual inclinometer probe readings. (Photograph by M. Darrow)

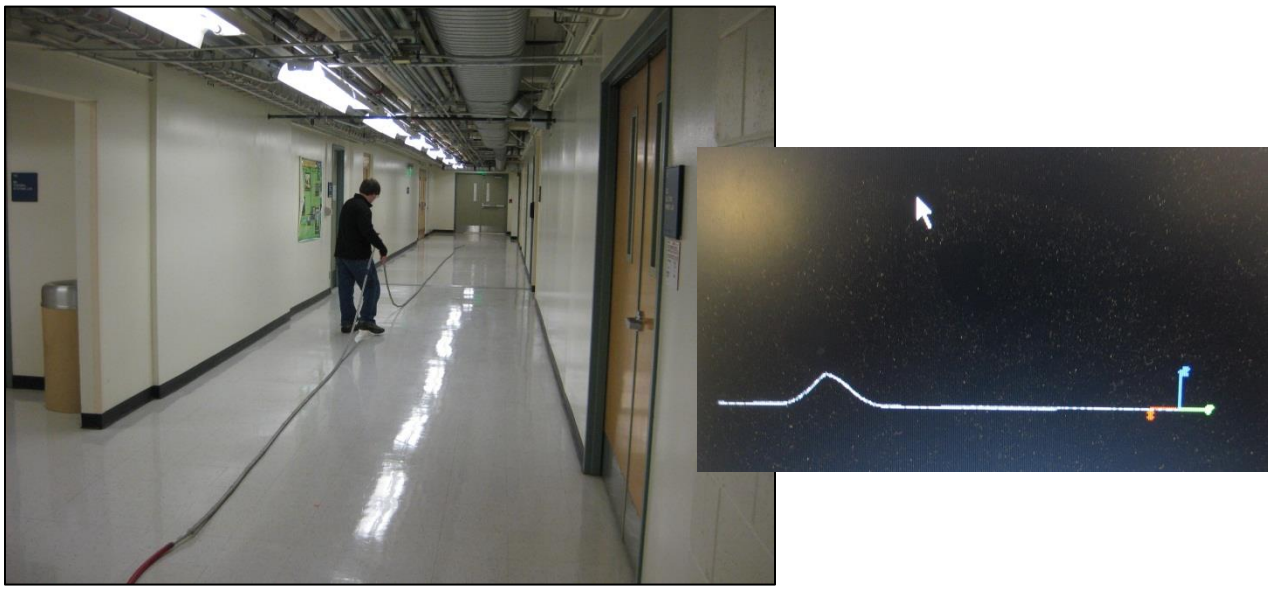

Figure A-24. "Hallway" test of the SAA device after retrieval from the Rich113 site. Inset shows a screen shot of the elevated portion of the M-IPI moving down the device. (Photographs by M. Darrow, Jan. 2012)

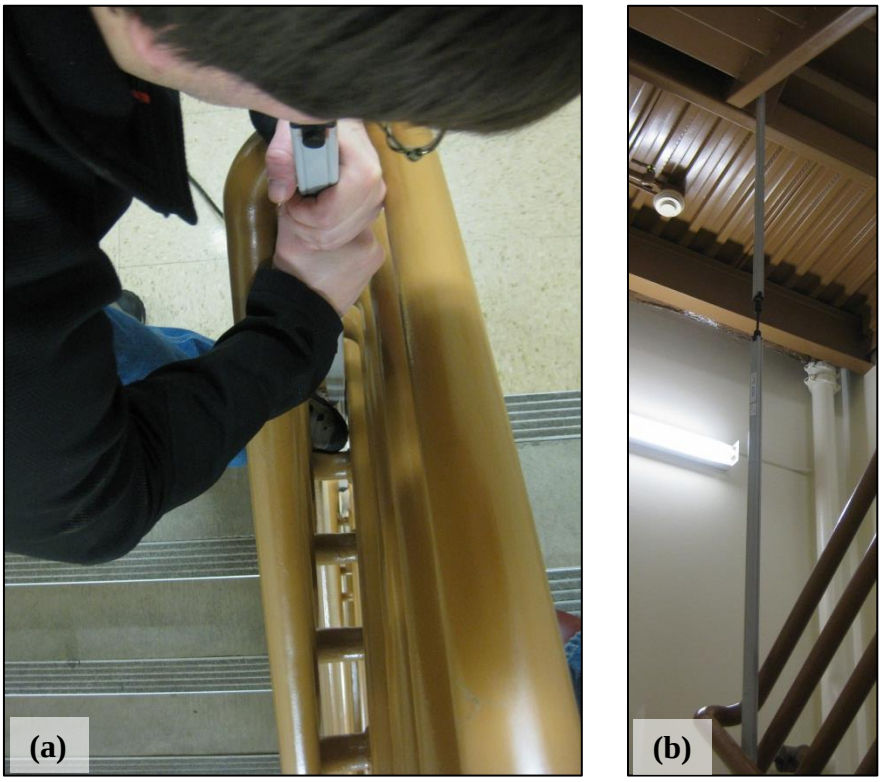

Figure A-25. "Hallway" test of the INC500 device after retrieval from the Rich113 site. Two to three modules were held tightly in a vertical orientation in a stairwell while the data was recorded. (Photographs by M. Darrow, Jan. 2012)

FINAL TEST HOLE LOG

STATE OF ALASKA DOT/PF
Northern Region Materials
Geology Section

ALASKA UNIVERSITY TRANSPORTATION CENTER
University of Alaska Fairbanks - INE

Project	Automated In-place MEMS Inclinometer Strings	Test Hole Number	TH09-1510
		Total Depth	70.5 feet
Field Geologist	M. DARROW	Dates Drilled	11/17/2009 - 11/19/2009
Field Crew	R. WAGSTER, C. ROACH, T. HALLER	Equipment Type	CME 75 Truck
		UTM	N, E
		Weather	-14 deg F
		Latitude, Longitude	N62.08337°, W145.43767°
TH Finalized By	M. DARROW	Vegetation	Bk spruce
		Elevation	

Ground Water Data	While Drilling	After Drilling
Depth in (ft.)		
Time		
Date		
Symbol		

GENERAL COMMENTS:
Located ~4 ft NE from TH07-1711

Drilling Method	Depth in (Feet)	Casing Blows/ft	Sample Data: Method	Number	Blow Count	Sample Interval	N-Value	Frozen	Graphic Log	SUBSURFACE MATERIAL
H-S Auger	0									Bn SILT dry to moist
	5		SS	09-4100	8 16 15 15		31			Gy Sandy Fat CLAY w/ occ. Gr SAMPLE 09-4100 (4.5-6.5): 30% recov., 37.0 deg F, used 140 lb hammer 0.0-59.5
	10		SS	09-4101	6 15 13 19		28			SAMPLE 09-4101 (9.5-11.5): 95% recov., 37.2 deg F on sample btm
	15		SS	09-4102	5 9 11 13		20			SAMPLE 09-4102 (14.5-16.5): 100% recov., 35.3 deg F on sample btm
	20		SS	09-4103	5 7 8 14		15			SAMPLE 09-4103 (19.5-21.5): 90% recov., 34.3 deg F on sample btm
	25		SS	09-4104	11 23 36 35		59			SAMPLE 09-4104 (24.5-26.5): 60% recov, 38.6 deg F on sample btm; temp. rise attributed to high blowcounts
	30		SS	09-4105	2 7 10 12		17			SAMPLE 09-4105 (29.5-31.5): 60% recov., 33.4 deg F on sample btm
	35				6			?		

Note: Unless otherwise noted, all samples are taken with 1-3/8-in. ID Standard Penetration Sampler driven with 140 lb. hammer with 30-in. drop. ☒ CME Auto Hammer ☐ Cathead Rope Method

NR AKDOT TEST HOLE LOG - USCS AIMS DRILLING.GPJ NR_AKDOT_PRECON_USCS_06_28_07.GDT 12/12/12

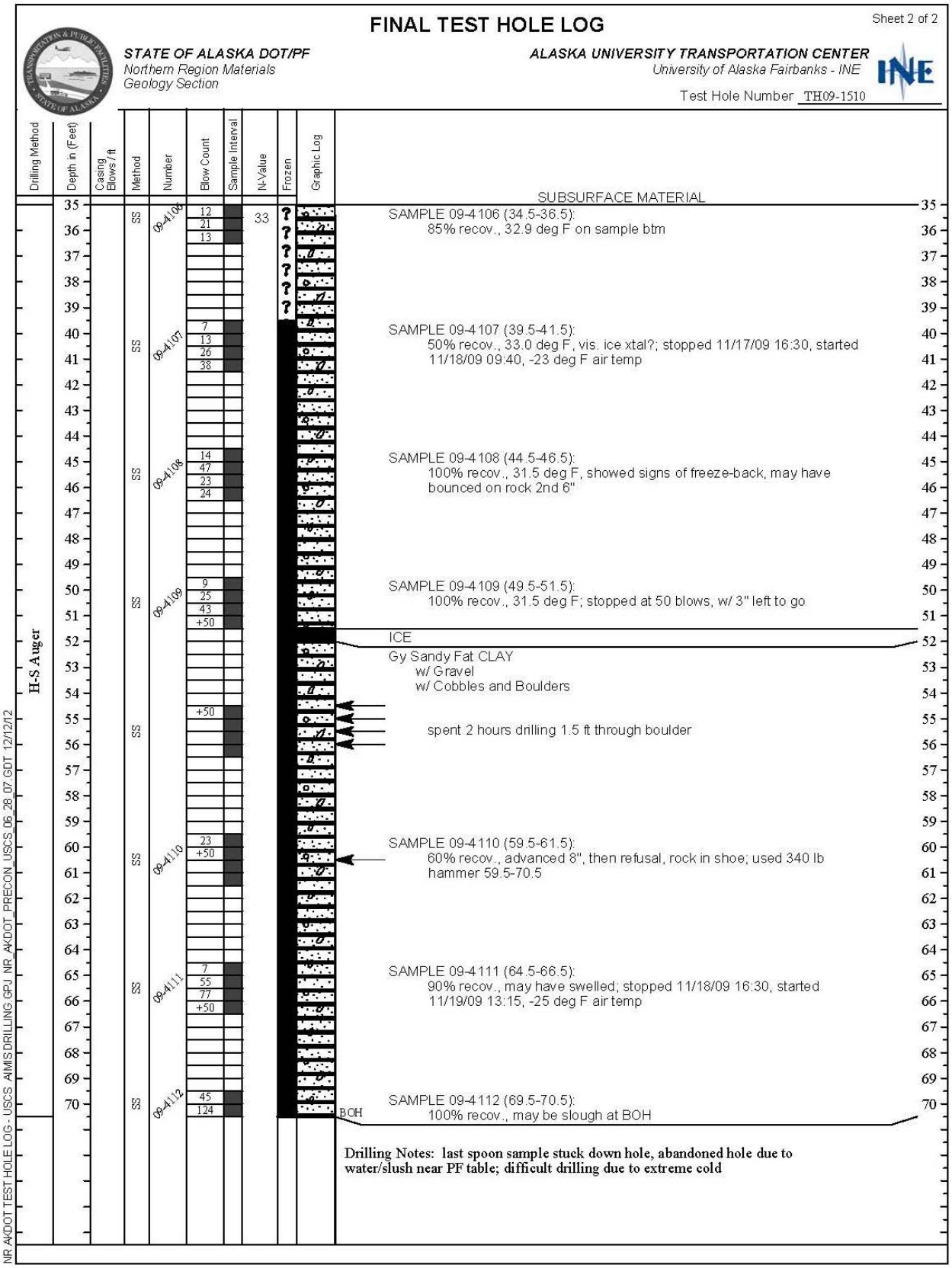
FINAL TEST HOLE LOG
Sheet 2 of 2
STATE OF ALASKA DOT/PF
Northern Region Materials
Geology Section
ALASKA UNIVERSITY TRANSPORTATION CENTER
University of Alaska Fairbanks - INE
Test Hole Number TH09-1510
Drilling Method
Depth in (Feet)
Casing Blows / ft
Method
Number
Blow Count
Sample Interval
N-Value
Frozen
Graphic Log
SUBSURFACE MATERIAL
H-S Auger
SS
09-4106
12
21
13
33
SAMPLE 09-4106 (34.5-36.5):
85% recov., 32.9 deg F on sample btm
09-4107
7
13
26
38
SAMPLE 09-4107 (39.5-41.5):
50% recov., 33.0 deg F, vis. ice xtal?; stopped 11/17/09 16:30, started 11/18/09 09:40, -23 deg F air temp
09-4108
14
47
23
24
SAMPLE 09-4108 (44.5-46.5):
100% recov., 31.5 deg F, showed signs of freeze-back, may have bounced on rock 2nd 6"
09-4109
9
25
43
+50
SAMPLE 09-4109 (49.5-51.5):
100% recov., 31.5 deg F; stopped at 50 blows, w/ 3" left to go
ICE
Gy Sandy Fat CLAY
w/ Gravel
w/ Cobbles and Boulders
+50
spent 2 hours drilling 1.5 ft through boulder
09-4110
23
+50
SAMPLE 09-4110 (59.5-61.5):
60% recov., advanced 8", then refusal, rock in shoe; used 340 lb hammer 59.5-70.5
09-4111
7
55
77
+50
SAMPLE 09-4111 (64.5-66.5):
90% recov., may have swelled; stopped 11/18/09 16:30, started 11/19/09 13:15, -25 deg F air temp
09-4112
45
124
BOH
SAMPLE 09-4112 (69.5-70.5):
100% recov., may be slough at BOH
Drilling Notes: last spoon sample stuck down hole, abandoned hole due to water/slush near PF table; difficult drilling due to extreme cold
NR AKDOT TEST HOLE LOG - USCS AIMS DRILLING.GPJ NR_AKDOT_PRECON_USCS_06_28_07.GDT 12/12/12

FINAL TEST HOLE LOG

STATE OF ALASKA DOT/PF
Northern Region Materials
Geology Section

ALASKA UNIVERSITY TRANSPORTATION CENTER
University of Alaska Fairbanks - INE

Project: Automated In-place MEMS Inclinometer Strings
Test Hole Number: TH09-1511
Total Depth: 85 feet
Field Geologist: M. DARROW
Dates Drilled: 11/20/2009 - 11/20/2009
Field Crew: R. WAGSTER, C. ROACH, T. HALLER
Equipment Type: CME 75 Truck
UTM: N, E
Weather: -22 deg F
Latitude, Longitude:
TH Finalized By: M. DARROW
Vegetation: Bk spruce
Elevation:

Ground Water Data	While Drilling	After Drilling
Depth in (ft.)		
Time		
Date		
Symbol		

GENERAL COMMENTS:
Located ~3 ft S of TH09-1510; back-filled w/ 30 50-lb bags of sand from 63.0; 2.7 ft stick-up on SI casing

Drilling Method: H-S Auger

Sample Data: Method | Number | Blow Count | Sample Interval | N-Value

Depth in (Feet) | Casing Blows / ft | Frozen | Graphic Log

SUBSURFACE MATERIAL

0 – 4: Bn SILT
dry to moist, w/ Gr 3.0-4.0

4 – 35: Gy Sandy Fat CLAY
w/ occ. Gr, w/ Cobbles below 35.0

Note: Unless otherwise noted, all samples are taken with 1-3/8-in. ID Standard Penetration Sampler driven with 140 lb. hammer with 30-in. drop. ☒ CME Auto Hammer ☐ Cathead Rope Method

NR AKDOT TEST HOLE LOG - USCS AIMS DRILLING.GPJ NR_AKDOT_PRECON_USCS_06_28_07.GDT 12/12/12

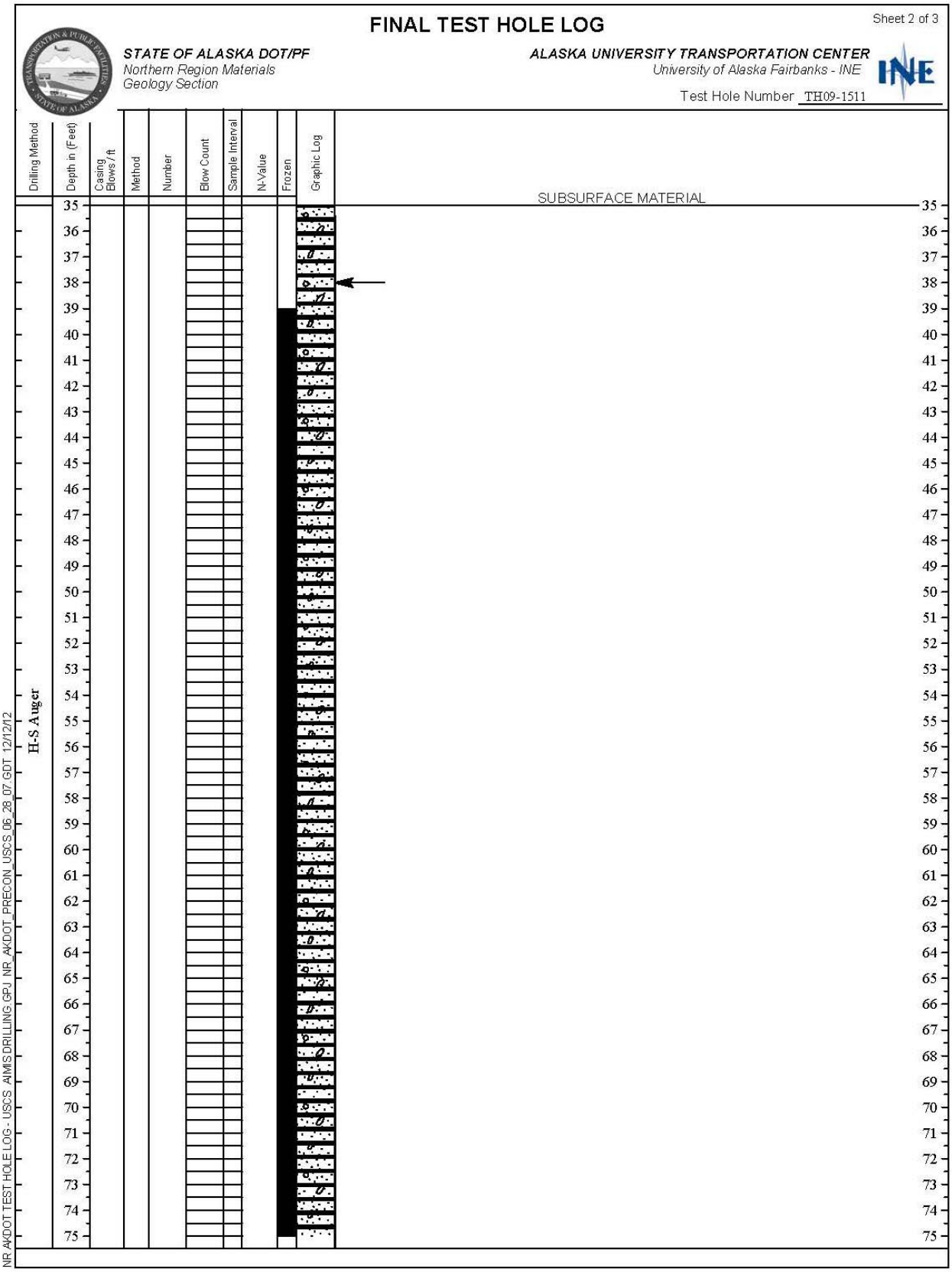
FINAL TEST HOLE LOG
Sheet 2 of 3
STATE OF ALASKA DOT/PF
Northern Region Materials
Geology Section
ALASKA UNIVERSITY TRANSPORTATION CENTER
University of Alaska Fairbanks - INE
Test Hole Number TH09-1511
Drilling Method
Depth in (Feet)
Casing Blows / ft
Method
Number
Blow Count
Sample Interval
N-Value
Frozen
Graphic Log
SUBSURFACE MATERIAL
H-S Auger
NR AKDOT TEST HOLE LOG - USCS AIMS DRILLING.GPJ NR_AKDOT_PRECON_USCS_06_28_07.GDT 12/12/12

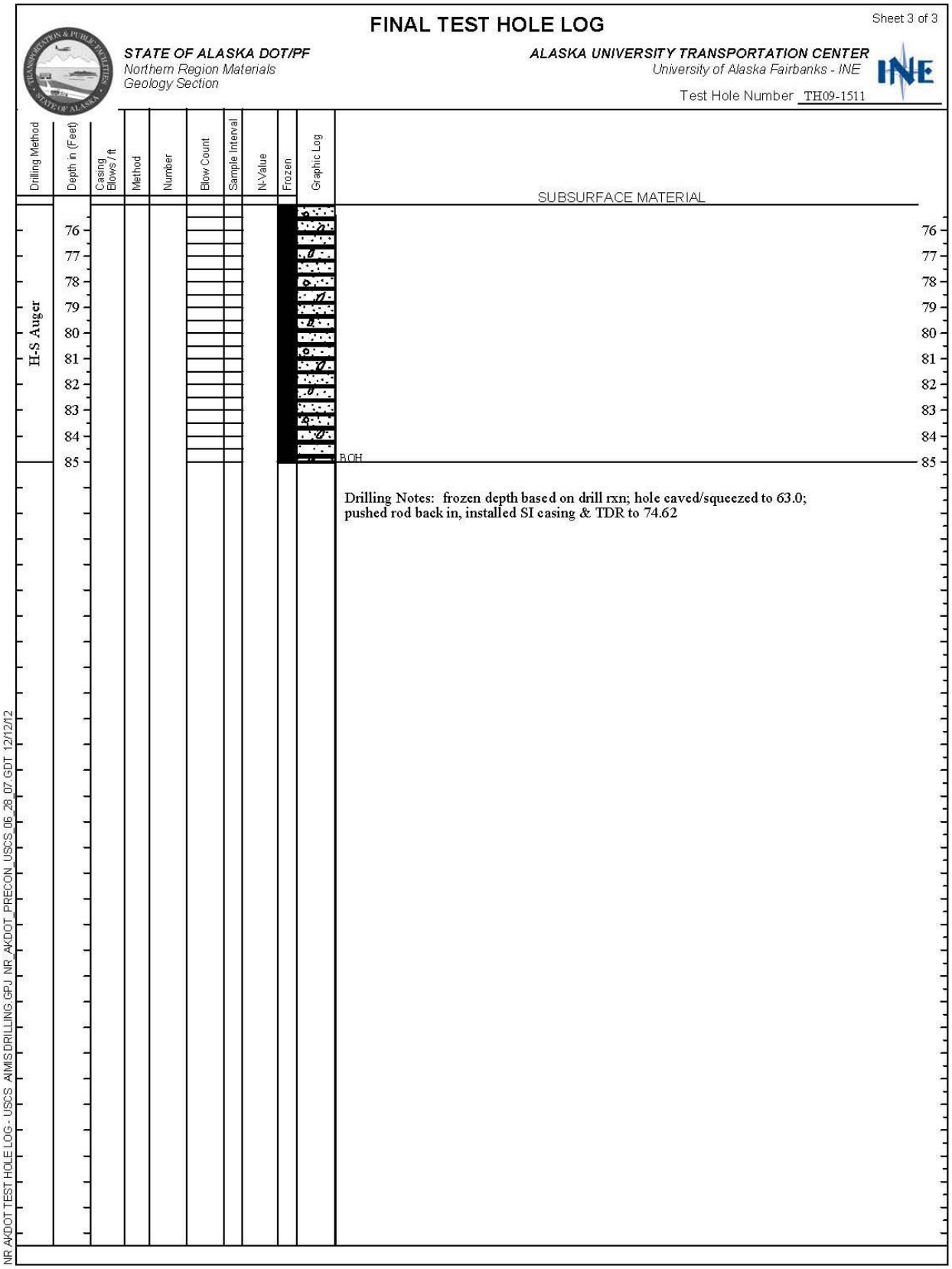
FINAL TEST HOLE LOG
Sheet 3 of 3
STATE OF ALASKA DOT/PF
Northern Region Materials
Geology Section
ALASKA UNIVERSITY TRANSPORTATION CENTER
University of Alaska Fairbanks - INE
Test Hole Number TH09-1511
Drilling Method
Depth in (Feet)
Casing Blows / ft
Method
Number
Blow Count
Sample Interval
N-Value
Frozen
Graphic Log
SUBSURFACE MATERIAL
H-S Auger
76
77
78
79
80
81
82
83
84
85
ROH
Drilling Notes: frozen depth based on drill rxn; hole caved/squeezed to 63.0; pushed rod back in, installed SI casing & TDR to 74.62
NR AKDOT TEST HOLE LOG - USCS AIMS DRILLING.GPJ NR_AKDOT_PRECON_USCS_06_28_07.GDT 12/12/12

FINAL TEST HOLE LOG

STATE OF ALASKA DOT/PF
Northern Region Materials
Geology Section

ALASKA UNIVERSITY TRANSPORTATION CENTER
University of Alaska Fairbanks - INE

Project: Automated In-place MEMS Inclinometer Strings

Test Hole Number: TH09-1512
Total Depth: 85 feet
Dates Drilled: 11/21/2009 - 11/21/2009
UTM: N, E
Latitude, Longitude:
Elevation:

Field Geologist: M. DARROW
Field Crew: R. WAGSTER, C. ROACH, T. HALLER, S. PARKER
Equipment Type: CME 75 Truck
Weather: -10 deg F
Vegetation: Bk spruce
TH Finalized By: M. DARROW

Ground Water Data	While Drilling	After Drilling
Depth in (ft.)		
Time		
Date		
Symbol		

GENERAL COMMENTS:
Located ~4 ft S of TH07-1711; 4.0 ft stick-up on SI casing & 1" PVC

Drilling Method	Depth in (Feet)	Casing Blows / ft	Sample Data: Method	Number	Blow Count	Sample Interval	N-Value	Frozen	Graphic Log	SUBSURFACE MATERIAL
H-S Auger	0									Gy Lean CLAY (debris on surface from previous drilling)
	1									
	2									Bn SILT dry, w/ wood frags
	3									
	4									Gy Sandy Fat CLAY w/ occ. Gr, w/ Cobbles below 50.0
	5									
	6									
	7									
	8									
	9									
	10									
	11									
	12									
	13									
	14									
	15									
	16									
	17									
	18									
	19									
	20									
	21									
	22									
	23									
	24									
	25									
	26									
	27									
	28									
	29									
	30									
	31									
	32									
	33									
	34									
	35									

Note: Unless otherwise noted, all samples are taken with 1-3/8-in. ID Standard Penetration Sampler driven with 140 lb. hammer with 30-in. drop. ☒ CME Auto Hammer ☐ Cathead Rope Method

NR AKDOT TEST HOLE LOG - USCS AIMS DRILLING.GPJ NR_AKDOT_PRECON_USCS_06_28_07.GDT 12/12/12

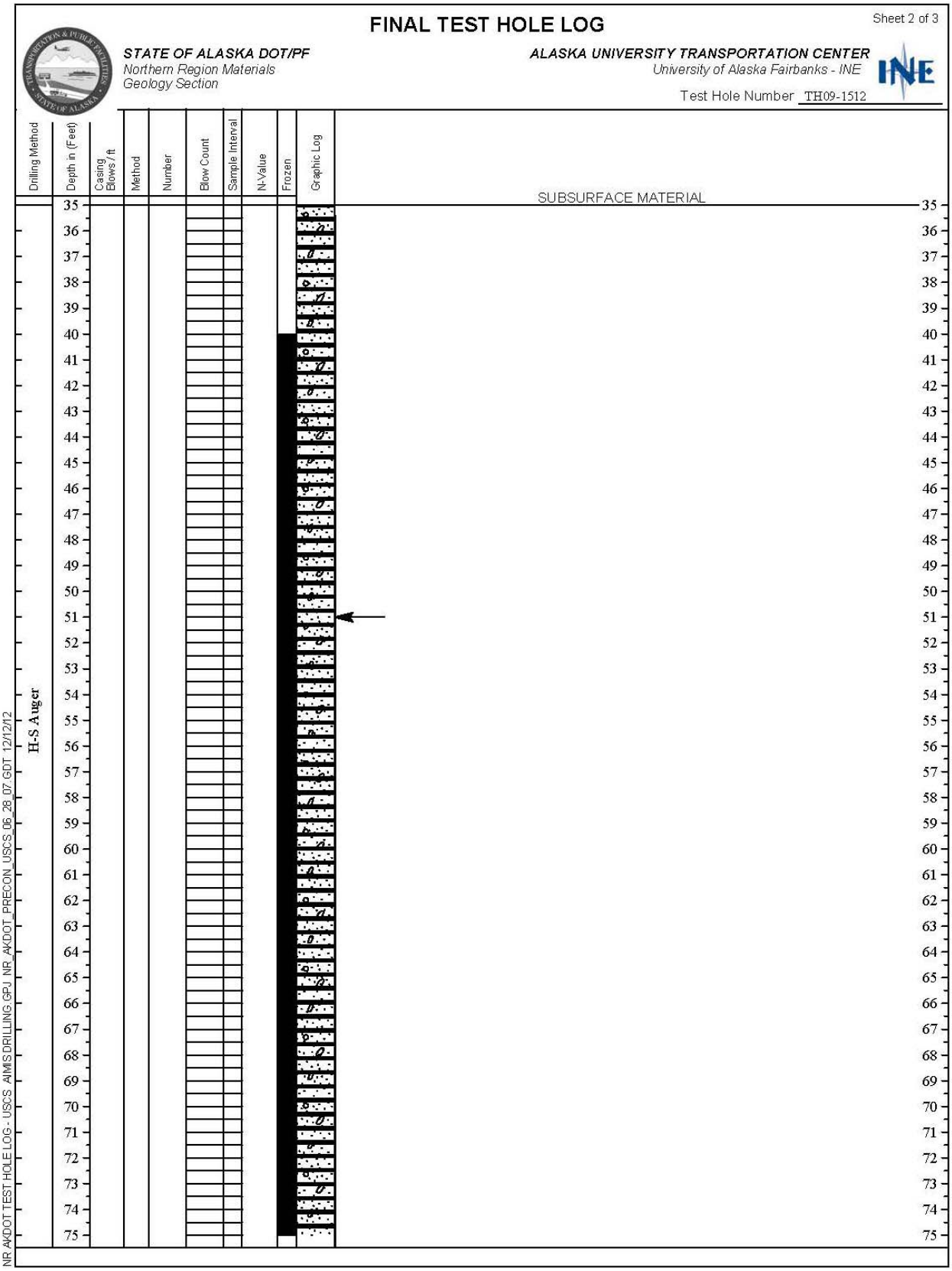
FINAL TEST HOLE LOG
Sheet 2 of 3
STATE OF ALASKA DOT/PF
Northern Region Materials
Geology Section
ALASKA UNIVERSITY TRANSPORTATION CENTER
University of Alaska Fairbanks - INE
Test Hole Number TH09-1512
Drilling Method
Depth in (Feet)
Casing Blows / ft
Method
Number
Blow Count
Sample Interval
N-Value
Frozen
Graphic Log
SUBSURFACE MATERIAL
H-S Auger
NR AKDOT TEST HOLE LOG - USCS AIMS DRILLING.GPJ NR_AKDOT_PRECON_USCS_06_28_07.GDT 12/12/12

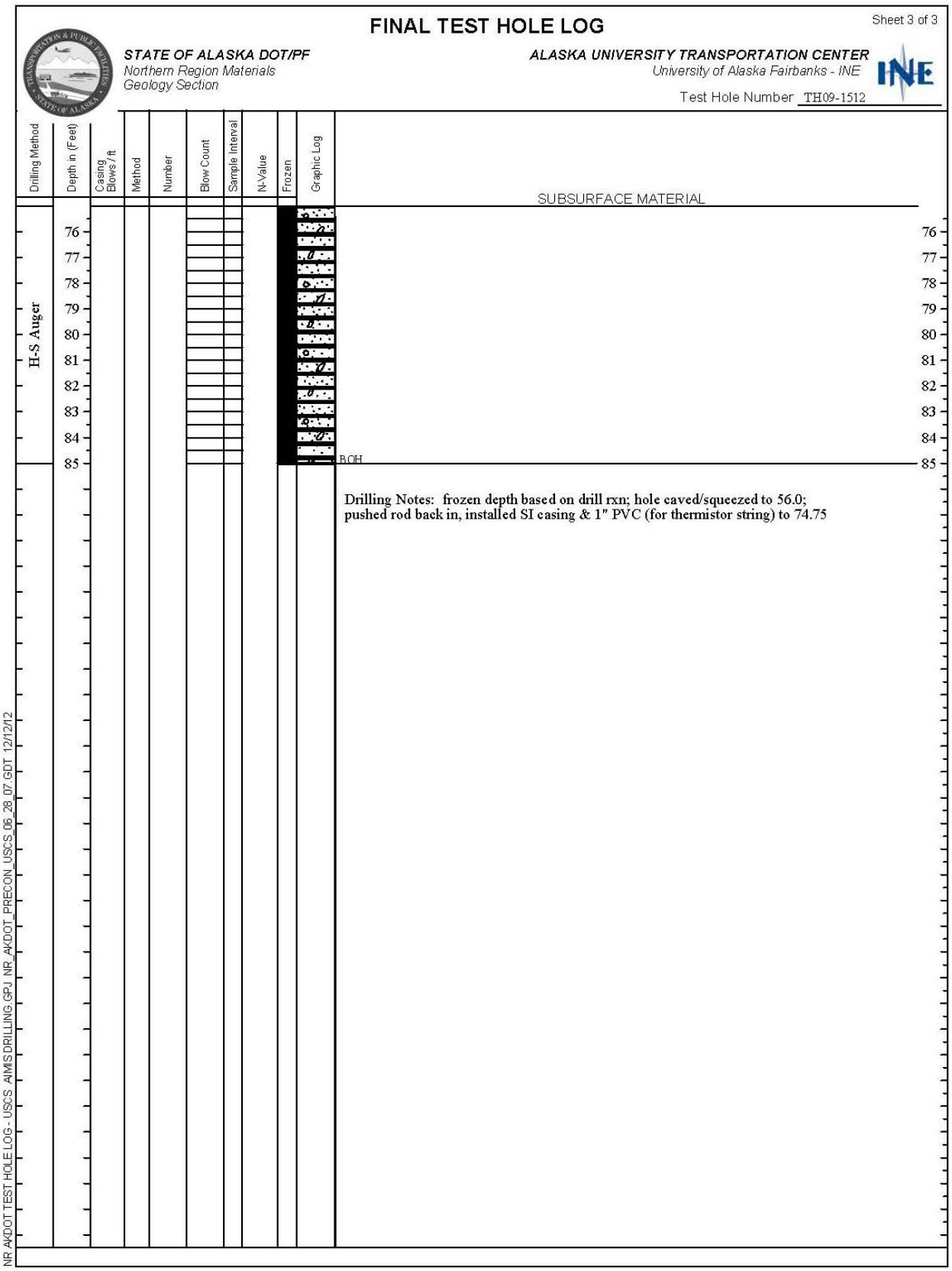
FINAL TEST HOLE LOG
Sheet 3 of 3
STATE OF ALASKA DOT/PF
Northern Region Materials
Geology Section
ALASKA UNIVERSITY TRANSPORTATION CENTER
University of Alaska Fairbanks - INE
Test Hole Number TH09-1512
Drilling Method
Depth in (Feet)
Casing Blows / ft
Method
Number
Blow Count
Sample Interval
N-Value
Frozen
Graphic Log
SUBSURFACE MATERIAL
H-S Auger
76
77
78
79
80
81
82
83
84
85
BOH
Drilling Notes: frozen depth based on drill rxn; hole caved/squeezed to 56.0; pushed rod back in, installed SI casing & 1" PVC (for thermistor string) to 74.75
NR AKDOT TEST HOLE LOG - USCS AIMS DRILLING.GPJ NR_AKDOT_PRECON_USCS_06_28_07.GDT 12/12/12

APPENDIX B: CHITINA INSTALLATION PHOTOGRAPHS AND BORING LOGS

Figure B-1. Tamping dry sand backfill around the guide casing. (Photograph by M. Darrow, June 2010)

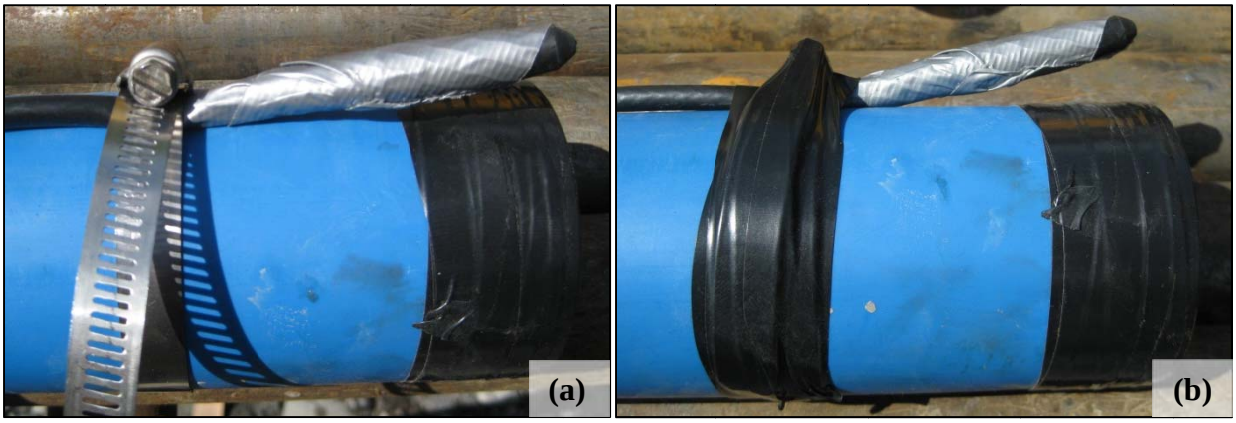

Figure B-2. Configuration of the coaxial (TDR) cable on the outside of the guide casing. Photograph (a) illustrates the crimp into the cable by the hose clamp; (b) the hose clamp was wrapped with tape to prevent snagging on the walls of the boring. (Photographs by M. Darrow, June 2010)

Figure B-3. Attaching the coaxial (TDR) cable with hose clamps at 10-ft intervals. (Photograph courtesy of T. Haller, June 2010)

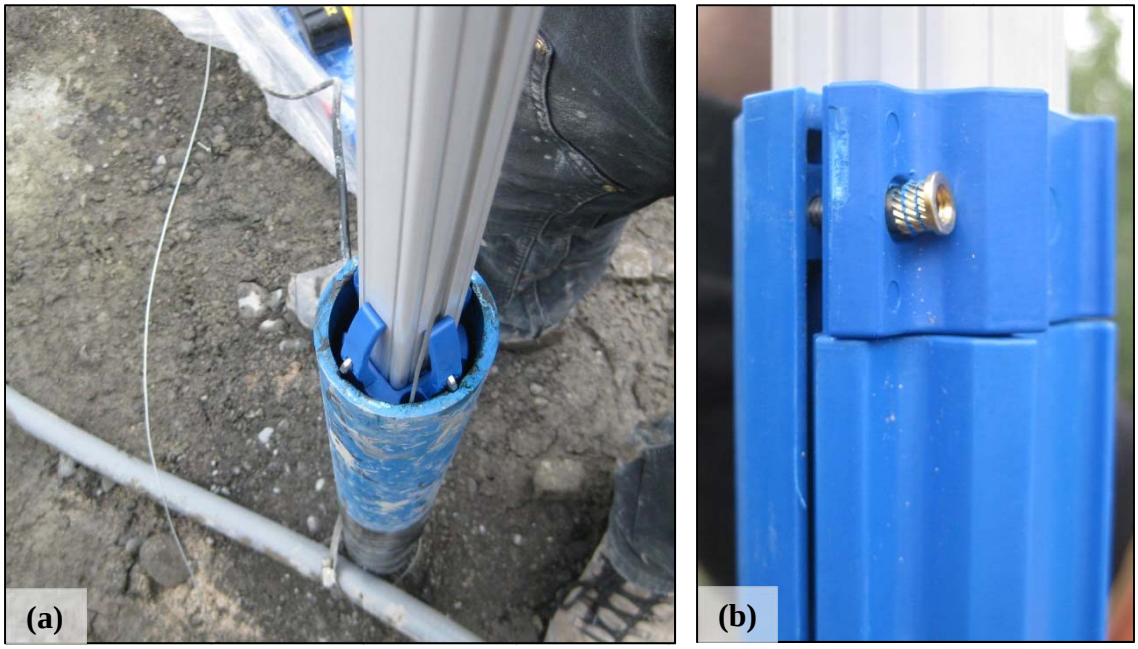

Figure B-4. Installing the INC500 within the guide casing. (a) This photograph shows the arrangement of the centralizers and the wire rope used as a safety line; (b) some of the insets for the machine screw popped out of the plastic housing. (Photographs by M. Darrow, June 2010)

Figure B-5. Placement of vibrating wire piezometer on PVC casing for installation into TH10-1553. (Photograph by M. Darrow, June 2010)

Figure B-6. Preparing the cement-bentonite grout for backfill into TH10-1553. (Photograph by M. Darrow, June 2010)

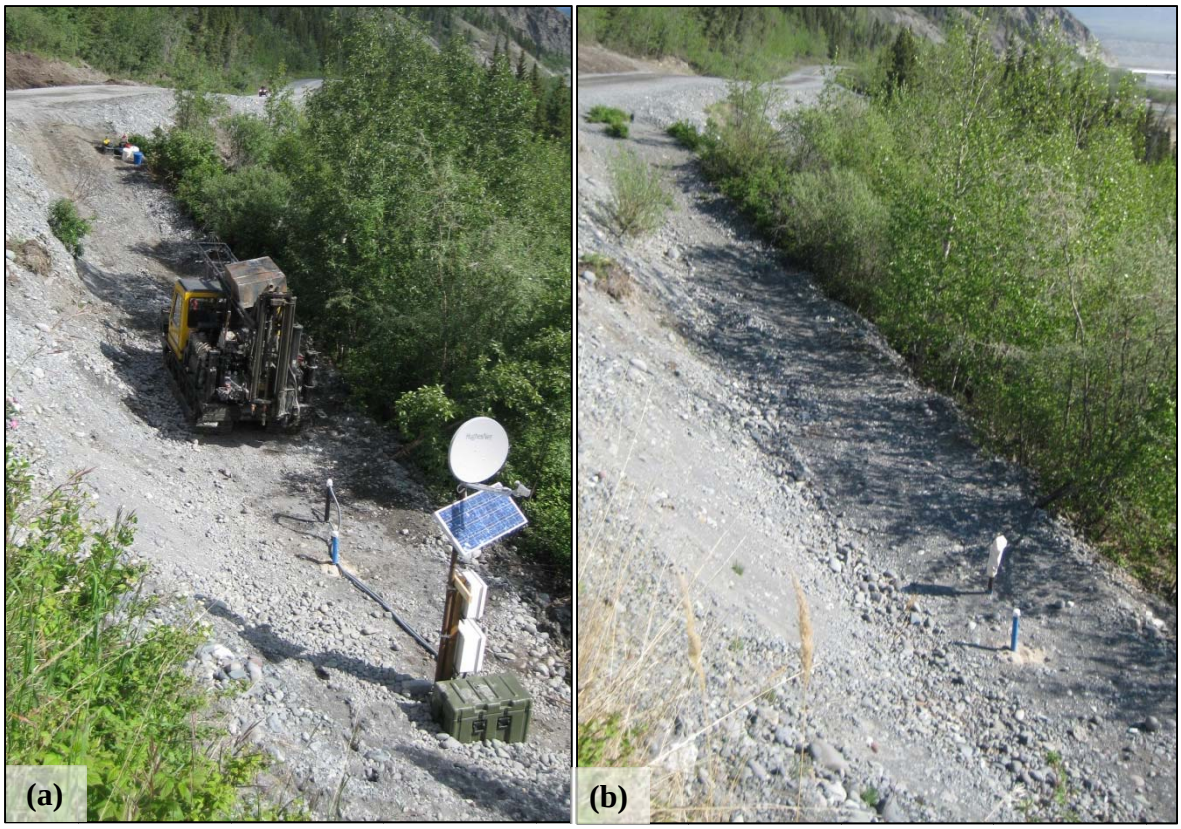

Figure B-7. Overview of the Chitina installation. (a) Final configuration showing the ADAS with satellite dish in the foreground, followed by the casing stick-up of TH10-1551 and TH10-1552, June 2010; (b) Chitina site after removal of the ADAS, May 2011. Only the guide casings remain visible on the drill pad. (Photographs by M. Darrow)

FINAL TEST HOLE LOG

STATE OF ALASKA DOT/PF
Northern Region Materials
Geology Section

ALASKA UNIVERSITY TRANSPORTATION CENTER
University of Alaska Fairbanks - INE

Project	Automated In-place MEMS Inclinometer Strings	Test Hole Number	TH10-1550
		Total Depth	20 feet
Field Geologist	M. DARROW	Dates Drilled	6/15/2010 - 6/15/2010
Field Crew	J. CLINE, P. LANIGAN, T. HALLER	UTM	N, E
Equipment Type	CME 45B	Latitude, Longitude	N61.51632°, W144.42664°
Weather	52 deg F, drizzle	Elevation	
TH Finalized By	M. DARROW	Vegetation	

Ground Water Data	While Drilling	After Drilling
Depth in (ft.)		
Time		
Date		
Symbol		

GENERAL COMMENTS:
Located to S end of drill pad, downhill and E of hwy

Drilling Method	Depth in (Feet)	Casing Blows / ft	Sample Data: Method	Number	Blow Count	Sample Interval	N-Value	Frozen	Graphic Log	SUBSURFACE MATERIAL
H-S Auger	0–8									Gy Well-graded GRAVEL w/ Sand (fill) w/ Cobbles dry to moist, loose, (cobbles on surface up to 1.0-ft dia.)
	8–11									Gy Well-graded GRAVEL w/ Silt & Sand (fill) w/ Cobbles dry to moist, loose
	11–15									Bn SILT wet, soft, *hi Org*, w/ Tr. Sa & Gr, w/ wood frags & shells; trash frags @ 11.0
	15–20									Gy Lean CLAY w/ Sand moist, w/ Tr. Gr
	20									BOH

Drilling Notes: overdrilled to coat boring w/ clay; installed timber post and steel rod for ADAS

Note: Unless otherwise noted, all samples are taken with 1-3/8-in. ID Standard Penetration Sampler driven with 140 lb. hammer with 30-in. drop. ☒ CME Auto Hammer ☐ Cathead Rope Method

NR AKDOT TEST HOLE LOG - USCS AIMS DRILLING.GPJ NR_AKDOT_PRECON_USCS_06_28_07.GDT 12/12/12

FINAL TEST HOLE LOG

STATE OF ALASKA DOT/PF
Northern Region Materials
Geology Section

ALASKA UNIVERSITY TRANSPORTATION CENTER
University of Alaska Fairbanks - INE

Project	Automated In-place MEMS Inclinometer Strings	Test Hole Number	TH10-1551
		Total Depth	50.2 feet
Field Geologist	M. DARROW	Dates Drilled	6/15/2010 - 6/16/2010
Field Crew	J. CLINE, P. LANIGAN, T. HALLER	Equipment Type	CME 45B
		UTM	N, E
Weather	55 deg F, overcast	Latitude, Longitude	N61.51639°, W144.42659°
TH Finalized By	M. DARROW	Vegetation	
		Elevation	

Ground Water Data	While Drilling	After Drilling
Depth in (ft.)		
Time		
Date		
Symbol		

GENERAL COMMENTS:
11.2 ft N of ADAS (TH10-1550)

Drilling Method	Depth in (Feet)	Casing Blows / ft	Sample Data: Method	Number	Blow Count	Sample Interval	N-Value	Frozen	Graphic Log
H-S Auger	0								
	1								
	2								
	3								
	4								
	5								
	6								
	7								
	8				WOR				
	9		SS	10-1000	1		3		
					2				
	10				1				
					WOR				
	11				1				
			SS	10-1001	1		2		
	12				1				
	13				1				
			SS	10-1002	1		3		
	14				2				
			SS	10-1003	1				
	15				3				
	16				3		6		
			SS	10-1004	3				
	17				4				
	18				4				
					6				
	19		SS	10-1005	8		14		
					7				
	20				2				
	21				3		7		
			SS	10-1006	4				
	22				8				
	23				2				
					3		7		
	24		SS	10-1007	4				
					5				
	25		SS	10-1008	3				
	26				5		11		
					6				
	27				9				
	28								
	29								
	30								
	31								
	32								
	33				4				
			SS		3		7		
	34				4				
					24				
	35								

SUBSURFACE MATERIAL

Gy Well-graded GRAVEL
w/ Sand (fill)
w/ Cobbles
dry, loose

Bn-Gy SILT
wet, soft, *hi Org*, w/ Tr. Gr; w/ snails, wood frags; trash frags @ 15.0;
wet below 12.5

SAMPLE 10-1000 (9.0-9.2): NM 69.2%
80% recov.

SAMPLE 10-1001 (11.5-11.7): NM 58.3%
100% recov., 38.5 degF

SAMPLE 10-1002 (13.2-13.3): NM 16.2%
NM taken from gravelly zone; 70% recov., schist clasts
SAMPLE 10-1003 (14.4-14.5): NM 53.4%
NM taken from hi Org Silt

40% recov., trash: can, styrofoam, glass

Gy Sandy Lean CLAY
w/ Gravel
w/ Cobbles
moist, stiff, trash frags @ 18.0; varves below 21.0, friable
SAMPLE 10-1004 (16.4-16.5): NM 22.1%

50% recov, 38.1 deg F, trash: glass, plastic X-mas tree
SAMPLE 10-1005 (19.0-19.1): NM 16.3%

100% recov., 38.1 deg F, varves
SAMPLE 10-1006 (21.7-21.8): NM 20.1%

100% recov., 39.7 deg F, varves
SAMPLE 10-1007 (24.4-24.5): NM 21.3%

80% recov., 37.4 deg F, varves, friable
SAMPLE 10-1008 (25.5-25.6): NM 26.3%

Gy Clayey GRAVEL
w/ Cobbles and Boulders
dry to moist, firm, schist, basalt, quartz clasts, boulder 14" min dia.
34.5-35.7

Note: Unless otherwise noted, all samples are taken with 1-3/8-in. ID Standard Penetration Sampler driven with 140 lb. hammer with 30-in. drop. ☒ CME Auto Hammer ☐ Cathead Rope Method

NR_AKDOT TEST HOLE LOG - USCS_AIMS DRILLING.GPJ NR_AKDOT_PRECON_USCS_06_28_07.GDT 12/12/12

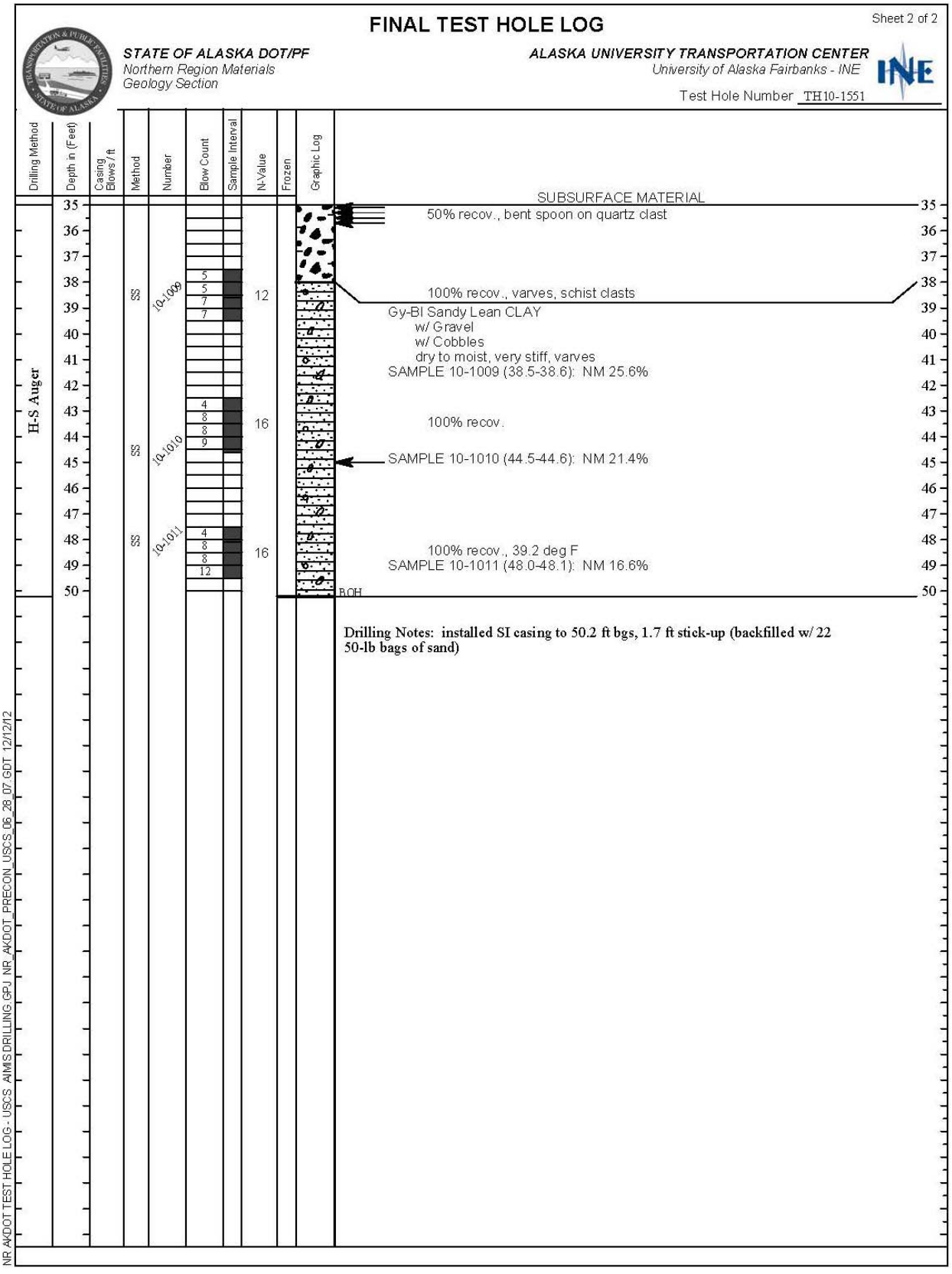
FINAL TEST HOLE LOG
Sheet 2 of 2
STATE OF ALASKA DOT/PF
Northern Region Materials
Geology Section
ALASKA UNIVERSITY TRANSPORTATION CENTER
University of Alaska Fairbanks - INE
Test Hole Number TH10-1551
Drilling Method
Depth in (Feet)
Casing Blows / ft
Method
Number
Blow Count
Sample Interval
N-Value
Frozen
Graphic Log
H-S Auger
SS
10-1009
10-1010
10-1011
5
5
7
7
12
4
8
8
9
16
4
8
8
12
16
SUBSURFACE MATERIAL
50% recov., bent spoon on quartz clast
100% recov., varves, schist clasts
Gy-Bl Sandy Lean CLAY
w/ Gravel
w/ Cobbles
dry to moist, very stiff, varves
SAMPLE 10-1009 (38.5-38.6): NM 25.6%
100% recov.
SAMPLE 10-1010 (44.5-44.6): NM 21.4%
100% recov., 39.2 deg F
SAMPLE 10-1011 (48.0-48.1): NM 16.6%
BOH
Drilling Notes: installed SI casing to 50.2 ft bgs, 1.7 ft stick-up (backfilled w/ 22 50-lb bags of sand)
NR AKDOT TEST HOLE LOG - USCS AIMS DRILLING.GPJ NR_AKDOT_PRECON_USCS_06_28_07.GDT 12/12/12

FINAL TEST HOLE LOG

Sheet 1 of 2

STATE OF ALASKA DOT/PF
Northern Region Materials
Geology Section

ALASKA UNIVERSITY TRANSPORTATION CENTER
University of Alaska Fairbanks - INE

Project: Automated In-place MEMS Inclinometer Strings
Test Hole Number: TH10-1552
Total Depth: 54 feet
Dates Drilled: 6/16/2010 - 6/17/2010
UTM: N, E
Latitude, Longitude: N61.51635°, W144.42668°
Elevation:

Field Geologist: M. DARROW
Field Crew: J. CLINE, P. LANIGAN, T. HALLER
TH Finalized By: M. DARROW
Equipment Type: CME 45B
Weather: 60 deg F, partly sunny
Vegetation:

Ground Water Data	While Drilling	After Drilling
Depth in (ft.)		
Time		
Date		
Symbol		

GENERAL COMMENTS:
4.2 ft N of TH10-1551

Drilling Method: H-S Auger

Sample Data: Depth in (Feet); Casing Blows / ft; Method; Number; Blow Count; Sample Interval; N-Value; Frozen; Graphic Log

SUBSURFACE MATERIAL

0 – Gy Well-graded GRAVEL
w/ Sand (fill)
w/ Cobbles
dry to moist

7 – Bn SILT
wet, soft, *hi Org*, w/ Tr. Gr., shells, wood frags

From Vane field test: Su ~ 90 kPa
SAMPLE 10-1014 (10.0-12.5):
Shelby collected for later Triaxial tests

16 – Gy Lean CLAY
w/ Gravel
moist

19 – Gy Gravelly Lean CLAY
w/ Cobbles and Boulders
dry to moist, up to 1.0-ft dia boulder 21.0-22.0

SAMPLE 10-1015 (25.0-27.5):
end of ST crumpled on rock; Shelby collected for later Triaxial tests

Method: ST VANE; ST
Number: 10-1014; 10-1015

Note: Unless otherwise noted, all samples are taken with 1-3/8-in. ID Standard Penetration Sampler driven with 140 lb. hammer with 30-in. drop. ☒ CME Auto Hammer ☐ Cathead Rope Method

NR AKDOT TEST HOLE LOG - USCS AIMS DRILLING.GPJ NR_AKDOT_PRECON_USCS_06_28_07.GDT 12/12/12

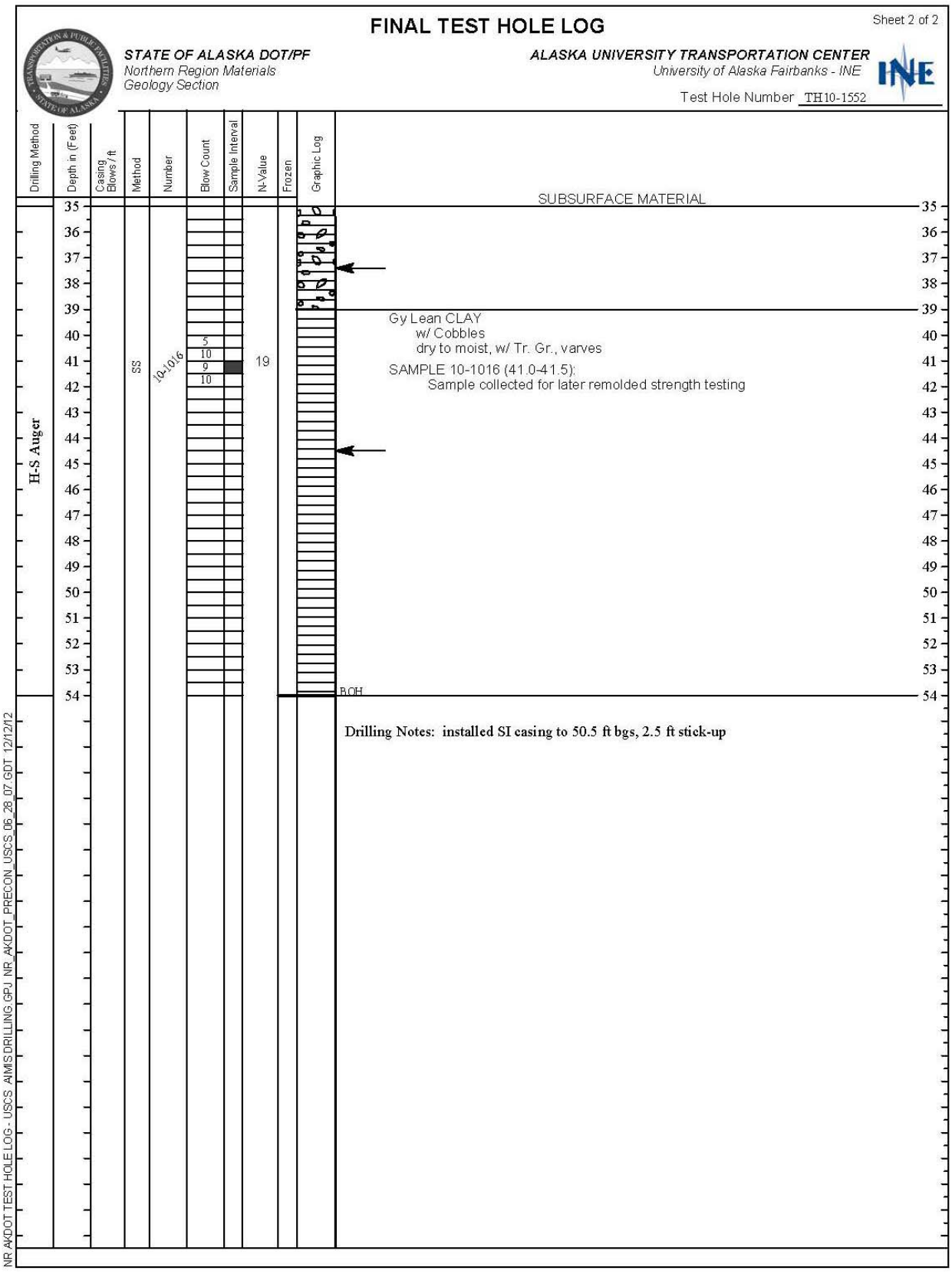
FINAL TEST HOLE LOG
Sheet 2 of 2
STATE OF ALASKA DOT/PF
Northern Region Materials
Geology Section
ALASKA UNIVERSITY TRANSPORTATION CENTER
University of Alaska Fairbanks - INE
Test Hole Number TH10-1552
Drilling Method
Depth in (Feet)
Casing Blows / ft
Method
Number
Blow Count
Sample Interval
N-Value
Frozen
Graphic Log
SUBSURFACE MATERIAL
H-S Auger
SS
10-1016
5
10
9
10
19
Gy Lean CLAY
w/ Cobbles
dry to moist, w/ Tr. Gr., varves
SAMPLE 10-1016 (41.0-41.5):
Sample collected for later remolded strength testing
BOH
Drilling Notes: installed SI casing to 50.5 ft bgs, 2.5 ft stick-up
NR AKDOT TEST HOLE LOG - USCS AIMS DRILLING.GPJ NR_AKDOT_PRECON_USCS_06_28_07.GDT 12/12/12

FINAL TEST HOLE LOG

STATE OF ALASKA DOT/PF
Northern Region Materials
Geology Section

ALASKA UNIVERSITY TRANSPORTATION CENTER
University of Alaska Fairbanks - INE

Project	Automated In-place MEMS Inclinometer Strings	Test Hole Number	TH10-1553
		Total Depth	16.5 feet
Field Geologist	M. DARROW	Dates Drilled	6/17/2010 - 6/17/2010
Field Crew	J. CLINE, P. LANIGAN, T. HALLER	Equipment Type	CME 45B
		UTM	N, E
		Weather	60 deg F, partly sunny
		Latitude, Longitude	N61.51645°, W144.42673°
TH Finalized By	M. DARROW	Vegetation	
		Elevation	

Ground Water Data	While Drilling	After Drilling
Depth in (ft.)		
Time		
Date		
Symbol		

GENERAL COMMENTS:
2.6 ft N of TH10-1552

Drilling Method: H-S Auger

Sample Data: Method | Number | Blow Count | Sample Interval | N-Value

Casing Blows / ft | Frozen | Graphic Log

SUBSURFACE MATERIAL

0 Gy Well-graded GRAVEL
w/ Sand (fill)
w/ Cobbles
dry to moist

6 Bn SILT
wet, soft, *hi Org*, w/ Tr. Gr., w/ wood frags

16 BOH

Drilling Notes: installed piezometer to 15.8 ft bgs on PVC casing; backfilled with cement bentonite grout

Note: Unless otherwise noted, all samples are taken with 1-3/8-in. ID Standard Penetration Sampler driven with 140 lb. hammer with 30-in. drop. ☒ CME Auto Hammer ☐ Cathead Rope Method

NR AKDOT TEST HOLE LOG - USCS AIMS DRILLING.GPJ NR_AKDOT_PRECON_USCS_06_28_07.GDT 12/12/12

APPENDIX C: LOST CHICKEN INSTALLATION PHOTOGRAPHS

Figure C-1. Looking southeast towards the instrumented cross section. Geotextile with some ACE material is present in the foreground. (Photograph by M. Darrow, June 2012)

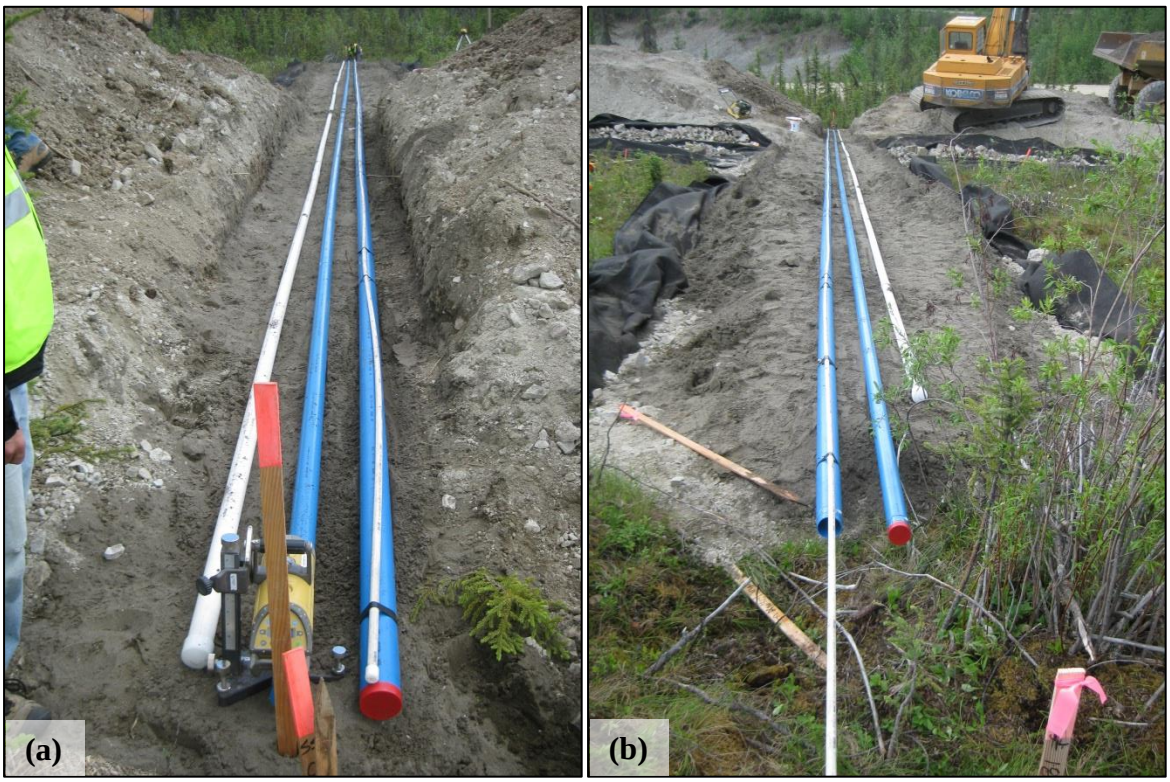

Figure C-2. Casings prior to backfill at the instrumented cross section, looking (a) upslope and (b) downslope. (Photographs by M. Darrow, June 2012)

Figure C-3. Covering the casings with sand bedding. (Photograph by M. Darrow, June 2012)

Figure C-4. Downhill toe of embankment with thermal berm and exposed casing ends. (Photograph by M. Darrow, July 2012)

Figure C-5. Wrapping BeadedStream temperature acquisition cable (TAC) to thermistor cable for installation. (Photograph by M. Darrow, July 2012)

Figure C-6. Alignment of TAC and thermistor cable. (a) Location of thermistor beads relative to TAC sensors was recorded, (b) as well as the location of the final thermistor bead. (Photographs by M. Darrow, July 2012)

Figure C-7. Attaching the pull rope to the end of the TAC device. (Photograph by M. Darrow, July 2012)

Figure C-8. Uphill termination of the casing containing the TAC and thermistor string. (Photograph by M. Darrow, July 2012)

Figure C-9. PVC casing to flexible conduit adapter for the temperature measurement cables. (Photograph by M. Darrow, July 2012)

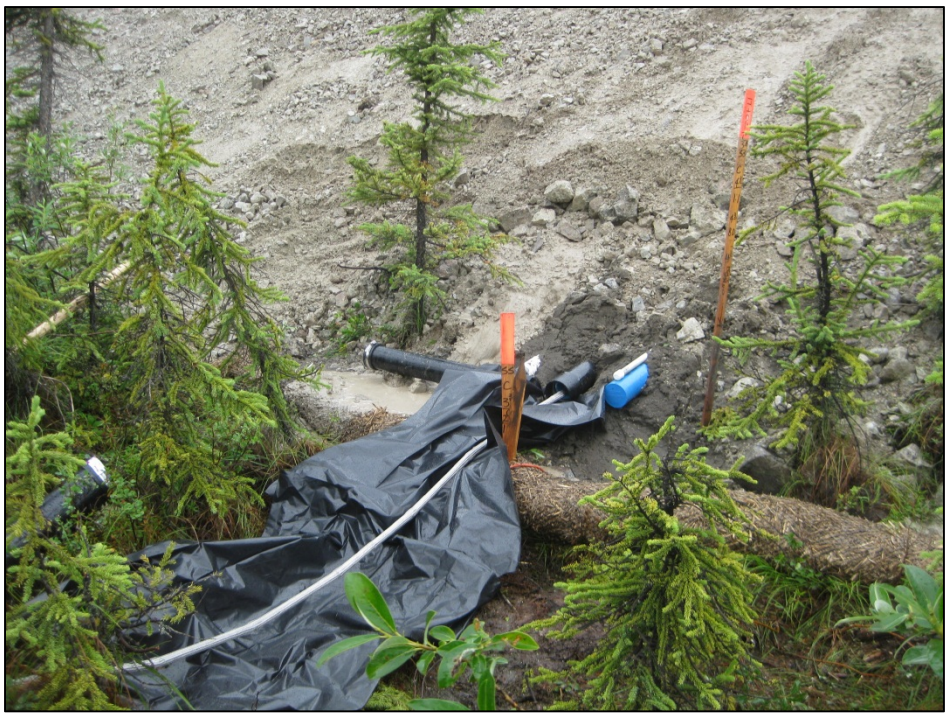

Figure C-10. Installing the SAA device from the downslope end, pulling from the upslope end. (Photograph by M. Darrow, July 2012)

Figure C-11. Installation of SAA device, showing shipping reel position relative to embankment and ADAS. (Photograph by M. Darrow, July 2012)

Figure C-12. PVC casing to flexible conduit adapter for SAA installation. (Photograph by M. Darrow, July 2012)

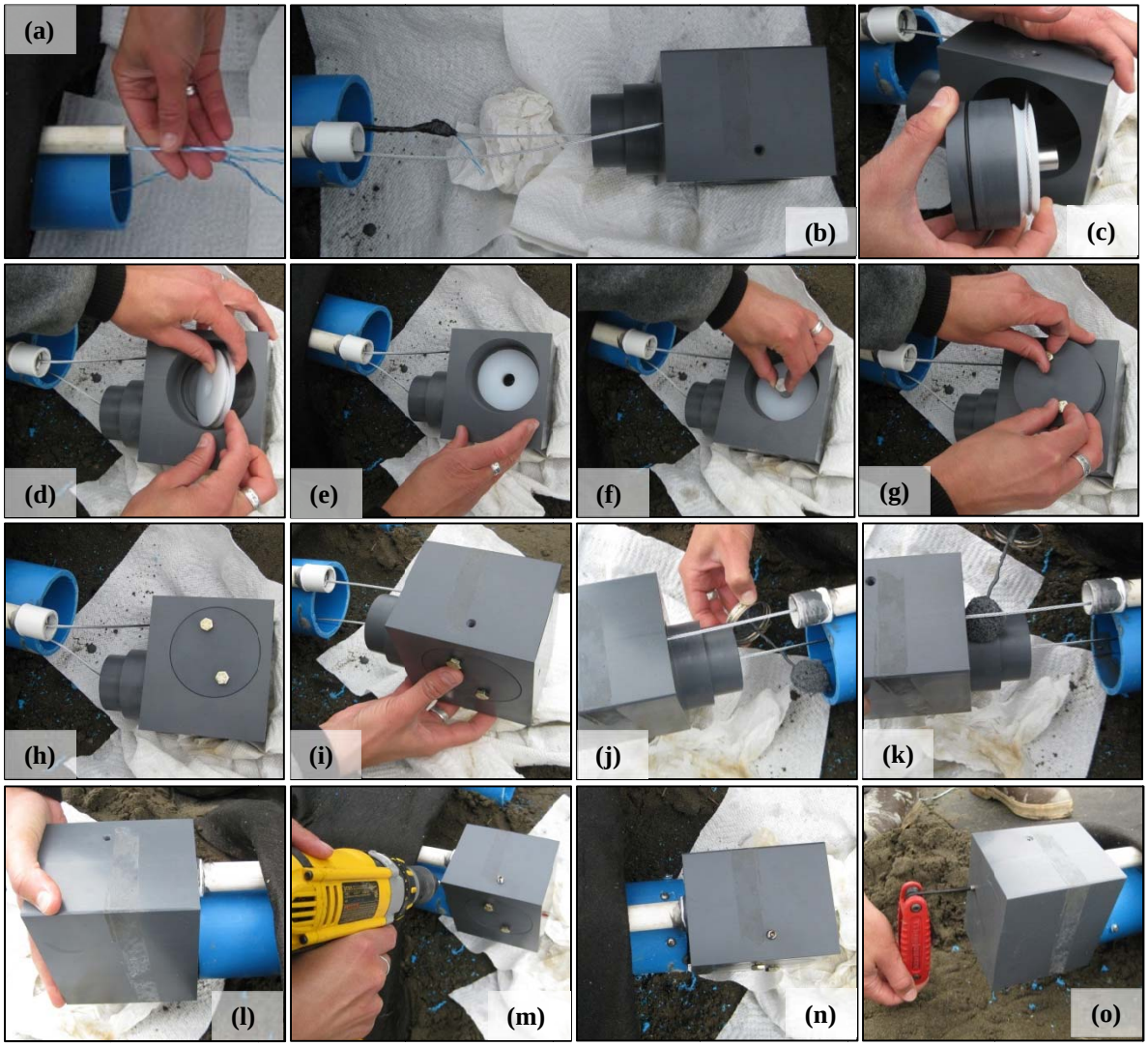

Figure C-13. Installing the dead-end pulley on the horizontal guide casing. (a) Identifying pull ropes within casing; (b) pulling wire rope through casing and dead-end housing; (c) positioning wire rope around pulley; (d) placing pulley within housing; (e) pulley seated within housing; (f) placing retaining pin through pulley; (g) placing access plug to seal housing; (h) access plug in place; (i) aligning dead-end pulley; (j) applying solvent cement to guide casing and 3/4-in. PVC casing; (k) applying PVC cement to dead-end pulley housing; (l) joining dead-end pulley housing to casing; (m) further attaching with screws; (n) dead-end housing in place with screws through casing and set screws for access plug; (o) tightening set screws to secure access plug. (Photographs courtesy of J. Zottola and D. Jensen, July 2012)

Figure C-14. Routing pull rope for SAA through ABS end cap adapter. (Photograph courtesy of J. Zottola, July 2012)

Figure C-15. Tapping ABS end cap adapter into the sand bedding to be flush with inner casing. (Photograph courtesy of J. Zottola, July 2012)

Figure C-16. Filling annulus space with expanding foam to seal outer ABS end cap adapter in place. (Photograph courtesy of J. Zottola, July 2012)

Figure C-17. Upslope casing ends secured. From left to right, dead-end pulley on guide casing for manual inclinometer probe measurements, sealed guide casing with tied-off SAA pull rope, sealed 2-in. PVC casing with tied-off TAC/thermistor string pull rope. (Photograph by M. Darrow, July 2012)

Figure C-18. Trimming the downslope guide casing for ABS end cap adapter. (Photograph by M. Darrow, July 2012)

Figure C-19. Tapping ABS end cap adapter into the sand bedding for downslope guide casing. (Photograph by M. Darrow, July 2012)

Figure C-20. Attaching 2 ¼-in. locking link to wire rope within guide casing. (Photograph by M. Darrow, July 2012)

Figure C-21. Winding up excess wire rope from within casing assembly. (Photograph by M. Darrow, July 2012)

Figure C-22. Taking manual inclinometer probe measurements. (a) Feeding inclinometer probe cable into casing by reeling up the wire rope; (c) taking readings as the cable is retracted from the casing. (Photographs by M. Darrow, July 2012)

Figure C-23. Downslope guide casing termination. Wire rope is tucked into casing for easy retrieval for next reading. (Photographs by M. Darrow, July 2012)

Figure C-24. Downslope casing ends secured. From left to right, ABS casing to flexible conduit adapters for TAC/thermistor cables and SAA device, and sealed guide casing for manual inclinometer probe measurements. (Photograph by M. Darrow, July 2012)

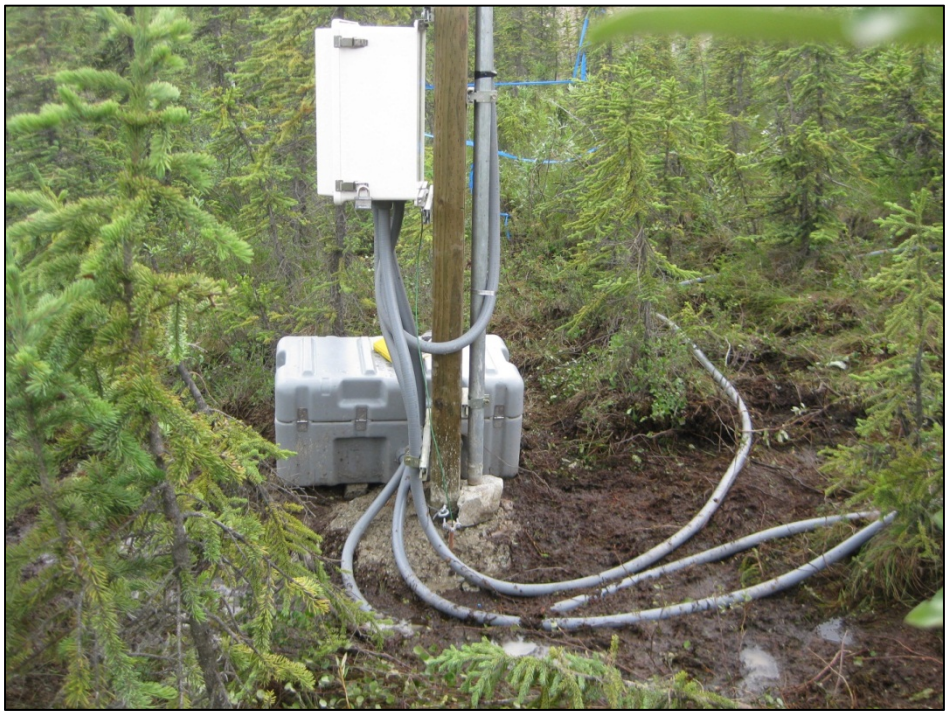

Figure C-25. Battery box and enclosure for ADAS. (Photograph by M. Darrow, July 2012)

Figure C-26. Final ADAS configuration located near the downslope toe of the embankment. The thermal berm is visible behind the ADAS. (Photograph by M. Darrow, July 2012)

Figure C-27. Cracks in the thermal berm on September 14, 2012. (Photograph by D. Jensen)

Figure C-28. Changes at the ADAS during the fall of 2012. (a) Post, solar panel support, and grounding rod on July 11, 2012; (b) Settlement of ground surface as of October 6, 2012. (Photographs by M. Darrow and D. Jensen)

APPENDIX D: FDL-A INSTALLATION PHOTOGRAPHS AND BORING LOG

Figure D-1. Drilling TH12-9004 with tricone and casing. (Photograph by M. Darrow, Sept. 2012)

Figure D-2. Cement-bentonite grout during the back-filling process. (Photograph by M. Darrow, Sept 2012)

Figure D-3. INC500 modules, staged and ready for installation. A safety line was attached to the lowest module (indicated by the yellow arrow). (Photograph by M. Darrow, Sept. 2012)

Figure D-4. Installing the INC500 within the guide casing in TH12-9004. (Photograph by J. Simpson, Sept. 2012)

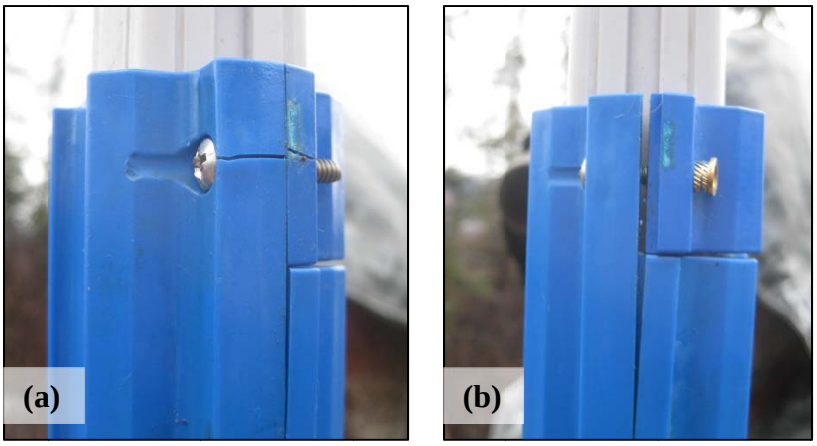

Figure D-5. Examples of coupler damage. (a) Cracked coupler, and (b) threaded insert that popped out of the plastic coupler and would not tighten. (Photographs courtesy of J. Simpson, Sept. 2012)

Figure D-6. Completed casing and instrument installation in TH12-9004. (Photograph by M. Darrow, Sept. 2012)

Figure D-7. Completed ADAS location and casing installation of TH12-9004. (Photograph by M. Darrow, Sept. 2012)

FINAL TEST HOLE LOG

STATE OF ALASKA DOT/PF
Northern Region Materials
Geology Section

ALASKA UNIVERSITY TRANSPORTATION CENTER
University of Alaska Fairbanks - INE

Project	Frozen Debris Lobe-A, Dalton Highway MP219	Test Hole Number	TH12-9004
		Total Depth	100 feet
Field Geologist	M. DARROW	Dates Drilled	9/19/2012 - 9/21/2012
Field Crew	J. CLINE, P. LANIGAN, K. MAXWELL, S. PARKER, R. DAANEN, J. SIMPSON	Equipment Type	CME 850
		UTM	N7524572, E381423
TH Finalized By	M. DARROW	Weather	~35degF, light rain
		Latitude, Longitude	
		Vegetation	wh. spruce, tea, alder, moss, lichen
		Elevation	

Ground Water Data	While Drilling	After Drilling
Depth in (ft.)		
Time		
Date		
Symbol		

GENERAL COMMENTS:
Location determined with handheld Garmin etrex GPS, UTM zone 6

Drilling Method	Depth in (Feet)	Casing Blows / ft	Sample Data: Method	Number	Blow Count	Sample Interval	N-Value	Frozen	Graphic Log
S-S Auger	0								
	1								
	2								
	3								
	4								
	5								
	6	12							
	7	11						?	
	8	28							
	9	52							
	10		SS	12-2510	5				
					6				
	11	14			7				
					10				
	12	39							
	13	52							
	14	83							
	15	102							
	16	132							
	17	78							
	18	92							
	19	115							
Tri-cone & Casing	20	7			8				
			SS SS	12-2511	5				
	21	18		12-2512	33				
					31				
	22	8							
	23	7							
	24	8							
	25	27							
	26	68							
	27	114							
	28	128							
	29	165							
	30	46			18				
					23				
	31	86	SS	12-2513	26				
					51				
	32	189							
	33	226							
	34	285							
	35				25				

SUBSURFACE MATERIAL

ORG MAT

Gy Silty SAND
w/ Gravel
pre-drilled 5.5-8.0, and 19.5-24.5; lost water @ 25.0; wood frags @ 38.5, water pressure in rod @~53.0

SAMPLE 12-2510 (9.5-11.5):
SS Liner (to be tested); 75% recov., washed to 10.0, wet to 10.5, fzn below 10.5

SAMPLE 12-2511 (19.5-21.5):
SS Liner (to be tested); 50% recov., clear ice layers w/in soil

SAMPLE 12-2512 (21.0-21.2): NM 13.7%
Vol. WC 27%

100% recov., clear ice coatings on gravel

SAMPLE 12-2513 (31.0-31.5): NM 16.4%

Note: Unless otherwise noted, all samples are taken with 1-3/8-in. ID Standard Penetration Sampler driven with 140 lb. hammer with 30-in. drop. ☒ CME Auto Hammer ☐ Cathead Rope Method

NR AKDOT TEST HOLE LOG - USCS FDLA_DALTON219.GPJ NR_AKDOT_PRECON_USCS_06_28_07.GDT 12/6/12

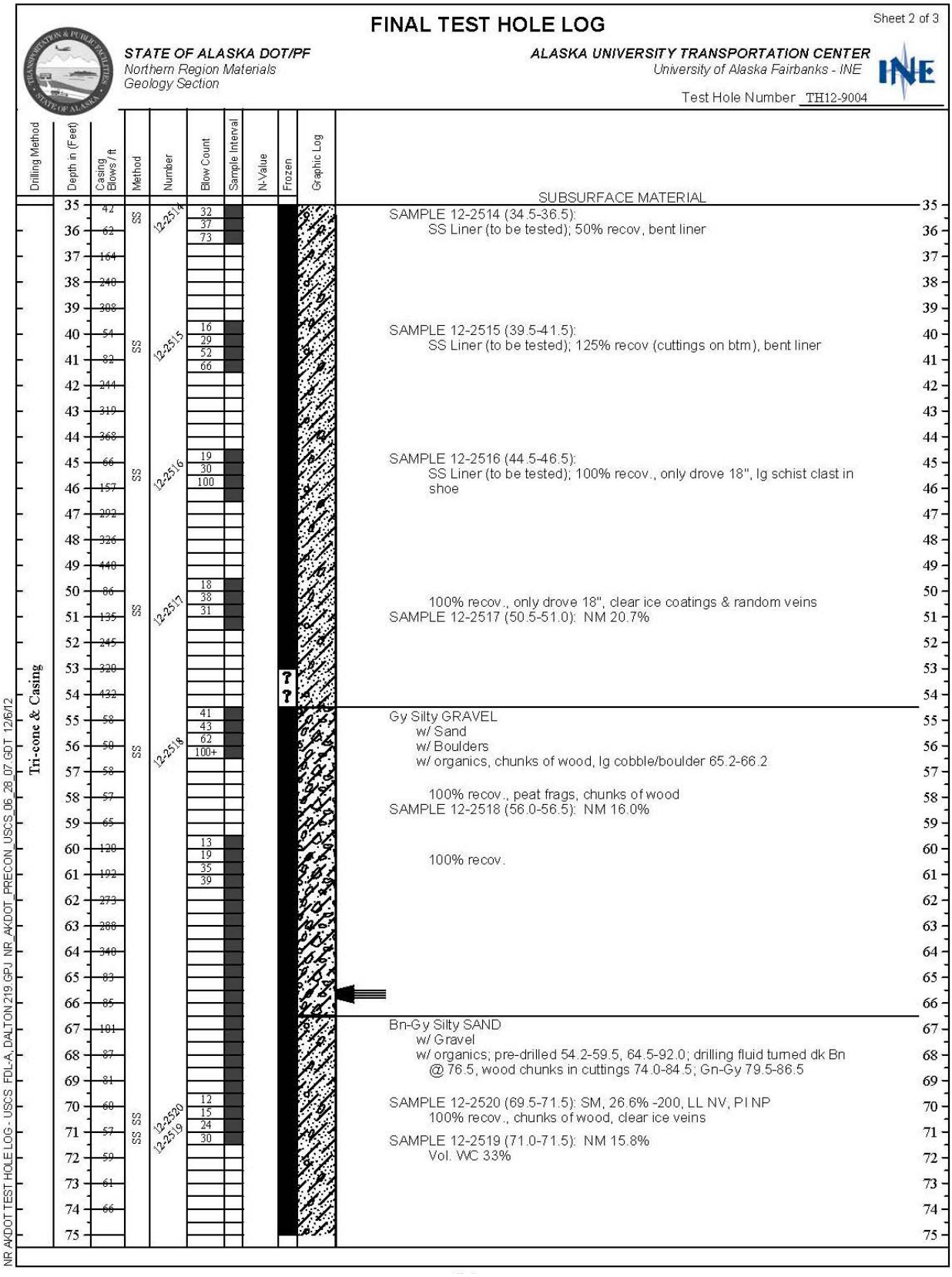
FINAL TEST HOLE LOG
Sheet 2 of 3
STATE OF ALASKA DOT/PF
Northern Region Materials
Geology Section
ALASKA UNIVERSITY TRANSPORTATION CENTER
University of Alaska Fairbanks - INE
Test Hole Number TH12-9004
Drilling Method
Depth in (Feet)
Casing Blows / ft
Method
Number
Blow Count
Sample Interval
N-Value
Frozen
Graphic Log
SUBSURFACE MATERIAL
Tri-cone & Casing
SAMPLE 12-2514 (34.5-36.5):
SS Liner (to be tested); 50% recov, bent liner
SAMPLE 12-2515 (39.5-41.5):
SS Liner (to be tested); 125% recov (cuttings on btm), bent liner
SAMPLE 12-2516 (44.5-46.5):
SS Liner (to be tested); 100% recov., only drove 18", lg schist clast in shoe
100% recov., only drove 18", clear ice coatings & random veins
SAMPLE 12-2517 (50.5-51.0): NM 20.7%
Gy Silty GRAVEL
w/ Sand
w/ Boulders
w/ organics, chunks of wood, lg cobble/boulder 65.2-66.2
100% recov., peat frags, chunks of wood
SAMPLE 12-2518 (56.0-56.5): NM 16.0%
100% recov.
Bn-Gy Silty SAND
w/ Gravel
w/ organics; pre-drilled 54.2-59.5, 64.5-92.0; drilling fluid turned dk Bn @ 76.5, wood chunks in cuttings 74.0-84.5; Gn-Gy 79.5-86.5
SAMPLE 12-2520 (69.5-71.5): SM, 26.6% -200, LL NV, PI NP
100% recov., chunks of wood, clear ice veins
SAMPLE 12-2519 (71.0-71.5): NM 15.8%
Vol. WC 33%
NR AKDOT TEST HOLE LOG - USCS FDL-A, DALTON 219.GPJ NR_AKDOT_PRECON_USCS_06_28_07.GDT 12/6/12

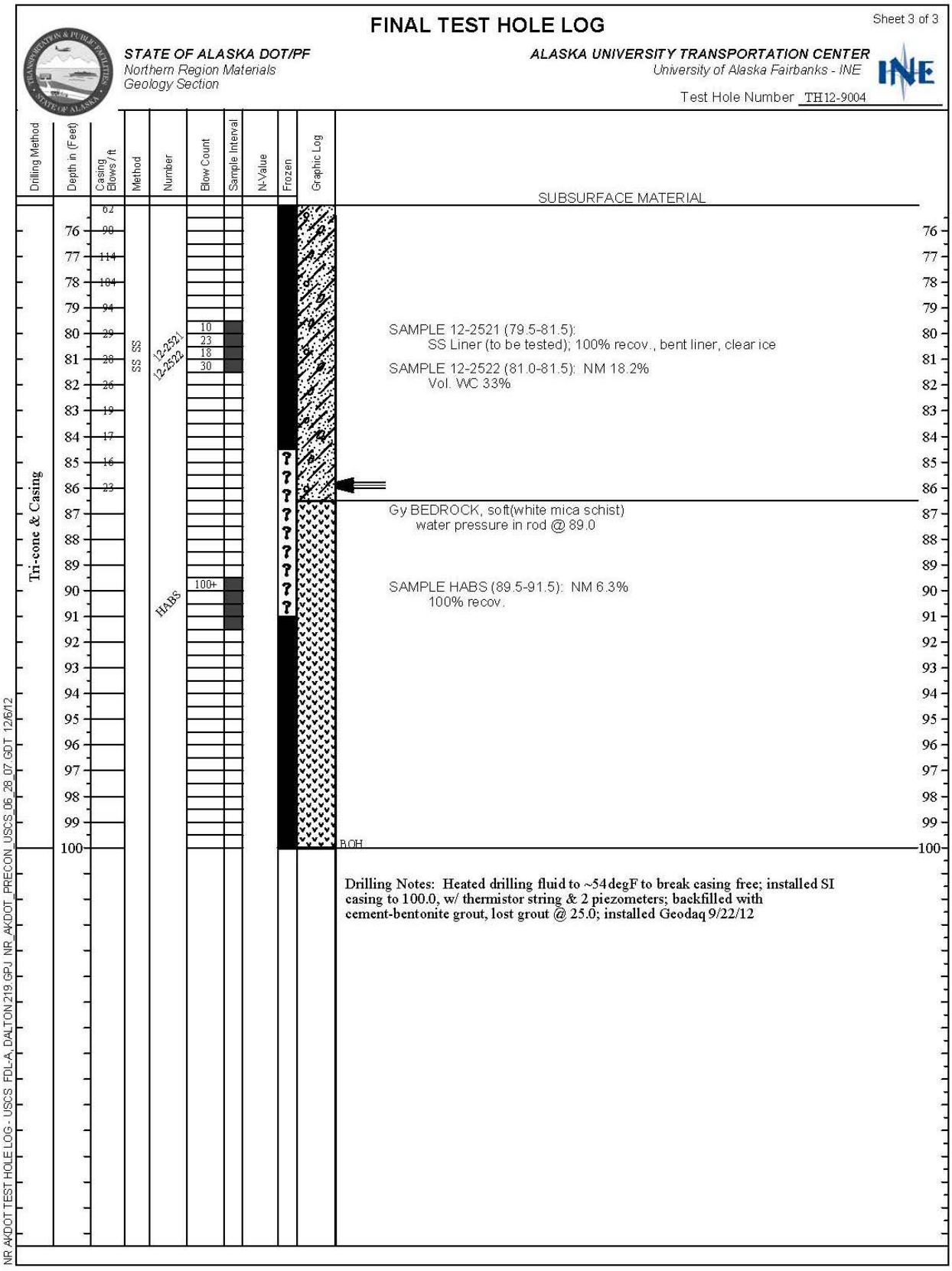
FINAL TEST HOLE LOG
Sheet 3 of 3
STATE OF ALASKA DOT/PF
Northern Region Materials
Geology Section
ALASKA UNIVERSITY TRANSPORTATION CENTER
University of Alaska Fairbanks - INE
Test Hole Number TH12-9004
Drilling Method
Depth in (Feet)
Casing Blows / ft
Method
Number
Blow Count
Sample Interval
N-Value
Frozen
Graphic Log
SUBSURFACE MATERIAL
Tri-cone & Casing
SS SS
12-2521
12-2522
10
23
18
30
HABS
100+
SAMPLE 12-2521 (79.5-81.5):
SS Liner (to be tested); 100% recov., bent liner, clear ice
SAMPLE 12-2522 (81.0-81.5): NM 18.2%
Vol. WC 33%
Gy BEDROCK, soft(white mica schist)
water pressure in rod @ 89.0
SAMPLE HABS (89.5-91.5): NM 6.3%
100% recov.
BOH
Drilling Notes: Heated drilling fluid to ~54degF to break casing free; installed SI casing to 100.0, w/ thermistor string & 2 piezometers; backfilled with cement-bentonite grout, lost grout @ 25.0; installed Geodaq 9/22/12
NR AKDOT TEST HOLE LOG - USCS FDLA_DALTON 219.GPJ NR_AKDOT_PRECON_USCS_06_28_07.GDT 12/6/12

APPENDIX E: MANUFACTURER'S WEBSITES

NOTE: These links were current as of December 2012. The websites are dynamic and constantly changing. We encourage the reader to use the information provided in this appendix with discretion.

Geodaq: www.geodaq.com

Specific devices used for this project: http://www.geodaq.com/inclinometer.html (product datasheet and white papers are available at this link)

For this project, we purchased a GCM Controller Module. As of December 2012, the website showed an updated version: http://www.geodaq.com/controller.html (product datasheet available at this link)

Received "Draft Installation Instructions for the INC500 In-Place Inclinometer, Geodaq, Inc., Sacramento, California" from manufacturer

Received "GCM1200 User Manual Ver. 2.0" from manufacturer

Measurand (geotechnical purposes): http://www.measurandgeotechnical.com/

Product information (including specifications, ordering guide, installation guide, and power and lightning protection information): http://www.measurandgeotechnical.com/products.html

Support manuals for instrumentation, interfaces (including using the CS CR1000 data logger), and accessories: http://www.measurandgeotechnical.com/support_manuals.html

Tutorial videos: (http://www.measurandgeotechnical.com/suppor_tutorial_videos.html)

Software downloads (http://www.measurandgeotechnical.com/software.html)

Examples of usage (http://www.measurandgeotechnical.com/examples.html)

For this project, we used "Integration of ShapeAccelArray (SAA) and Campbell Scientific's CR1000 Data Logger", "Measurand ShapeAccelArray (SAA) Specifications including ordering guide", and "ShapeAccelArray (SAA) Installation Guide" documents from the website.

APPENDIX F: "PARTS LISTS" FOR M-IPI DEVICES AND ADAS INSTALLATIONS

Table F-1. "Parts list" for Geodaq M-IPI device.

Item	Quantity
In-place inclinometer module, Model INC500; included four centralizers per module and needed couplers	21
Geodaq Controller Module with RS232 cable	2
Software for the INC500 inclinometer	1

Table F-2. "Parts list" for Measurand M-IPI device.

Item	Quantity
68' ShapeAccelArray – Field (SAAF); sensorized with 66 304.8-mm segments; custom build with 2 segment partial octet; total length with unsensorized segments 67.5'	1
50' of cable with connector	1
SAA232 converter with surge protection and auto power off feature; used for connecting to COM port on Campbell Scientific CR1000 data logger	1
SAA+CR1000 Software Suite; includes CR1000 program for collecting SAA data, SAACR_raw2data utility for converting raw SAA data to Cartesian coordinates, SAA3D Viewer software for displaying results	1
SAA232 to USC direct connection cable for pre-installation SAA diagnostics	1

Table F-3. “Parts list” for typical ADAS installation. This list is by no means exhaustive, and hardware dimensions are not provided as this must be adjusted for the materials on hand. Although not listed, a well-stocked toolbox, ratchet and socket set, and cordless drill, circular saw, and reciprocating saw are extremely valuable in the assembling an ADAS. “CS” stands for Campbell Scientific. *Telemetry not incorporated at all sites.

DATA ACQUISITION
CS CR1000 data logger w/ extended temperature testing
CS AM 16/32B 16 or 32 channel relay multiplexer w/ extended temperature testing
CS MUXPOWER-L-2 multiplexer power/reset cable
CS MUXSIGNAL-L-2 multiplexer signal cable
USB to serial interface connector
POWER
CSI SP70W solar panel, w/ mounting hardware and 20’ cable
MorningStar SunSaver 10A 12V control regulator
12V deep cycle batteries, 100 Amp-hour
TELEMETRY*
CS 900MHz 1W spread spectrum radio
Field power cable 12vdc plug to pigtail, 2 ft
8 dB omni-directional antenna
Coaxial cable, 20 ft
Moxa Portserver (2 port)
SUPPORT, SHELTER, AND HARDWARE
CS weather-resistant 16x18” enclosure
Battery enclosure
4” x 6” x 10’ pressure treated wood post
1-1/2” steel pipe, bolts, washers, nuts
Metal framing channel (various lengths), clamps, lag screws, washers, spring nuts
Liquidtite flexible conduit, Liquidtite connectors
8’ copper grounding rod, grounding rod clamp, 12ga grounding wire
Hose clamps, various sizes
Zip ties (black plastic), various sizes
Wire rope, ferrule set, padlocks
U-bolts, washers, nuts